Detection of Solar, Geo and Supernova Neutrinos
(recent progress)

Steve Biller, Oxford University

pp chain

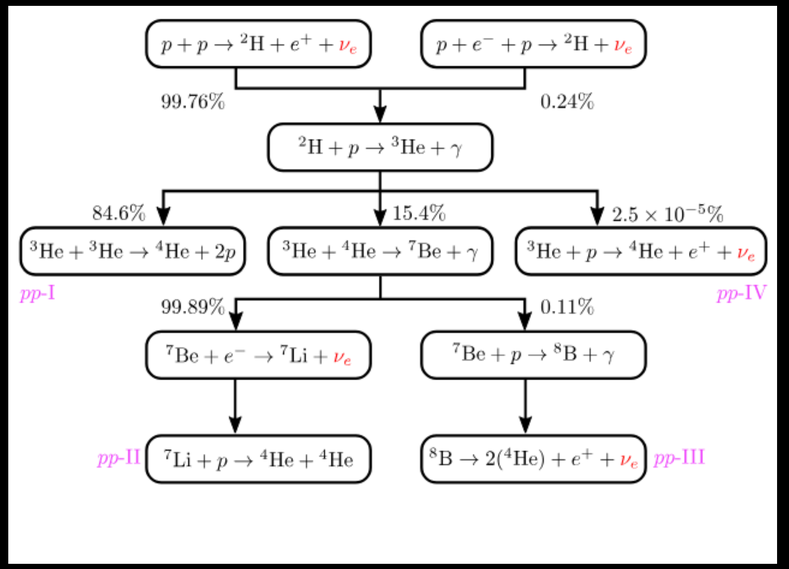

CNO cycle

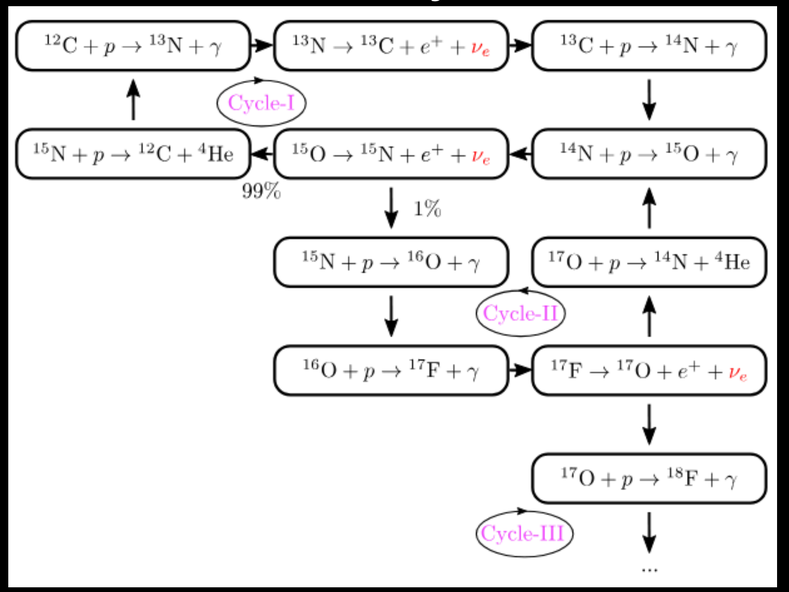


CNO

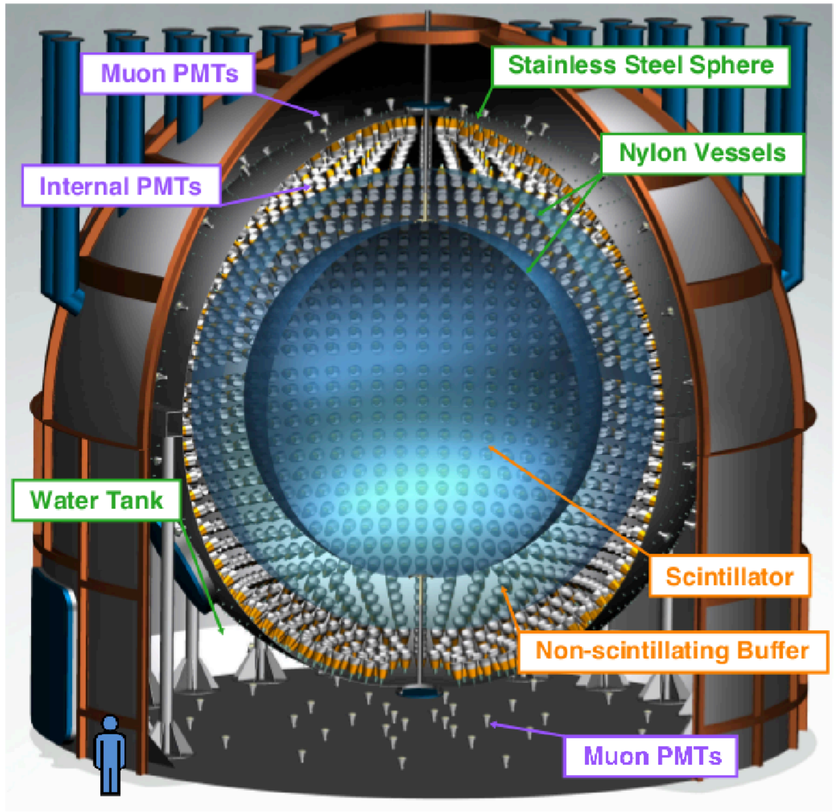

CNO

Final results of Borexino on CNO solar neutrinos
Phys. Rev. D **108**, 102005 – **14 November, 2023**
(arXiv:2307.14636 [hep-ex])

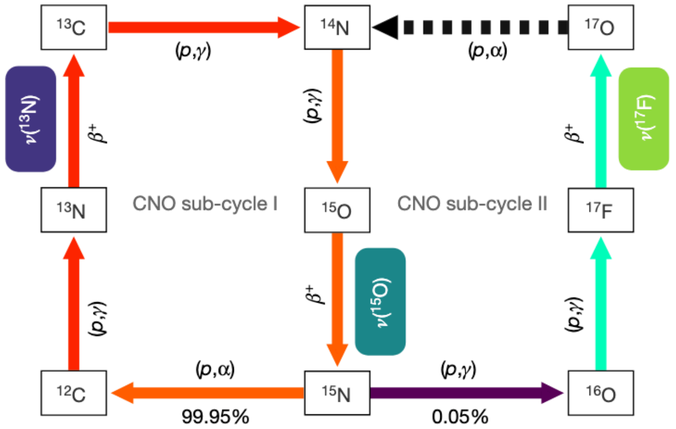

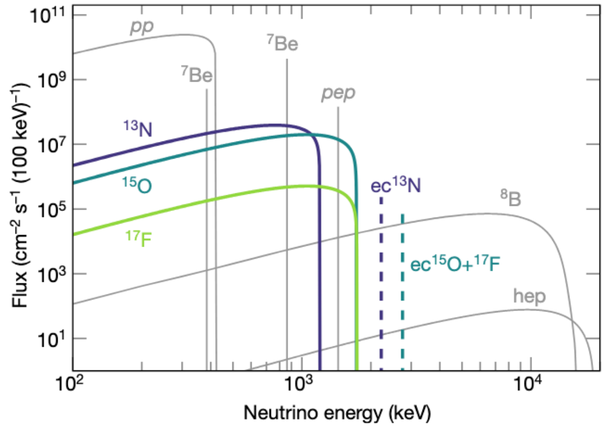

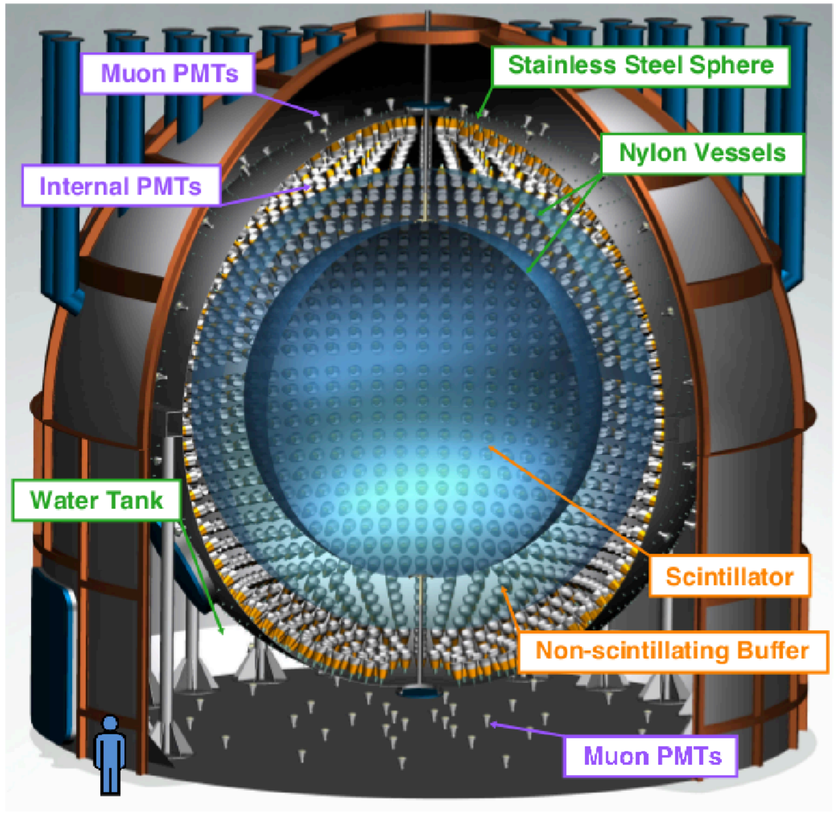

CNO

Final results of Borexino on CNO solar neutrinos
Phys. Rev. D **108**, 102005 – **14 November, 2023**
(arXiv:2307.14636 [hep-ex])

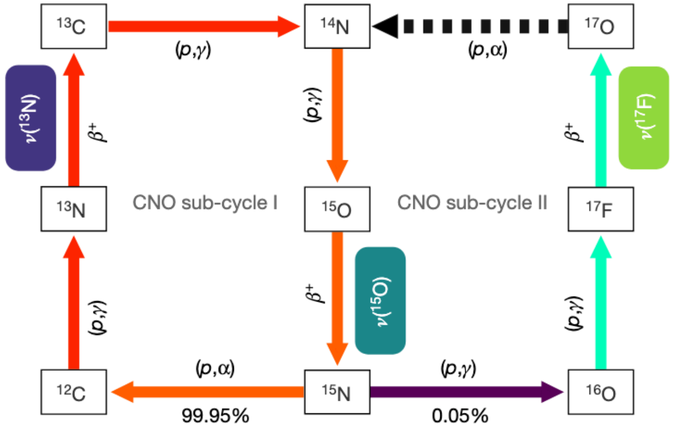

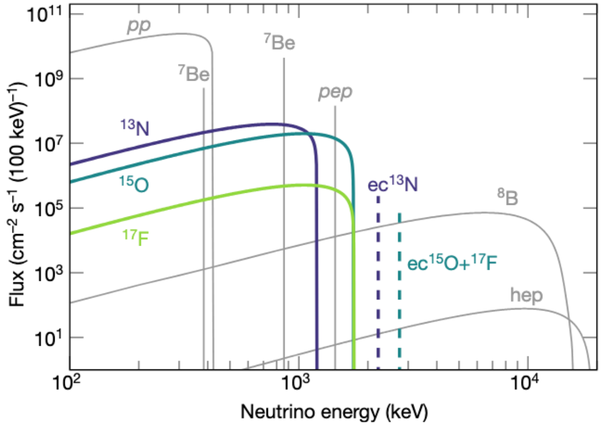

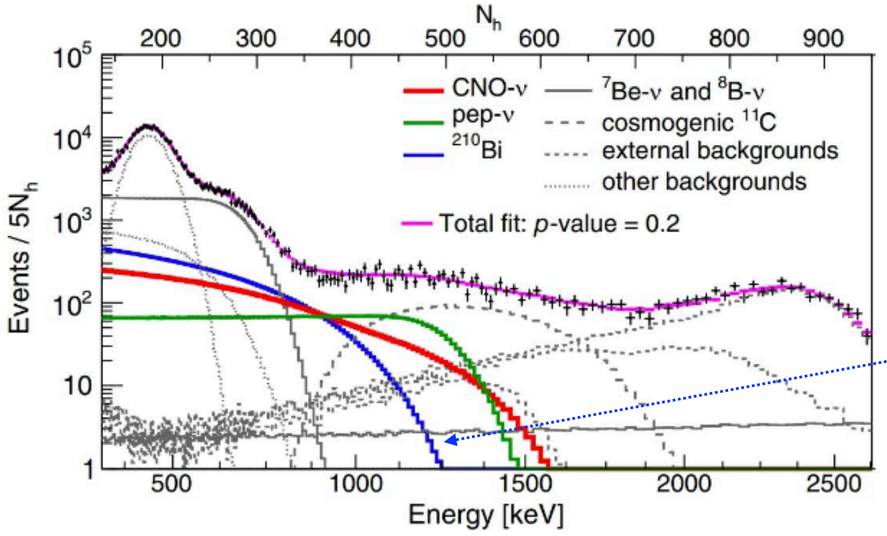

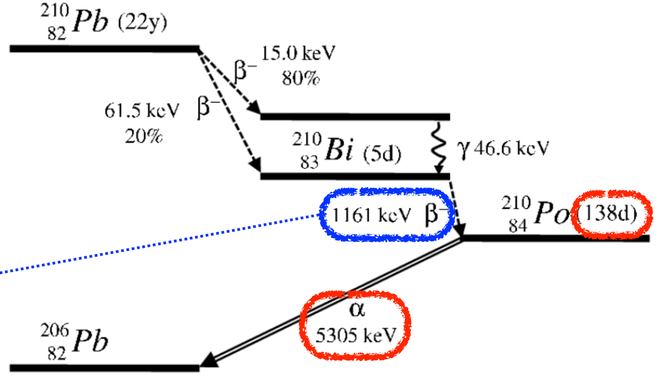

Improved thermal stability allows Bi-Po tagging to map ^{210}Bi (5d) distribution from ^{210}Po

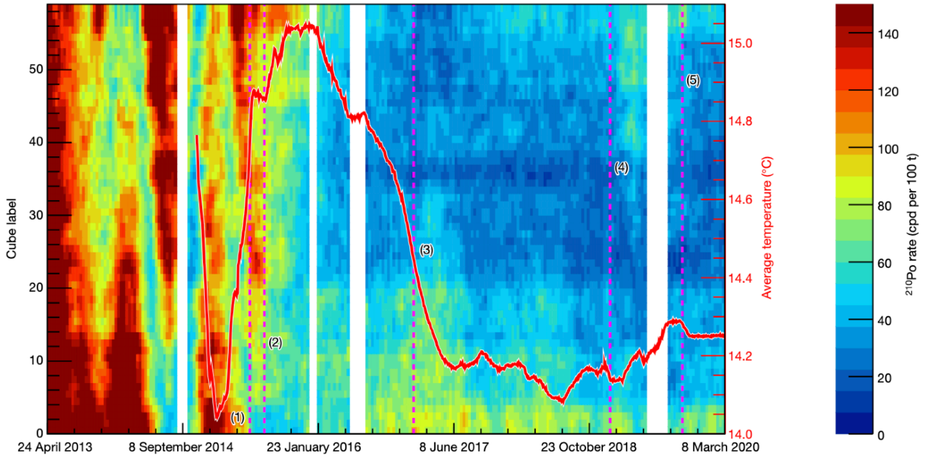

Experimental evidence of neutrinos produced in the CNO fusion cycle in the Sun

Nature **volume 587**, pages 577–582 (2020)

Improved thermal stability allows Bi-Po tagging to map ^{210}Bi (5d) distribution from ^{210}Po

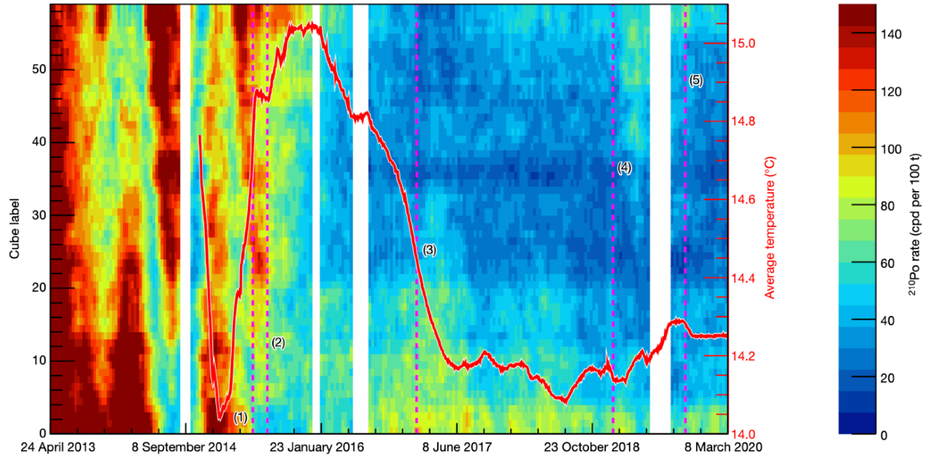

Experimental evidence of neutrinos produced in the CNO fusion cycle in the Sun
Nature **volume 587**, pages 577–582 (2020)

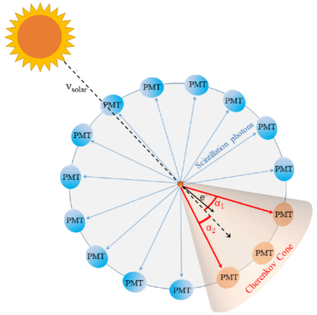

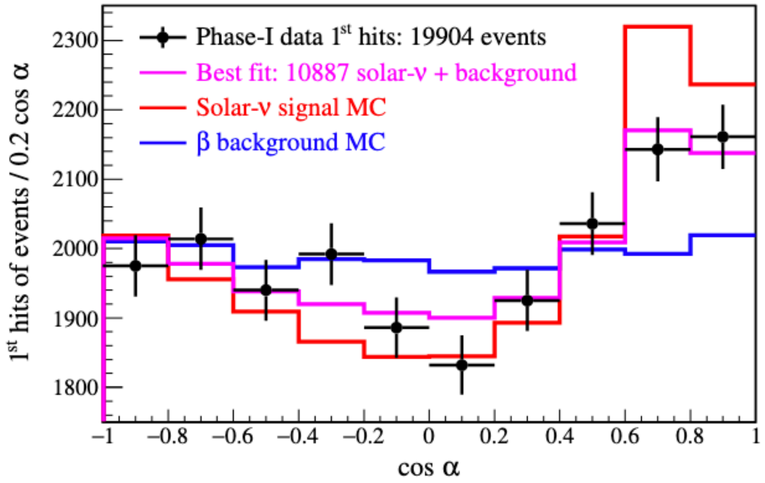

First Directional Measurement of Sub-MeV Solar Neutrinos with Borexino
Phys. Rev. Lett. **128**, 091803 – **Published 3 March, 2022**

Improved thermal stability allows Bi-Po tagging to map ^{210}Bi (5d) distribution from ^{210}Po

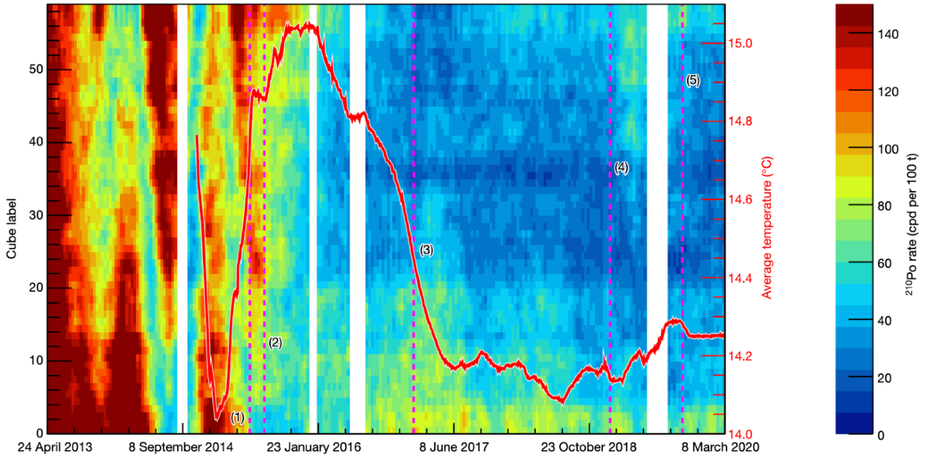

Experimental evidence of neutrinos produced in the CNO fusion cycle in the Sun

Nature **volume 587**, pages 577–582 (2020)

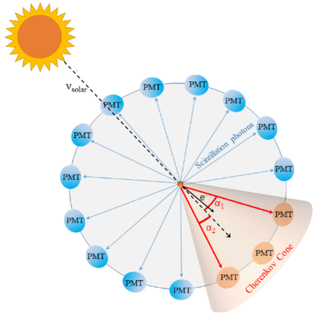

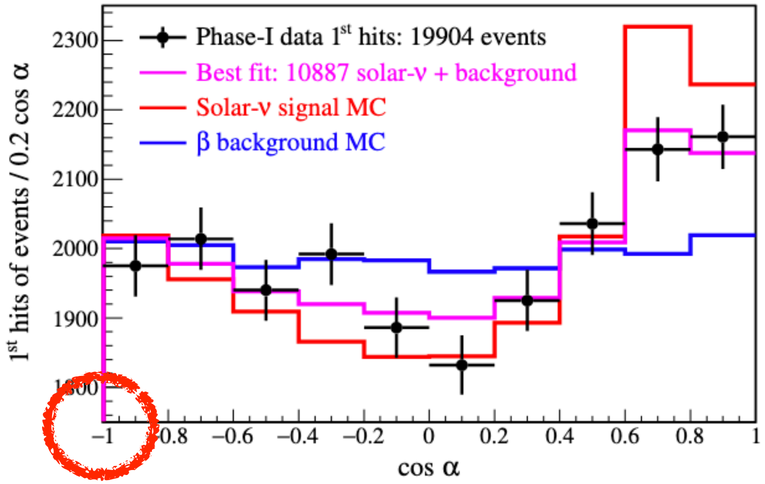

First Directional Measurement of Sub-MeV Solar Neutrinos with Borexino

Phys. Rev. Lett. **128**, 091803 – **Published 3 March, 2022**

Improved thermal stability allows Bi-Po tagging to map ^{210}Bi (5d) distribution from ^{210}Po

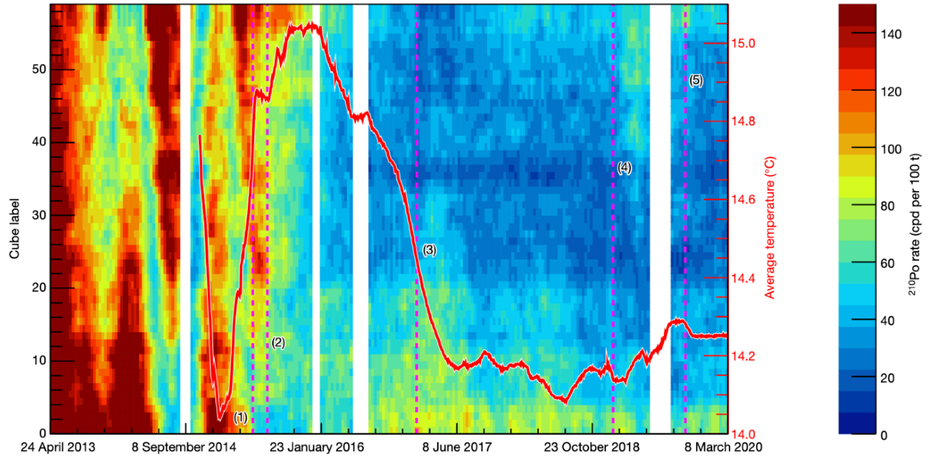

Experimental evidence of neutrinos produced in the CNO fusion cycle in the Sun
Nature **volume 587**, pages 577–582 (2020)

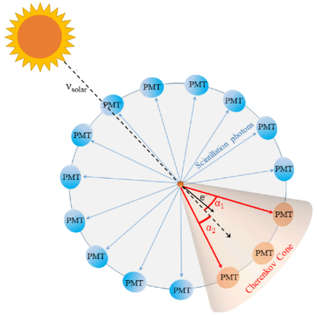

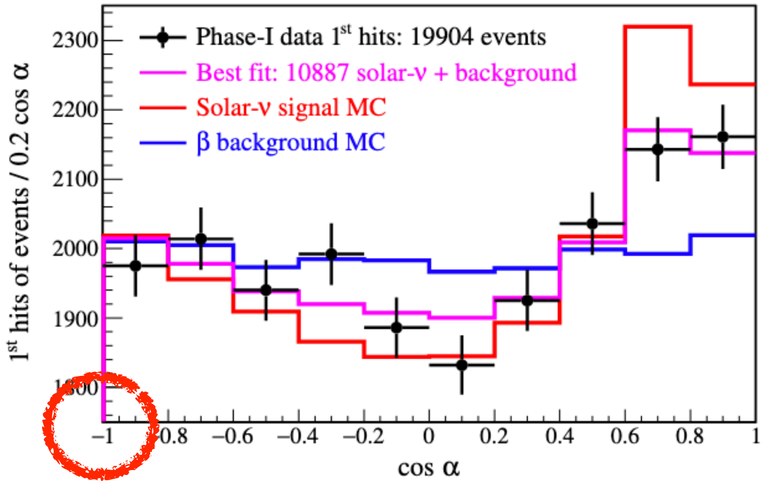

First Directional Measurement of Sub-MeV Solar Neutrinos with Borexino
Phys. Rev. Lett. **128**, 091803 – **Published 3 March, 2022**

Combined analysis, Phase-III dataset

2D multivariate analysis (energy and radial position) + **directionality** information

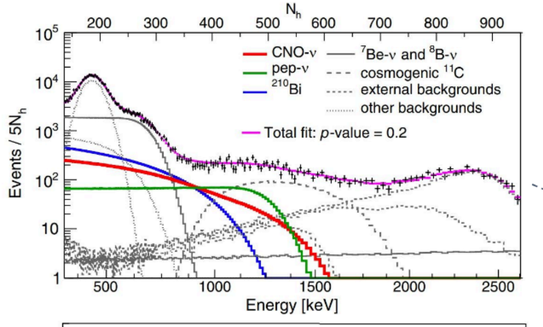

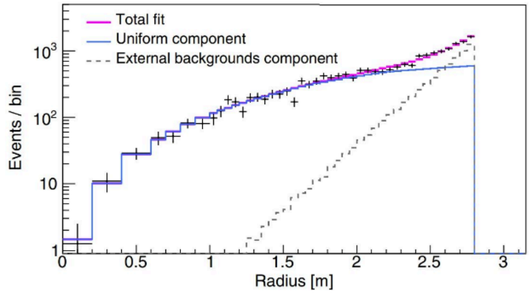

$$\mathcal{L}_{\mathrm{MV+CID}} = \underbrace{\mathcal{L}_{\mathrm{MV}}}_{\text{2D multivariate fit (energy + radius)}} \cdot \overbrace{\mathcal{L}_{\mathrm{pep}} \cdot \mathcal{L}_{^{210}\mathrm{Bi}} \cdot \underbrace{\mathcal{L}_{\mathrm{CID}}^{\mathrm{P-I}} \cdot \mathcal{L}_{\mathrm{CID}}^{\mathrm{P-II+III}}}_{\text{directionality constraints (new)}}}^{\text{independent constraints}}$$

pep ν 1.4% rate constraint (solar physics + flavor oscill.)

210Bi rate 10%. constraint (thermal insulation)

Davide Basilico (Milan), WIN 2025

Solar Composition Question:

high metallicity (HZ) → agreement with helioseismology low metallicity (LZ) → observed from solar photosphere

Solar Composition Question:

high metallicity (HZ) → agreement with helioseismology low metallicity (LZ) → observed from solar photosphere

LZ disfavoured by 3.2σ

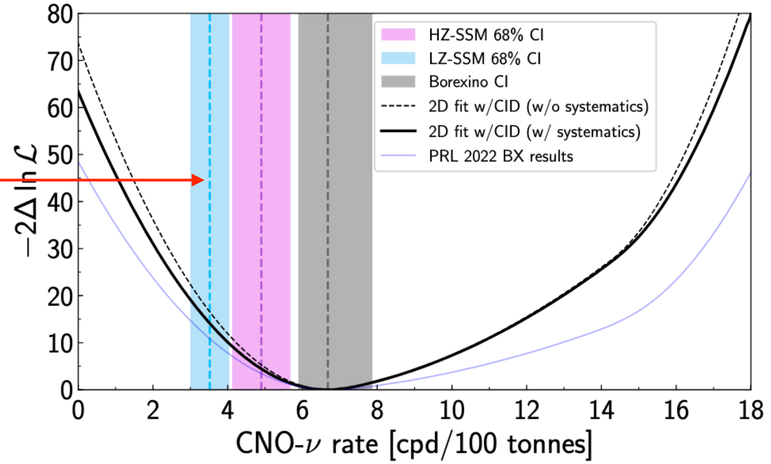

Solar Composition Question:

high metallicity (HZ) → agreement with helioseismology low metallicity (LZ) → observed from solar photosphere

LZ disfavoured by 3.2σ

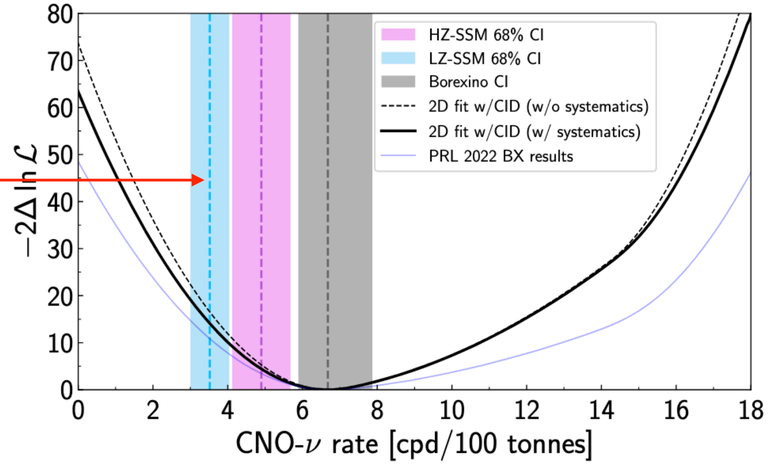

However…

	FIT	B23-SSM	FULL			Be+B+CNO			CNO		
	CNO-Rfixed		n=6			n=3			n=1		
			$\Delta\chi^2$	p_{GF}	CL [σ]	$\Delta\chi^2$	p_{GF}	CL [σ]	$\Delta\chi^2$	p_{GF}	CL [σ]
Low Z		AGSS09-met	14.5	0.024	2.3	9.8	0.020	2.3	7.2	0.0073	2.7
High Z		GS98	8.1	0.24	1.2	3.0	0.39	0.86	2.4	0.12	1.5
Low Z		AAG21	12.5	0.052	1.9	7.8	0.05	2.0	6.2	0.013	2.5
High Z		MB22-met/phot	7.1	0.31	1.0	2.2	0.53	0.62	2.0	0.16	1.4
	CNO-Rbound		n=8			n=5			n=3		
			$\Delta\chi^2$	p_{GF}	CL [σ]	$\Delta\chi^2$	p_{GF}	CL [σ]	$\Delta\chi^2$	p_{GF}	CL [σ]
Low Z		AGSS09-met	14.1	0.079	1.8	9.3	0.098	1.7	7.2	0.066	1.8
High Z		GS98	6.7	0.57	0.57	1.7	0.88	0.14	1.6	0.66	0.44
Low Z		AAG21	11.7	0.16	1.4	6.8	0.24	1.2	5.7	0.13	1.5
High Z		MB22-met/phot	5.9	0.66	0.44	1.1	0.95	0.06	1.0	0.80	0.25

Status of direct determination of solar neutrino fluxes after Borexino
M. C. Gonzalez-Garcia et al., JHEP02 (2024) 064

Solar Composition Question:

high metallicity (HZ) → agreement with helioseismology low metallicity (LZ) → observed from solar photosphere

LZ disfavoured by 3.2σ

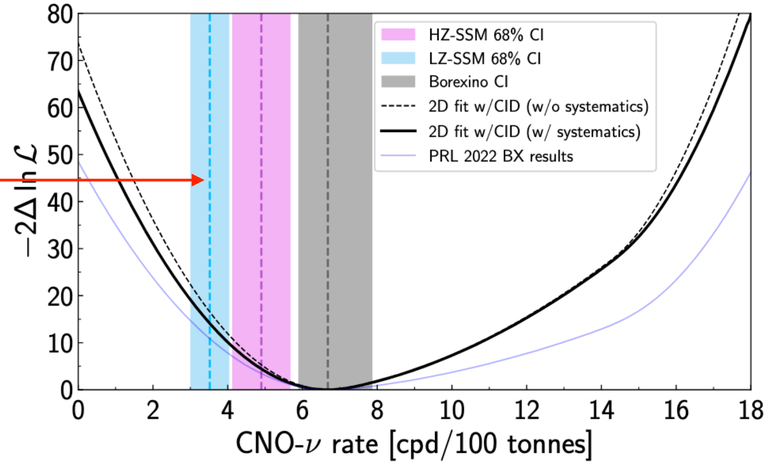

Question remains open!

However…

	FIT	B23-SSM	FULL			Be+B+CNO			CNO		
	CNO-Rfixed		n=6			n=3			n=1		
			$\Delta\chi^2$	p_{GF}	CL [σ]	$\Delta\chi^2$	p_{GF}	CL [σ]	$\Delta\chi^2$	p_{GF}	CL [σ]
Low Z		AGSS09-met	14.5	0.024	2.3	9.8	0.020	2.3	7.2	0.0073	2.7
High Z		GS98	8.1	0.24	1.2	3.0	0.39	0.86	2.4	0.12	1.5
Low Z		AAG21	12.5	0.052	1.9	7.8	0.05	2.0	6.2	0.013	2.5
High Z		MB22-met/phot	7.1	0.31	1.0	2.2	0.53	0.62	2.0	0.16	1.4
	CNO-Rbound		n=8			n=5			n=3		
			$\Delta\chi^2$	p_{GF}	CL [σ]	$\Delta\chi^2$	p_{GF}	CL [σ]	$\Delta\chi^2$	p_{GF}	CL [σ]
Low Z		AGSS09-met	14.1	0.079	1.8	9.3	0.098	1.7	7.2	0.066	1.8
High Z		GS98	6.7	0.57	0.57	1.7	0.88	0.14	1.6	0.66	0.44
Low Z		AAG21	11.7	0.16	1.4	6.8	0.24	1.2	5.7	0.13	1.5
High Z		MB22-met/phot	5.9	0.66	0.44	1.1	0.95	0.06	1.0	0.80	0.25

Status of direct determination of solar neutrino fluxes after Borexino
M. C. Gonzalez-Garcia et al., JHEP02 (2024) 064


8B

Solar neutrino measurements using the full data period of Super-Kamiokande-IV

Phys. Rev. D 109, 092001 (2024)

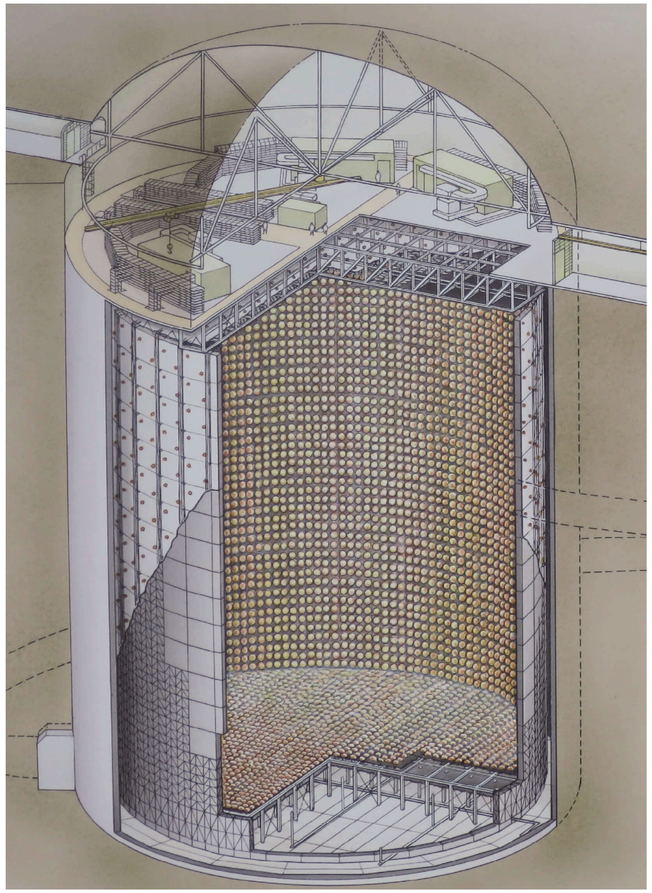

Phase	SK-I	SK-II	SK-III	SK-IV
Period (Start)	Apr. '96	Oct. '02	Jul. '06	Sep. '08
Period (End)	Jul. '01	Oct. '05	Aug. '08	May '18
Livetime [days]	1,496	791	548	2,970
ID PMTs	11,146	5,182	11,129	11,129
OD PMTs	1,885	1,885	1,885	1,885
PMT coverage [%]	40	19	40	40
Energy thr. [MeV]	4.49	6.49	3.99	3.49

^{8}B

Solar neutrino measurements using the full data period of Super-Kamiokande-IV

Phys. Rev. D 109, 092001 (2024)

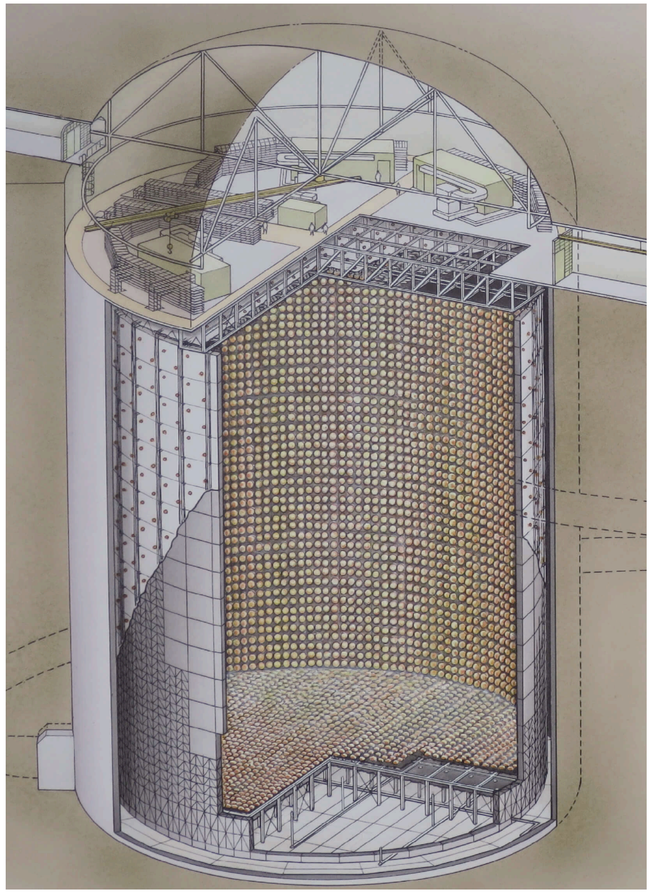

Phase	SK-I	SK-II	SK-III	SK-IV
Period (Start)	Apr. '96	Oct. '02	Jul. '06	Sep. '08
Period (End)	Jul. '01	Oct. '05	Aug. '08	May '18
Livetime [days]	1,496	791	548	2,970
ID PMTs	11,146	5,182	11,129	11,129
OD PMTs	1,885	1,885	1,885	1,885
PMT coverage [%]	40	19	40	40
Energy thr. [MeV]	4.49	6.49	3.99	3.49

^{8}B

Best fit oscillation parameters from SK-IV

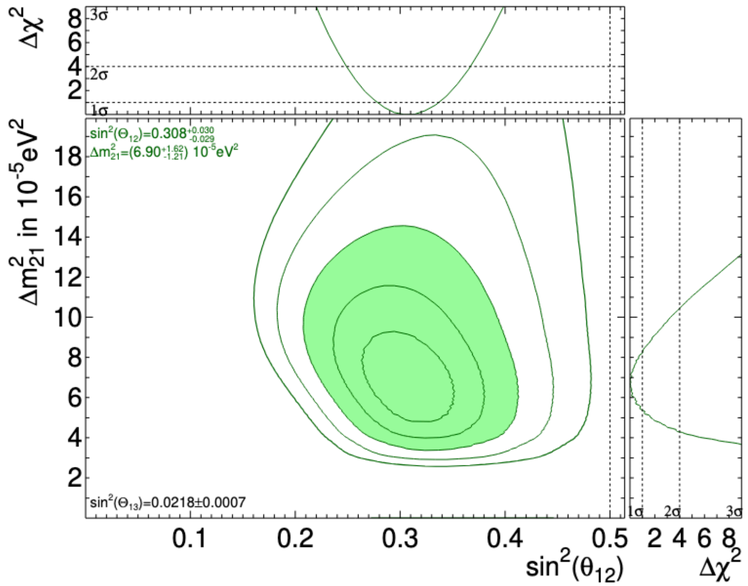

Combined SK I-IV and with SNO (dotted) compared with KamLAND (blue)

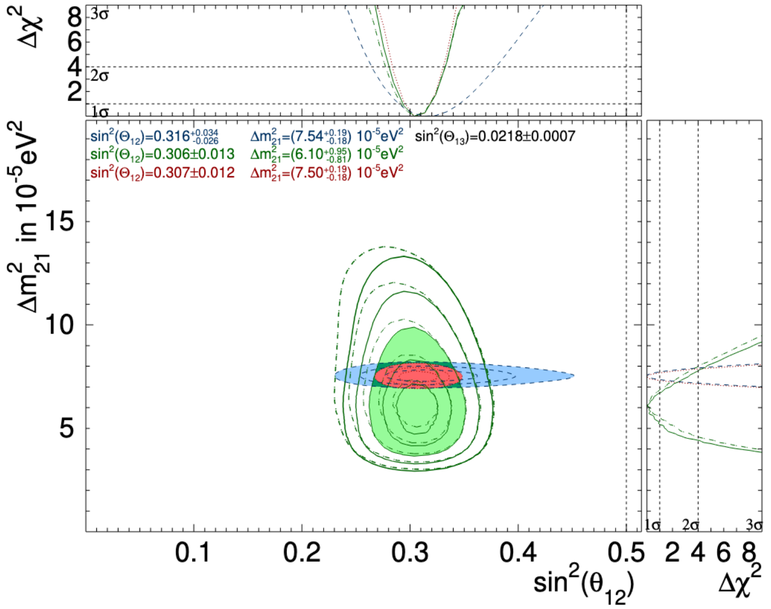

Solar neutrino measurements using the full data period of Super-Kamiokande-IV

Phys. Rev. D 109, 092001 (2024)

^{8}B

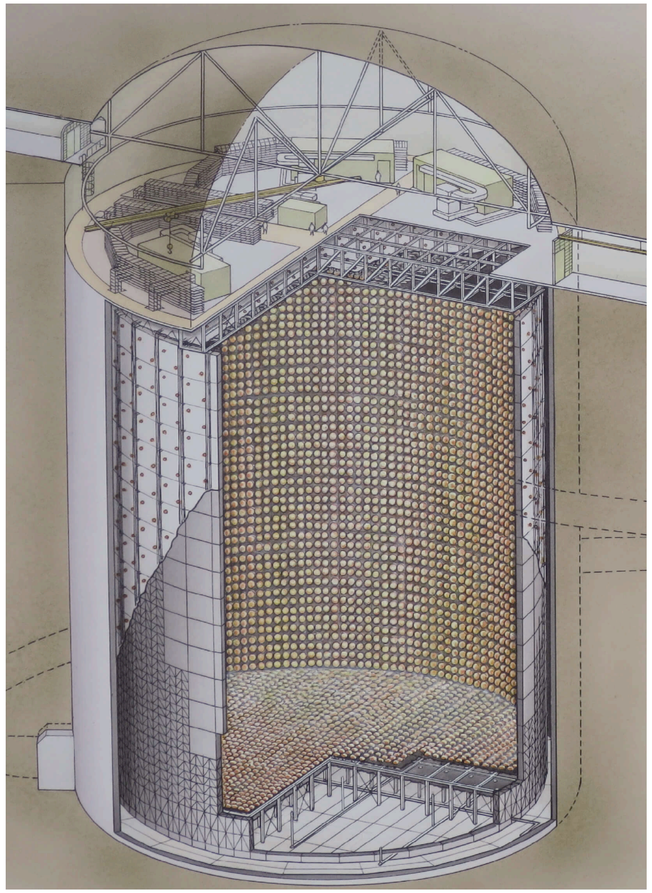

Phase	SK-I	SK-II	SK-III	SK-IV
Period (Start)	Apr. '96	Oct. '02	Jul. '06	Sep. '08
Period (End)	Jul. '01	Oct. '05	Aug. '08	May '18
Livetime [days]	1,496	791	548	2,970
ID PMTs	11,146	5,182	11,129	11,129
OD PMTs	1,885	1,885	1,885	1,885
PMT coverage [%]	40	19	40	40
Energy thr. [MeV]	4.49	6.49	3.99	3.49

Best fit oscillation parameters from SK-IV

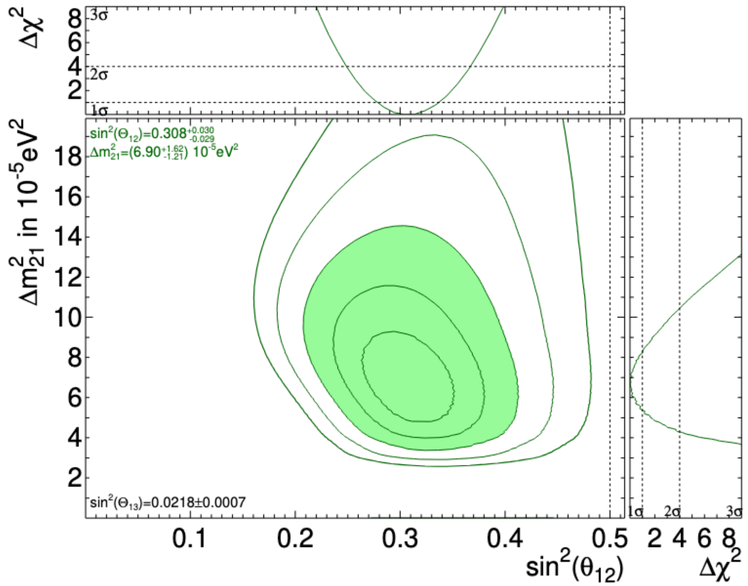

Combined SK I-IV and with SNO (dotted) compared with KamLAND (blue)

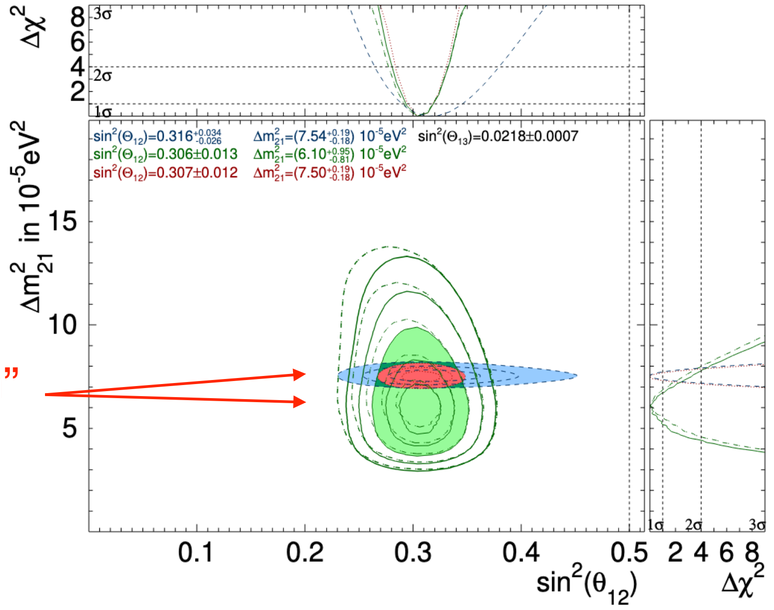

1.5σ "tension"

Solar neutrino measurements using the full data period of Super-Kamiokande-IV
Phys. Rev. D 109, 092001 (2024)

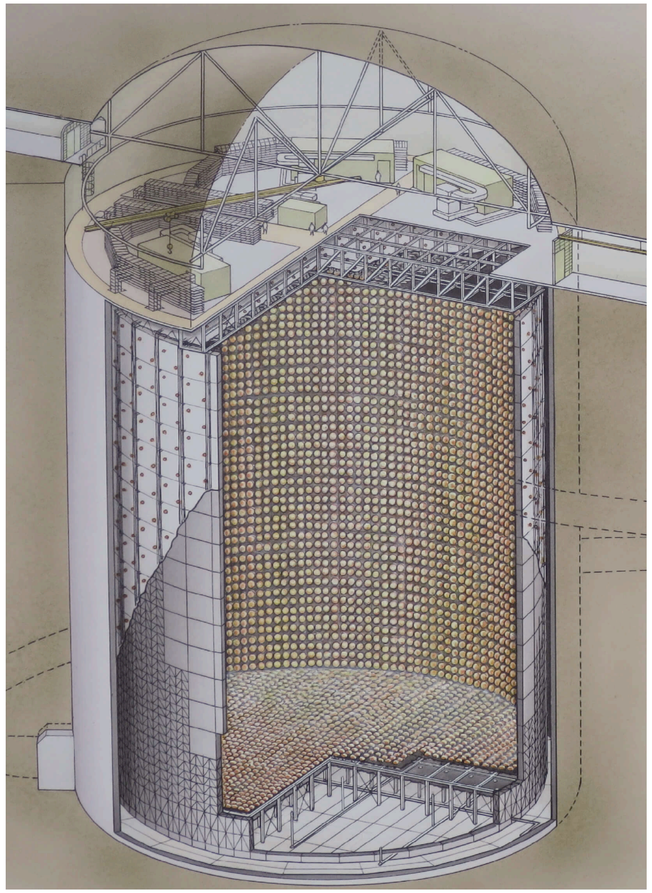

Phase	SK-I	SK-II	SK-III	SK-IV
Period (Start)	Apr. '96	Oct. '02	Jul. '06	Sep. '08
Period (End)	Jul. '01	Oct. '05	Aug. '08	May '18
Livetime [days]	1,496	791	548	2,970
ID PMTs	11,146	5,182	11,129	11,129
OD PMTs	1,885	1,885	1,885	1,885
PMT coverage [%]	40	19	40	40
Energy thr. [MeV]	4.49	6.49	3.99	3.49

^{8}B

tension - noun (ten· sion ˈten(t)-shən'): Perfectly consistent.

Best fit oscillation parameters from SK-IV

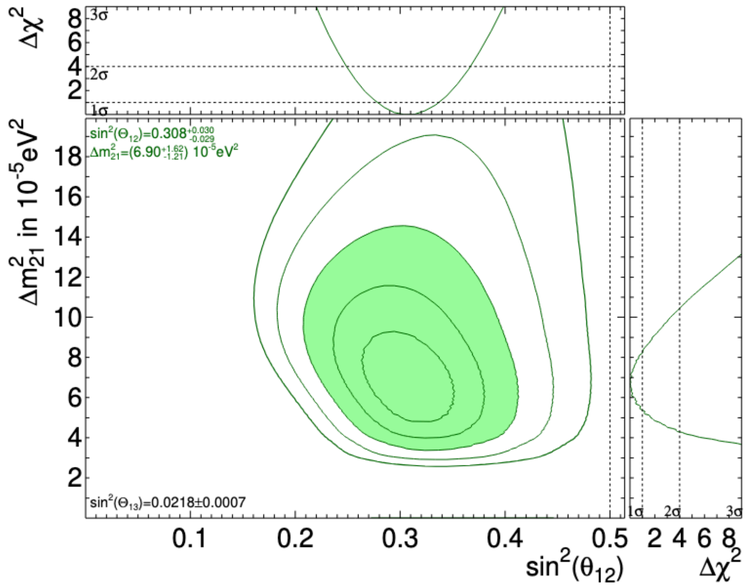

Combined SK I-IV and with SNO (dotted) compared with KamLAND (blue)

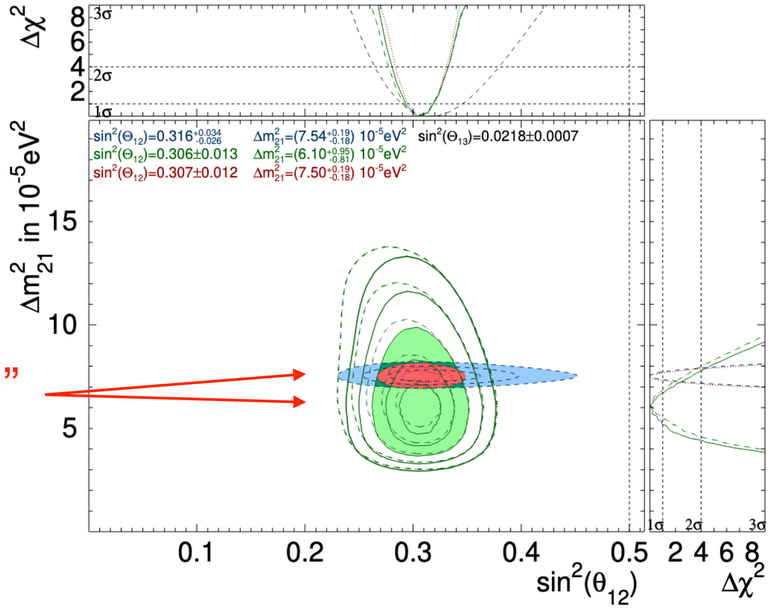

1.5σ "tension"

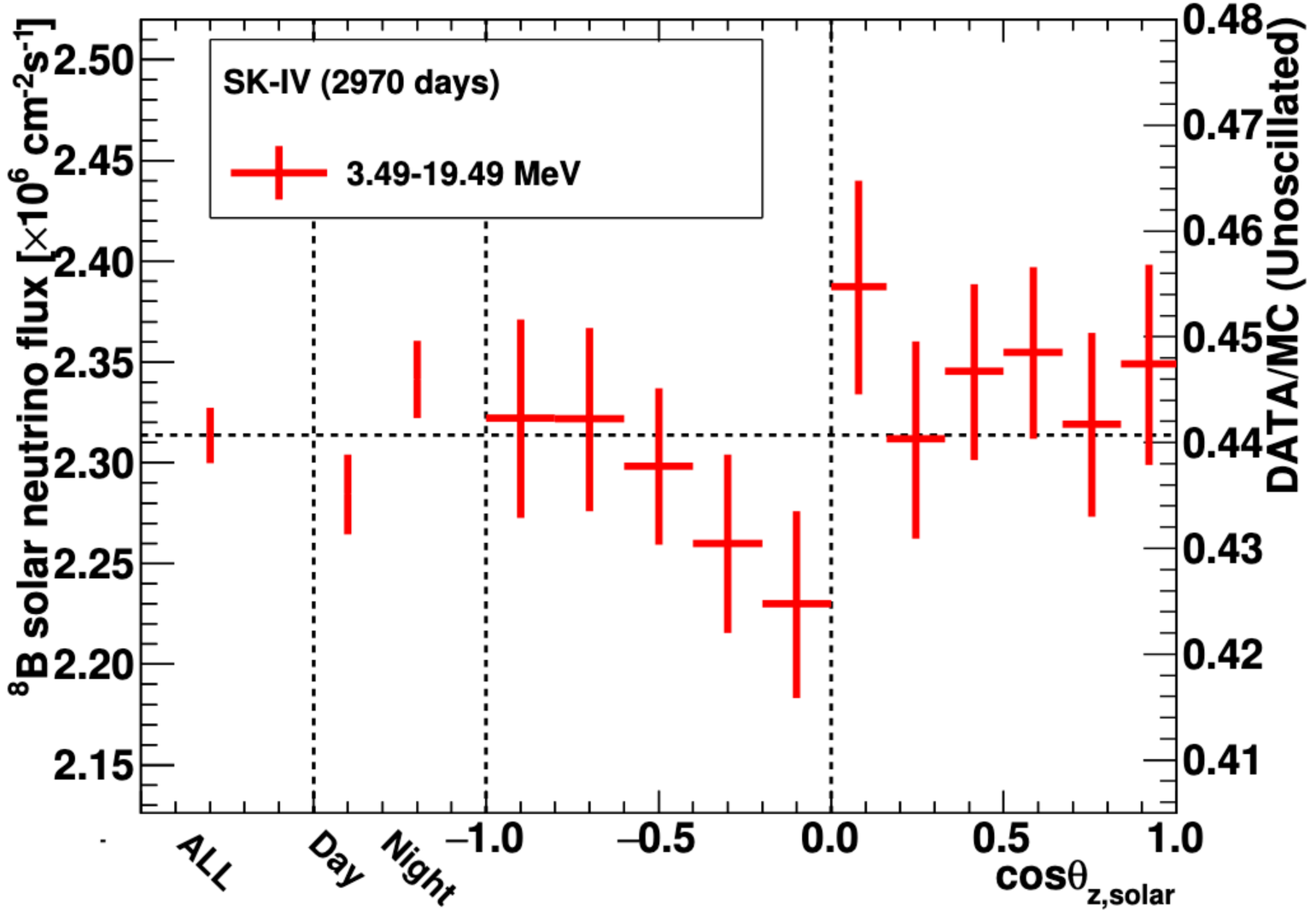

SK IV: $A_{\mathrm{D/N}}^{\mathrm{SK-IV,fit}} = -0.0262 \pm 0.0107(\mathrm{stat.}) \pm 0.0030(\mathrm{syst})$

SK I-IV: $A_{\mathrm{D/N}}^{\mathrm{SK,fit}} = -0.0286 \pm 0.0085(\mathrm{stat.}) \pm 0.0032(\mathrm{syst})$ ⟶ 3.36σ

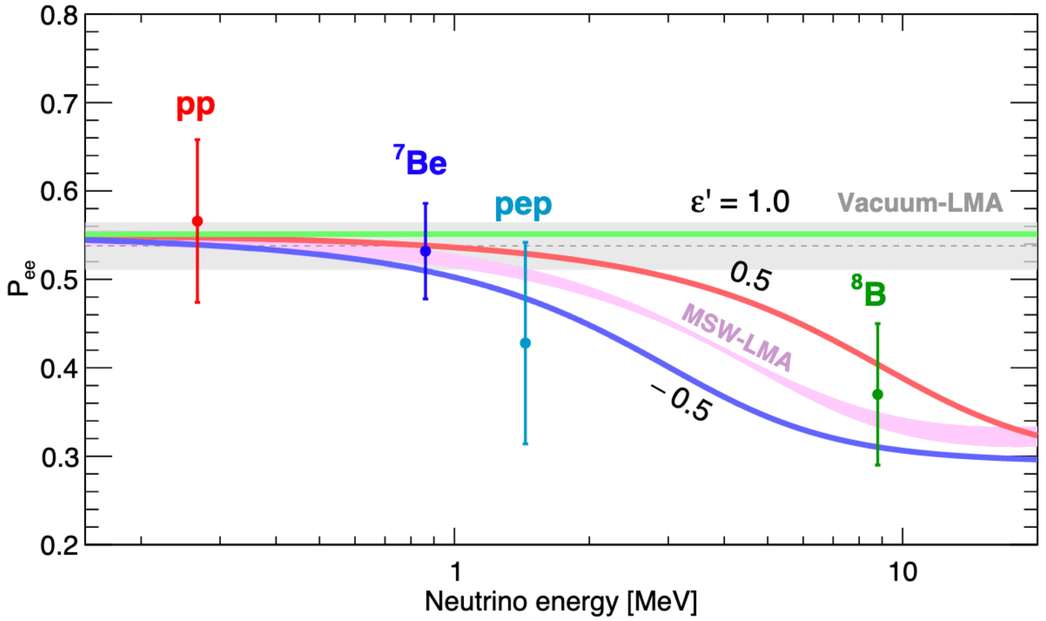

Constraints on Flavor-Diagonal Non-Standard Neutrino Interactions from Borexino Phase-II
JHEP 2002 (2020) 038

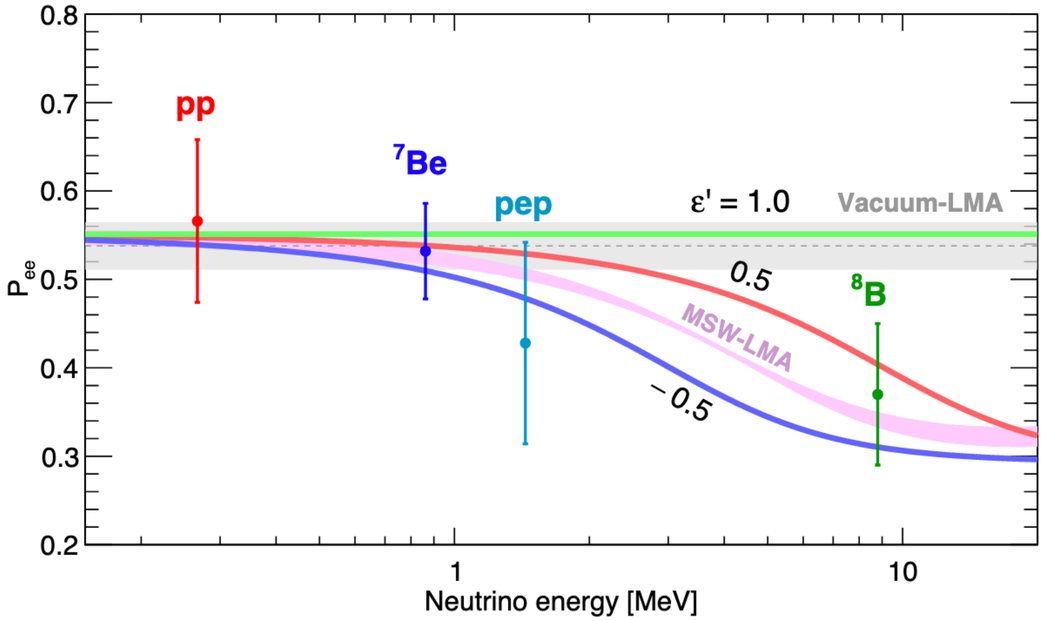

Constraints on Flavor-Diagonal Non-Standard Neutrino Interactions from Borexino Phase-II
JHEP 2002 (2020) 038

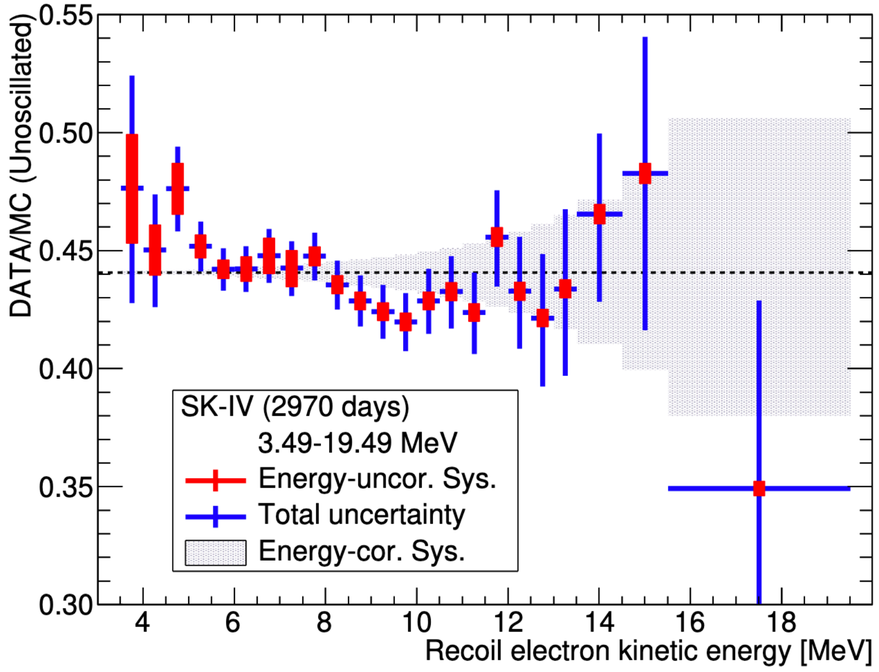

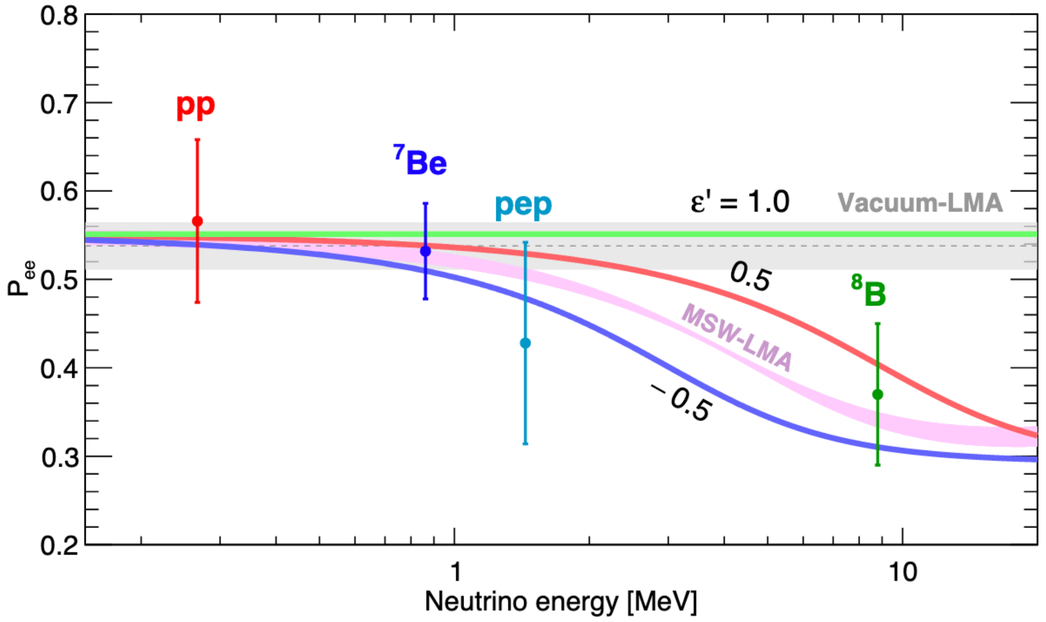

Constraints on Flavor-Diagonal Non-Standard Neutrino Interactions from Borexino Phase-II
JHEP 2002 (2020) 038

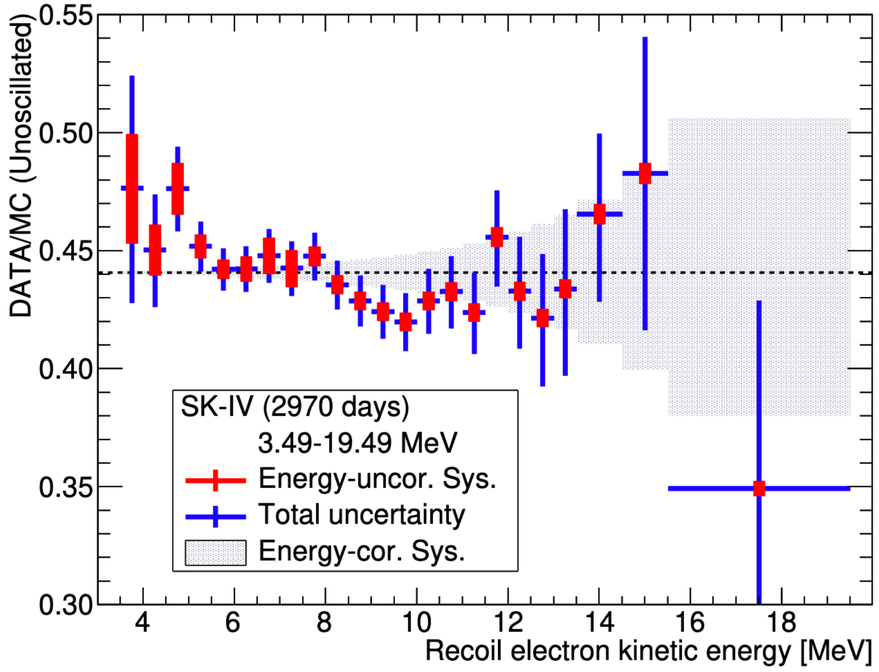

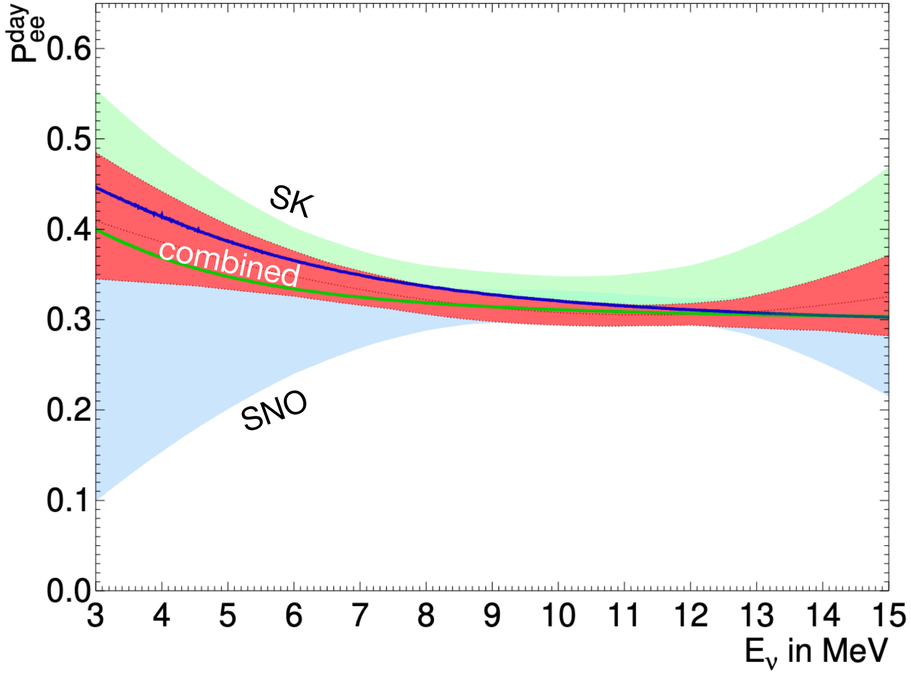

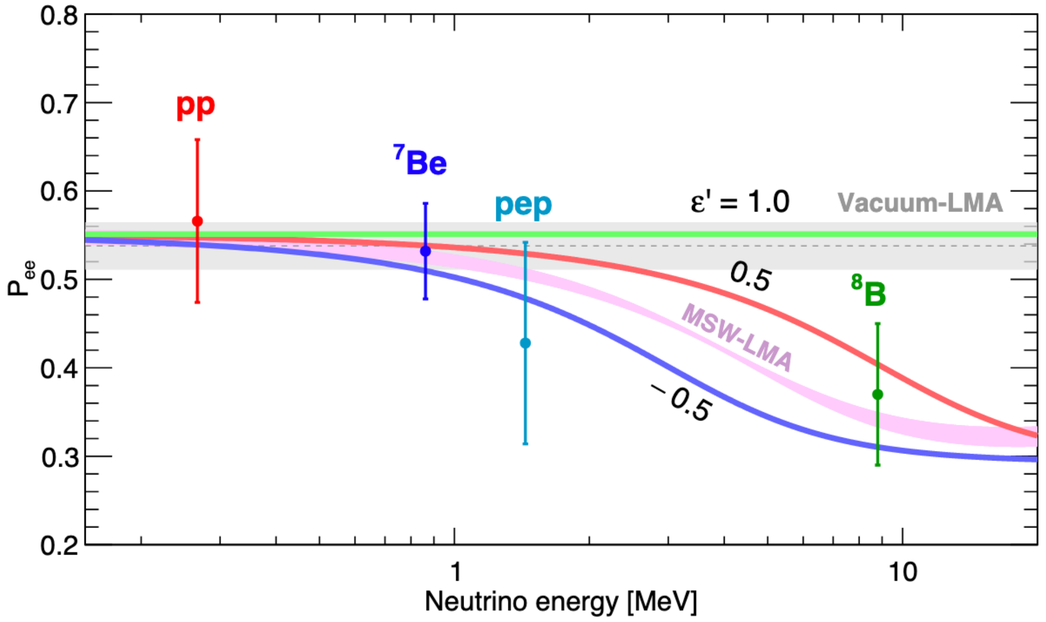

Constraints on Flavor-Diagonal Non-Standard Neutrino Interactions from Borexino Phase-II
JHEP 2002 (2020) 038

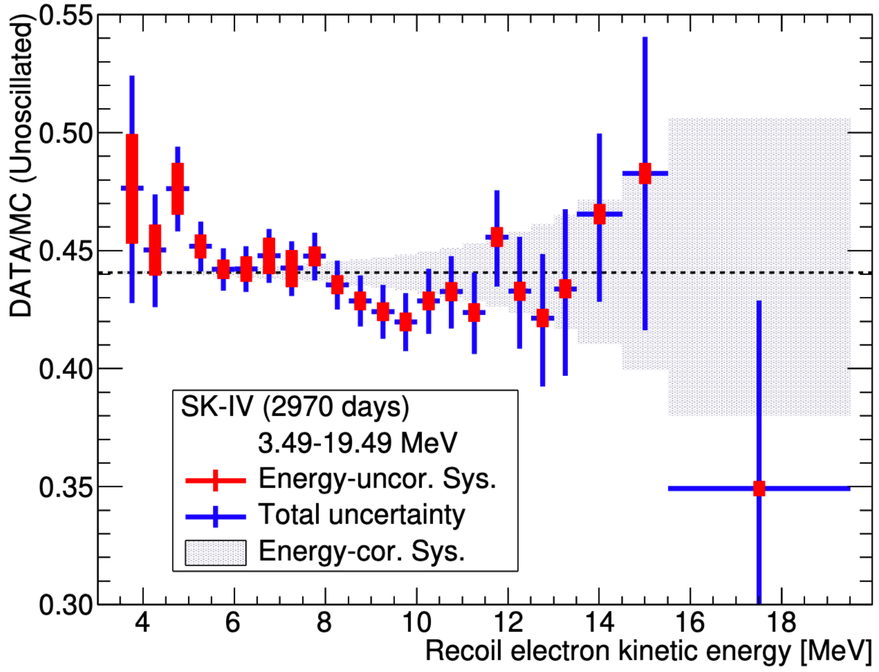

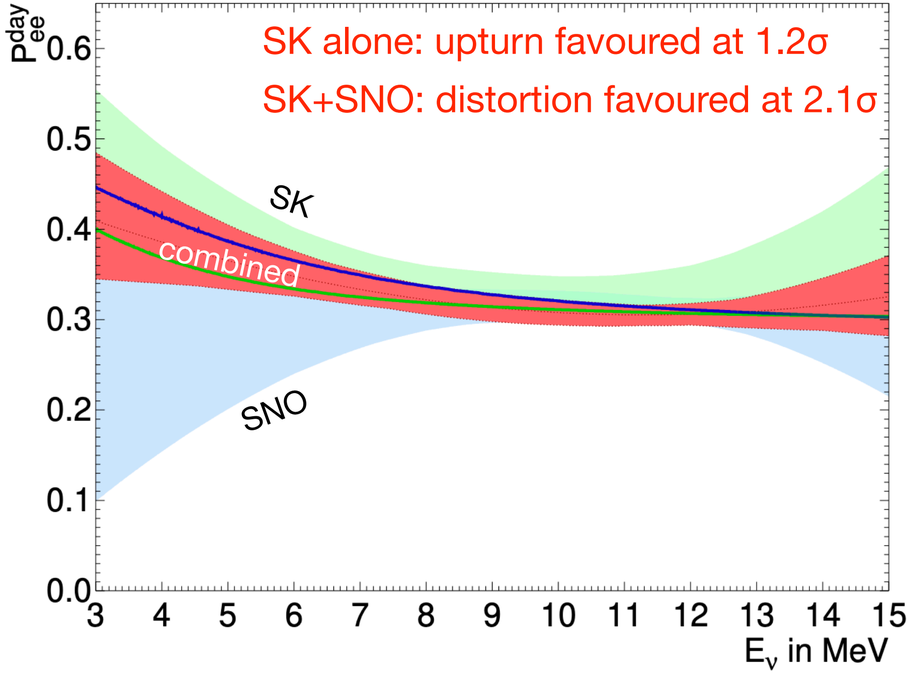

Question remains open!

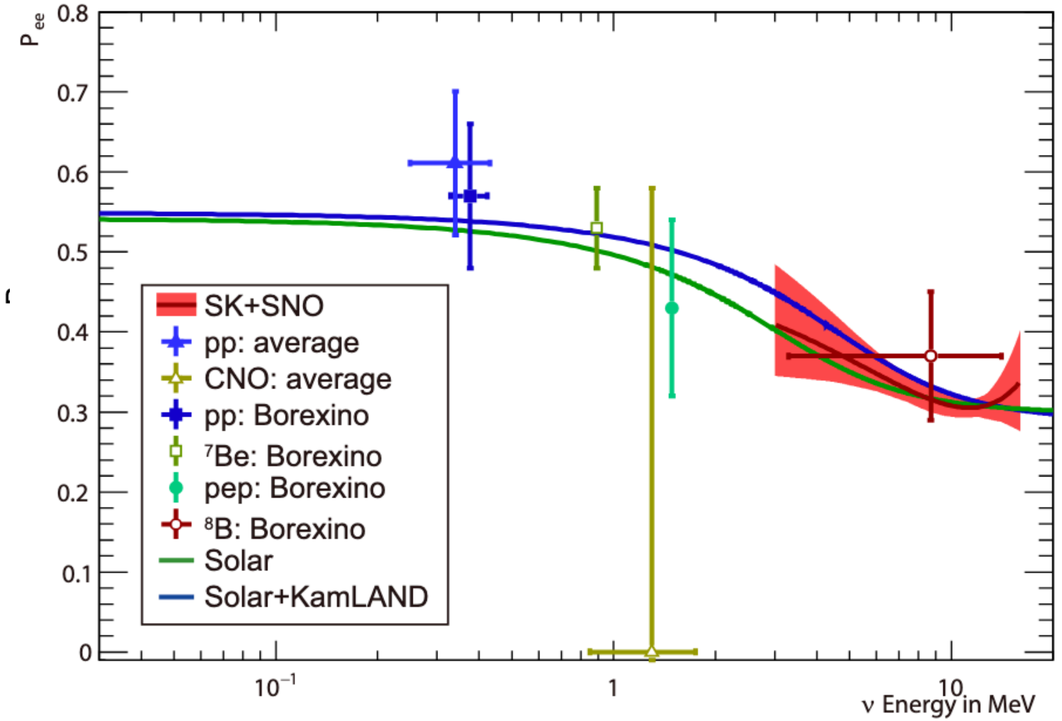

Constraints on Flavor-Diagonal Non-Standard Neutrino Interactions from Borexino Phase-II
JHEP 2002 (2020) 038

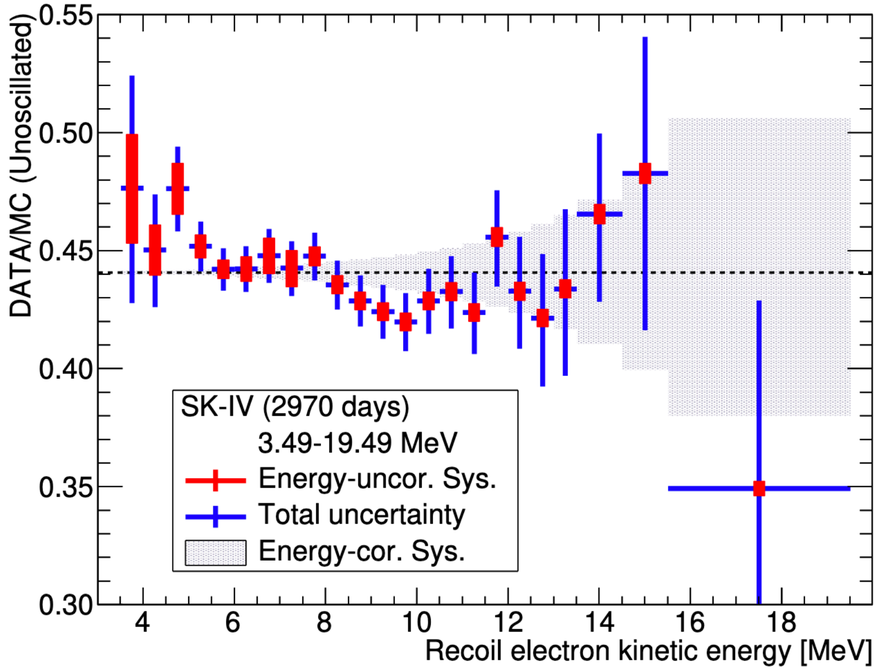

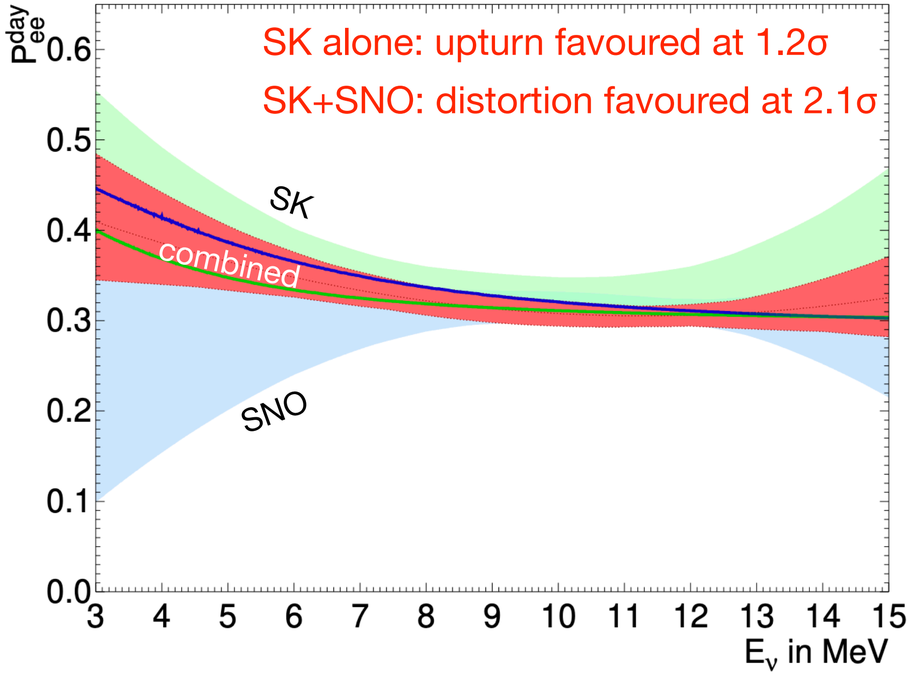

Potentially new information in the pipeline:

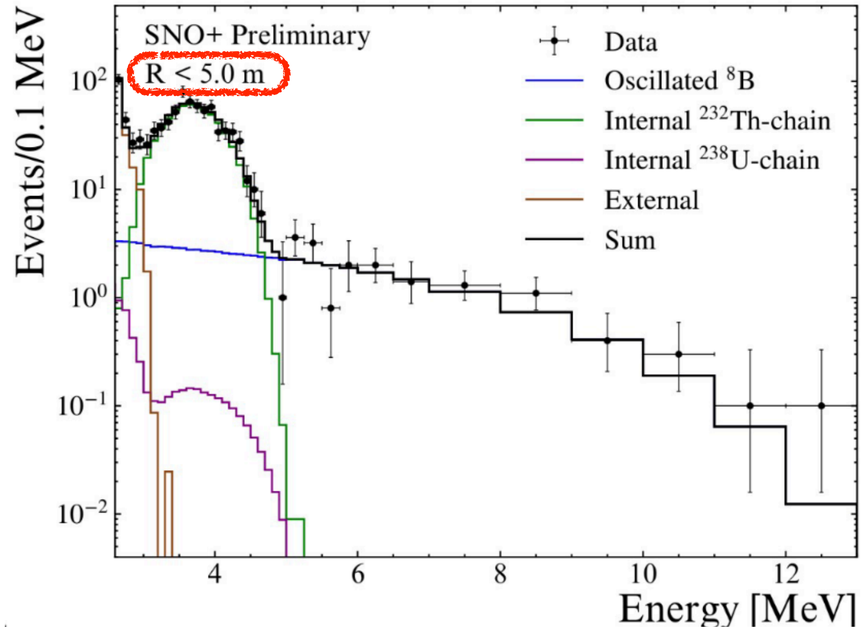

Potentially new information in the pipeline:

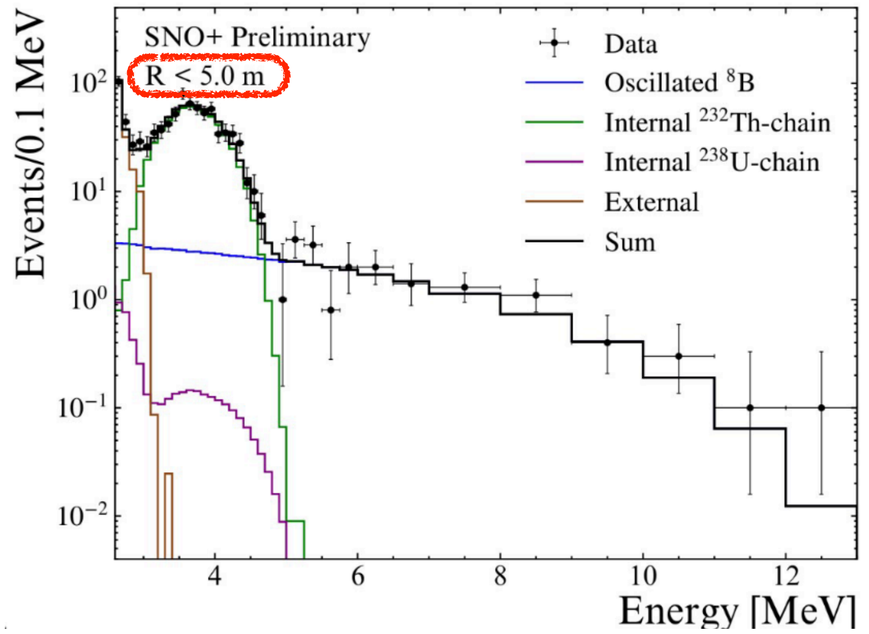

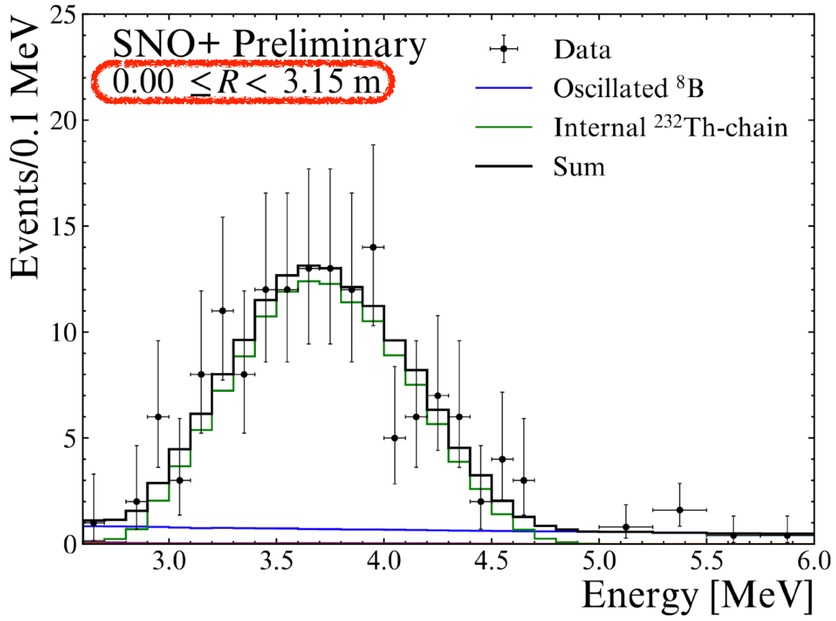

Potentially new information in the pipeline:

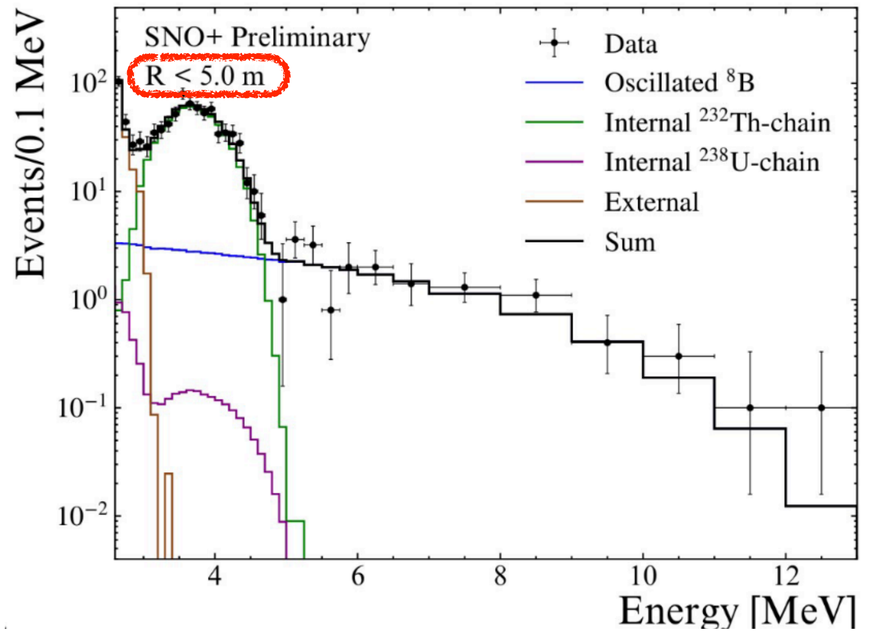

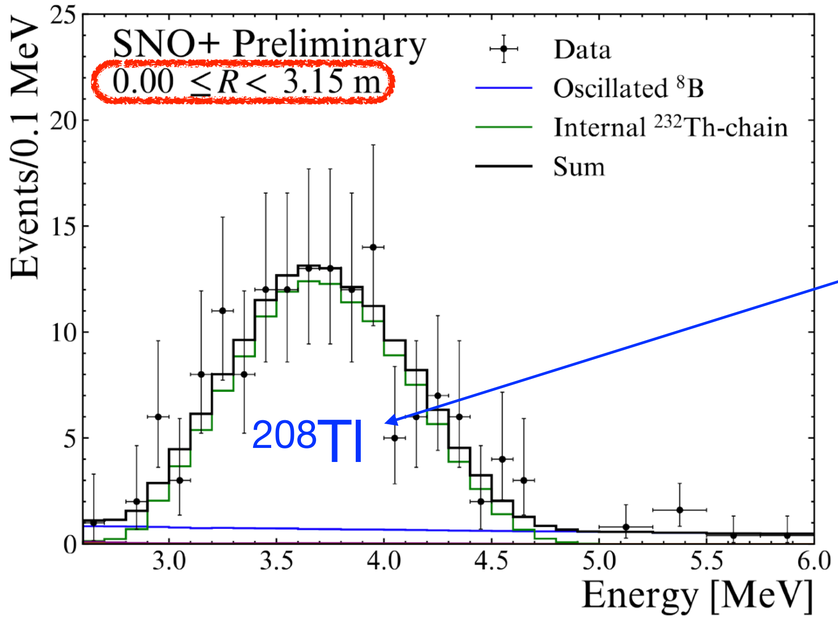

Can be reduced via tagging and multi-site discrimination methods

Potentially new information in the pipeline:

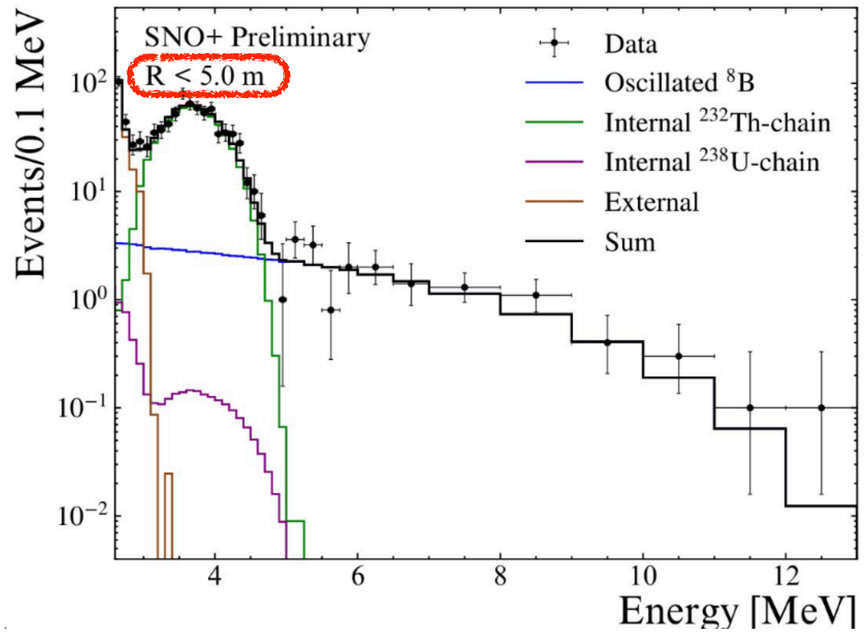

Aiming for low-energy measurement in the 2-3 MeV region

(currently under study for 0νββ background characterisation)

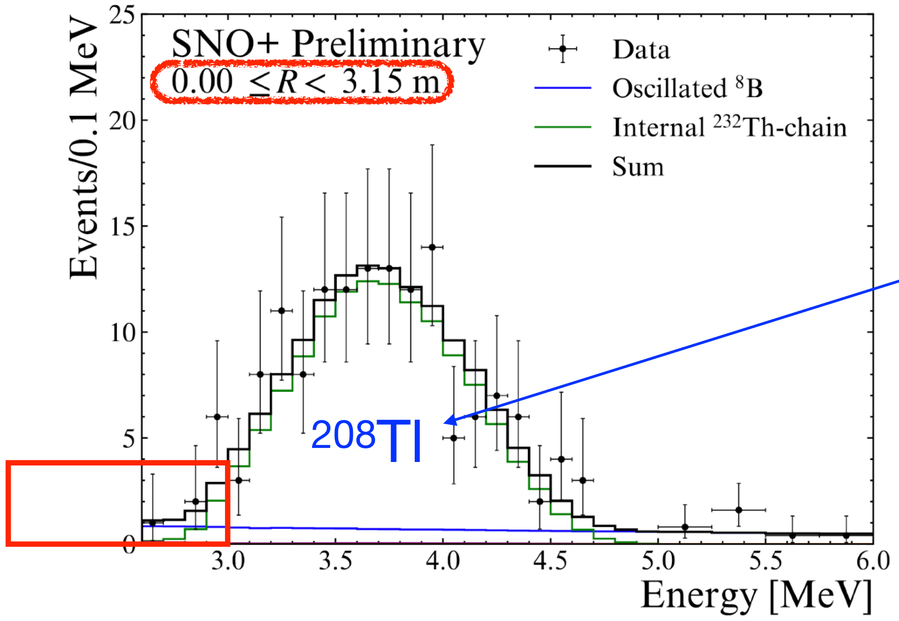

Can be reduced via tagging and multi-site discrimination methods

Event-by-event direction reconstruction of solar neutrinos in a high light-yield liquid scintillator

Phys. Rev. D **109**, 072002 – **Published 3 April, 2024**

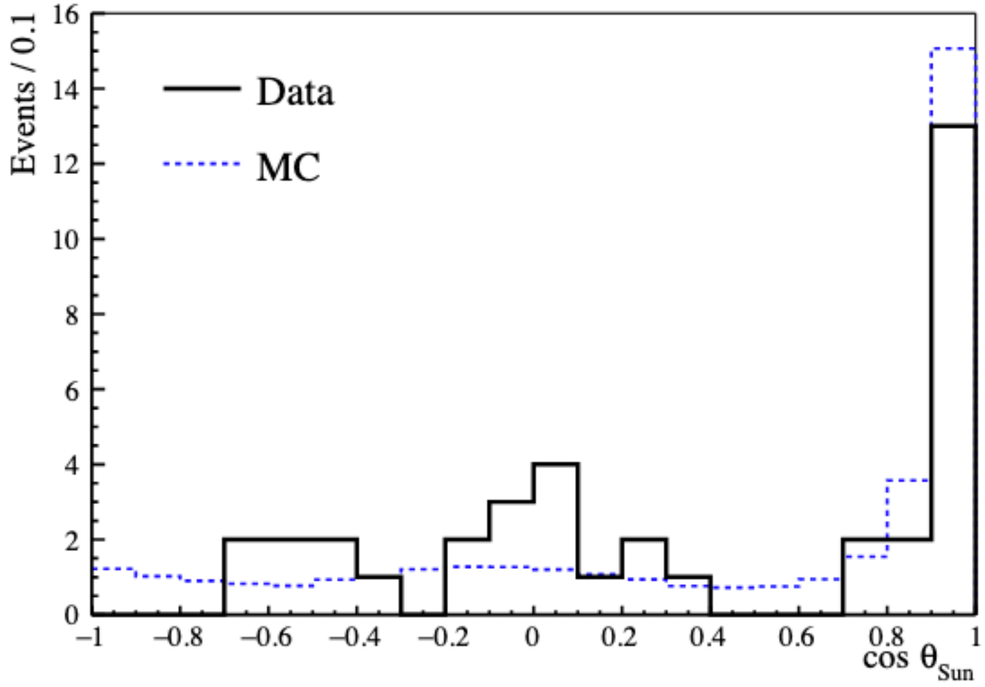

Cherenkov peak
at earlier times

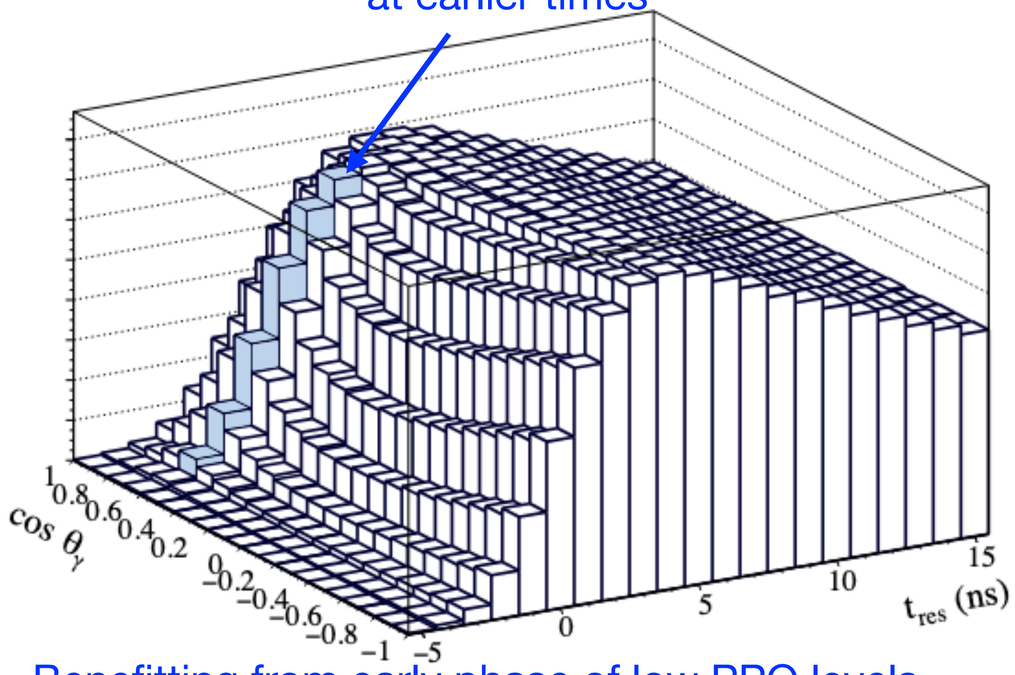

Benefitting from early phase of low PPO levels,
leading to increased flourescence decay time (~10ns)

Event-by-event direction reconstruction of solar neutrinos in a high light-yield liquid scintillator

Phys. Rev. D **109**, 072002 – **Published 3 April, 2024**

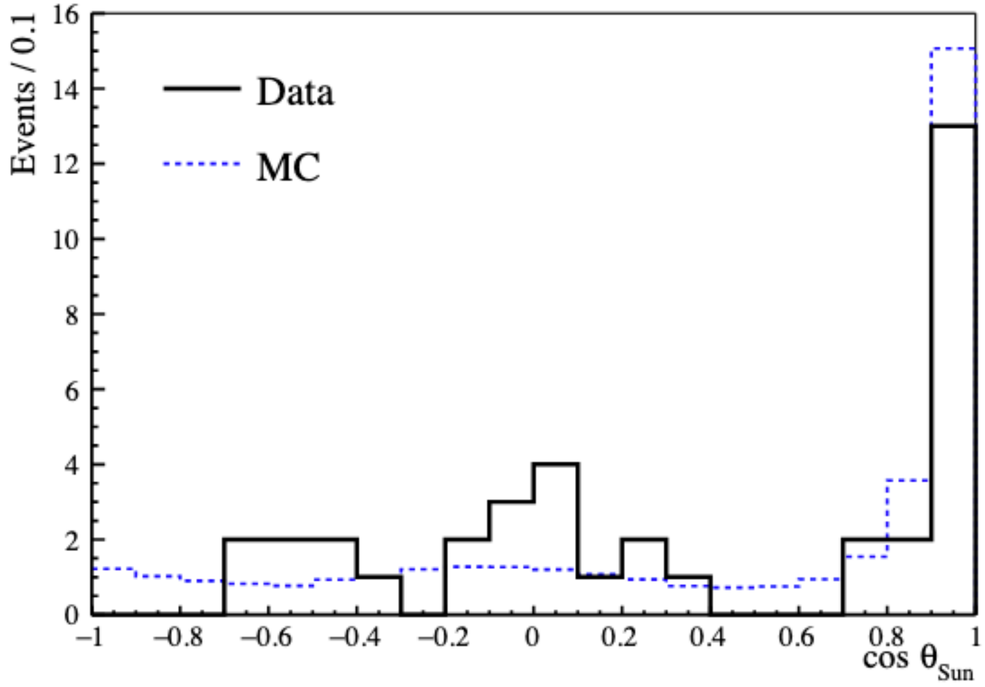

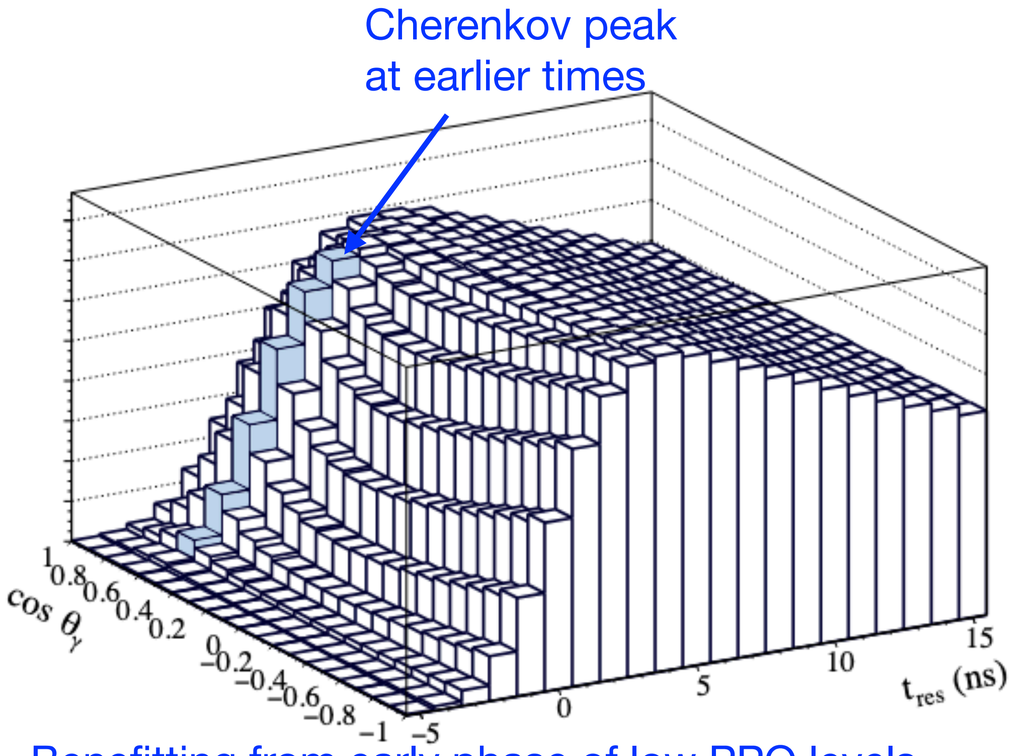

Benefitting from early phase of low PPO levels, leading to increased flourescence decay time (~10ns)

However, we also see some directionality in our current data and JUNO ought to be able to take some advantage of this with their subset of fast Hamamatsu PMTs and higher statistics

New Result:

First First Observation of Solar Neutrino Interactions on ^{13}C

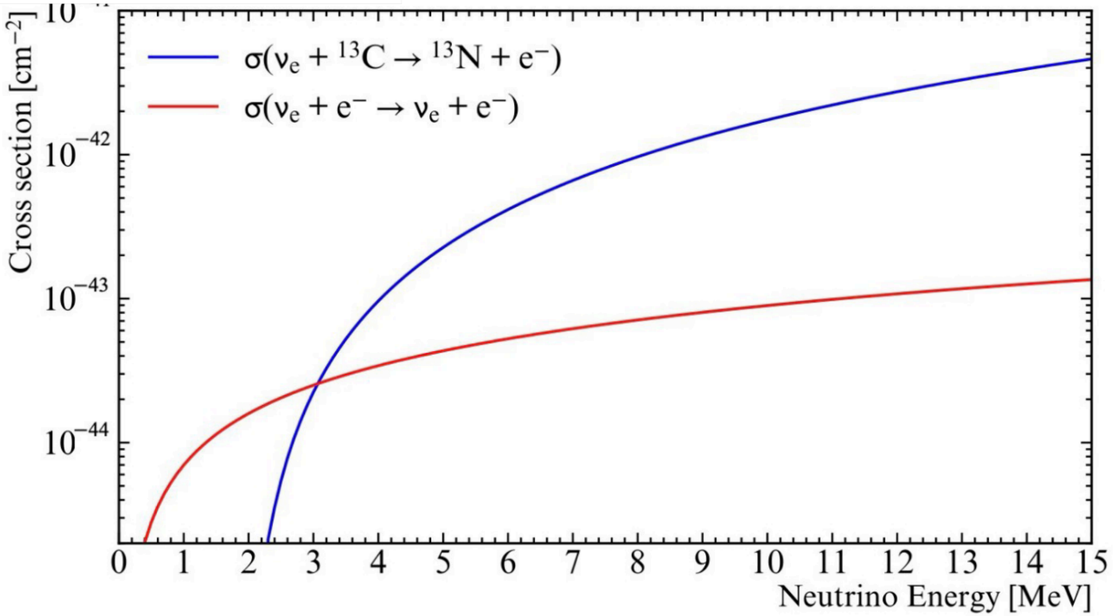

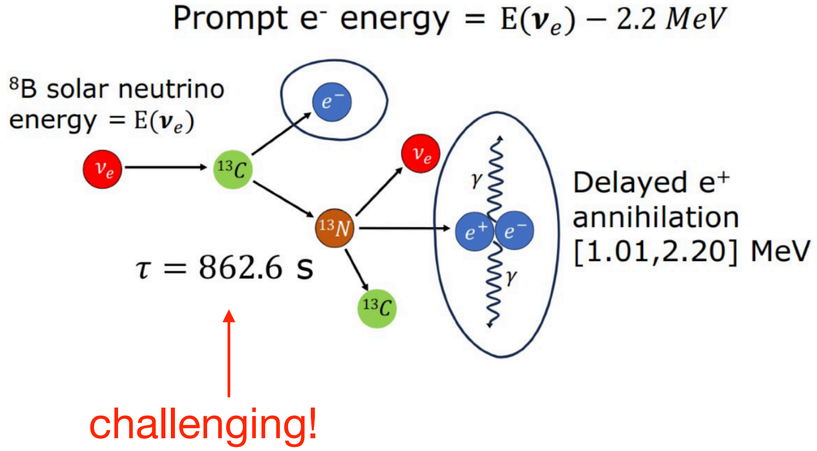

challenging!

New Result:

First First Observation of Solar Neutrino Interactions on ^{13}C

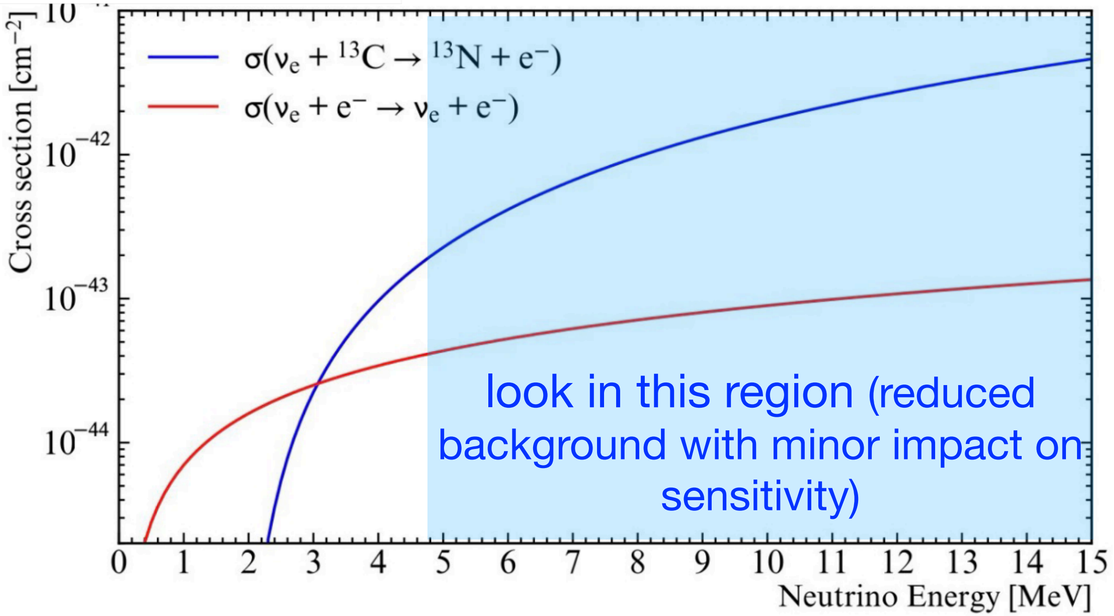

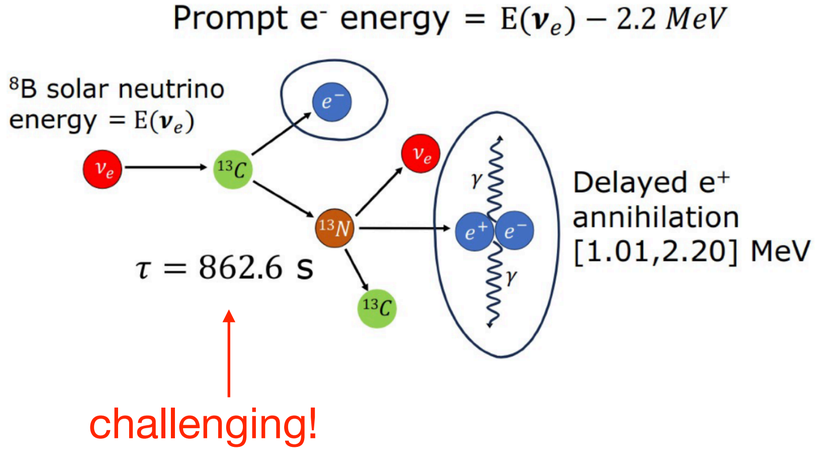

Depth of SNOLAB was critical to reduce muon-induced backgrounds (*e.g.* ^{11}C) to negligible levels.

New Result:

First First Observation of Solar Neutrino Interactions on ^{13}C

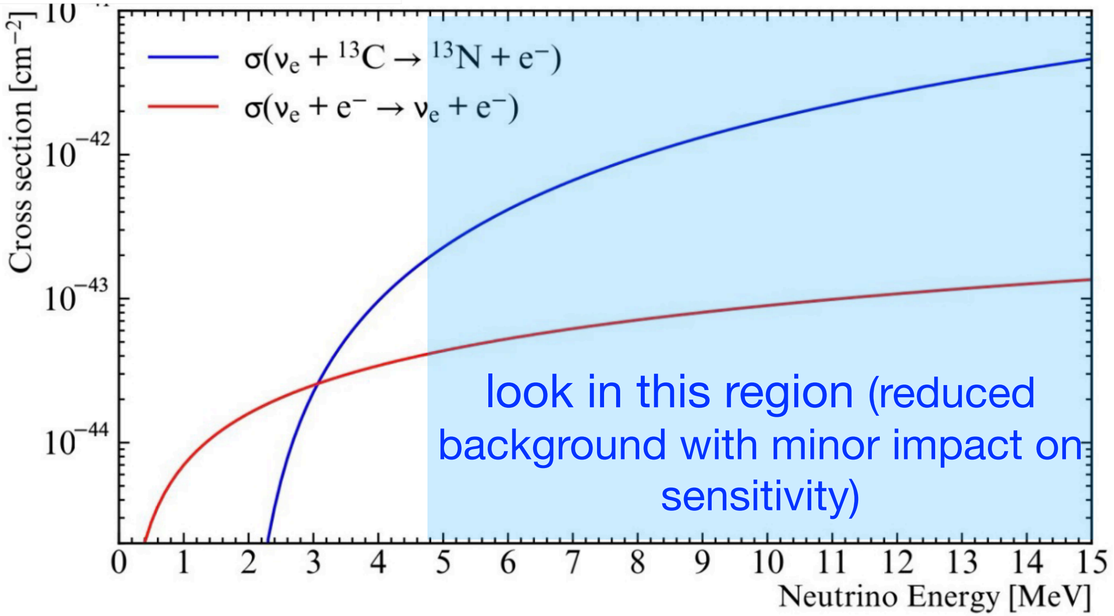

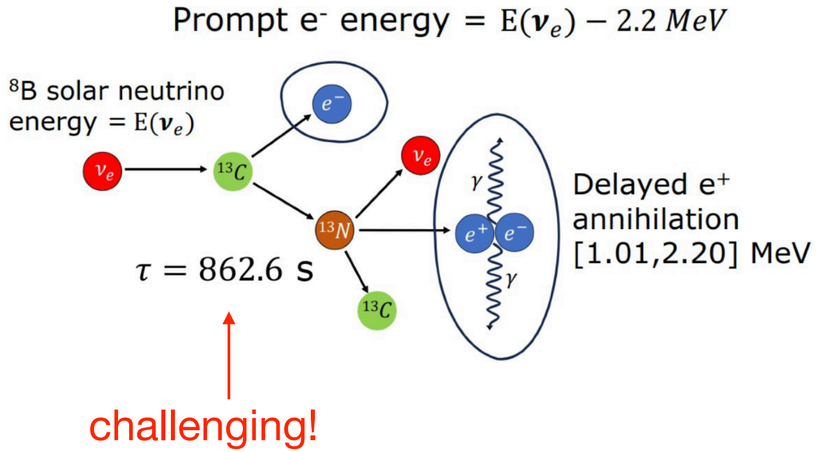

Depth of SNOLAB was critical to reduce muon-induced backgrounds (*e.g.* ^{11}C) to negligible levels.

Use data-driven calculation of accidental backgrounds and form a likelihood ratio statistic based on distance and time separation between prompt and delayed candidate events:

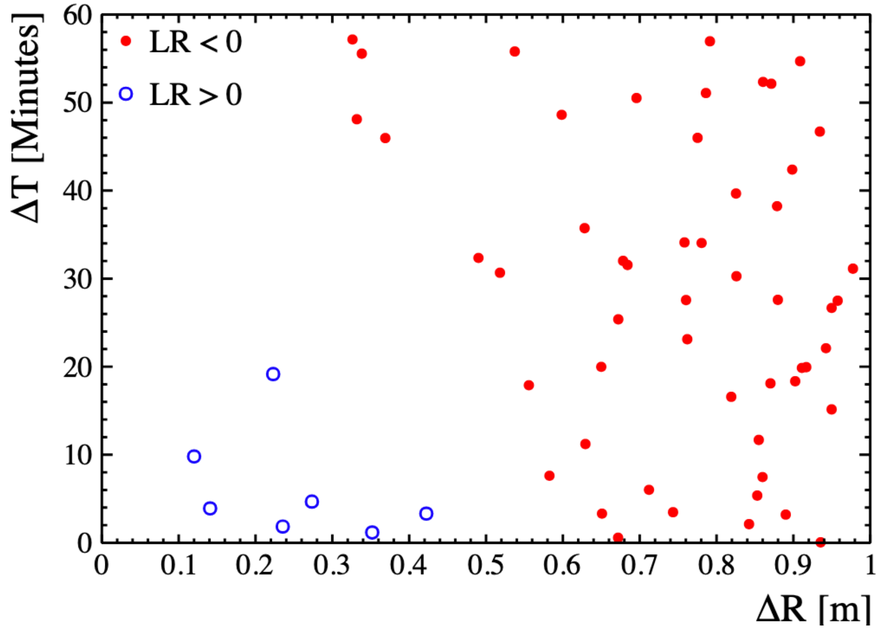

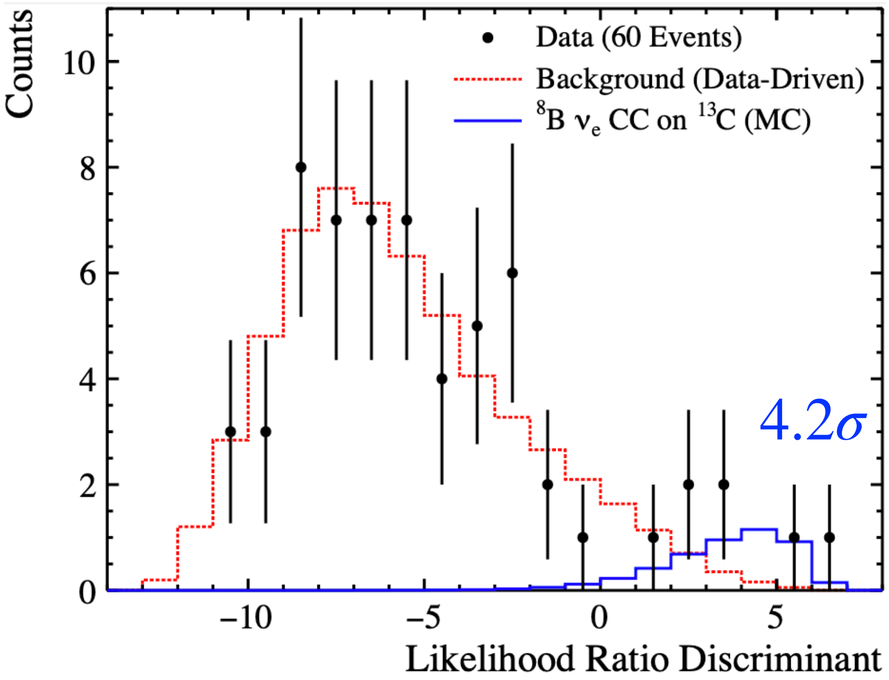
Counts
Data (60 Events)
Background (Data-Driven)
^{8}B ν_e CC on ^{13}C (MC)
4.2σ
Likelihood Ratio Discriminant

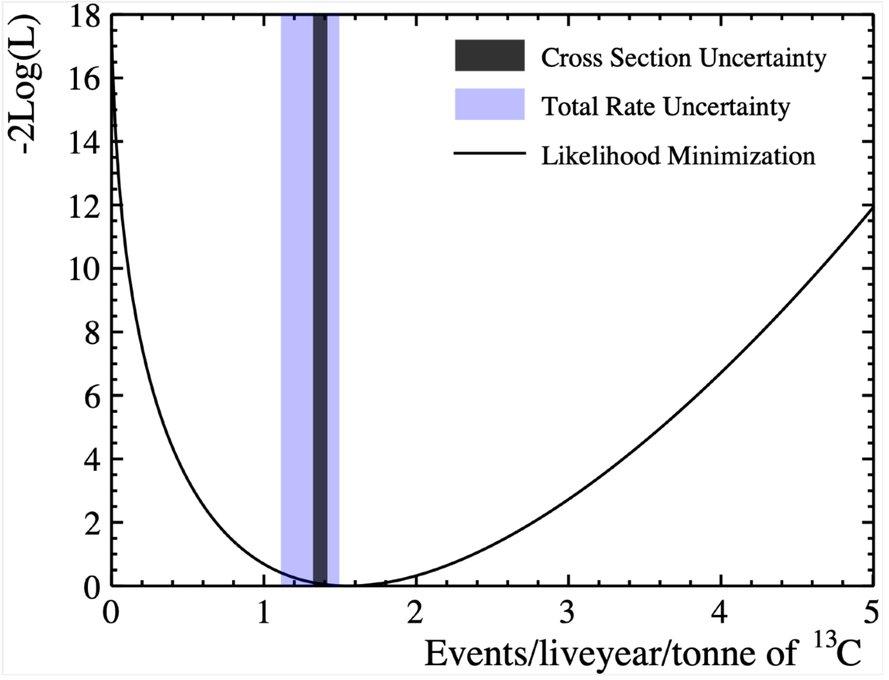
-2Log(L)
Cross Section Uncertainty
Total Rate Uncertainty
Likelihood Minimization
Events/liveyear/tonne of ^{13}C

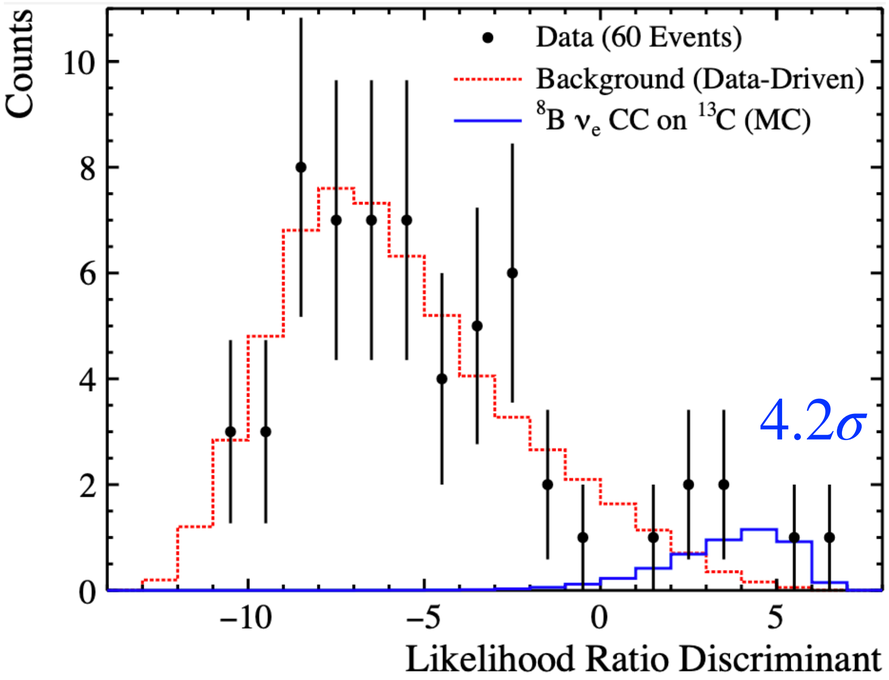

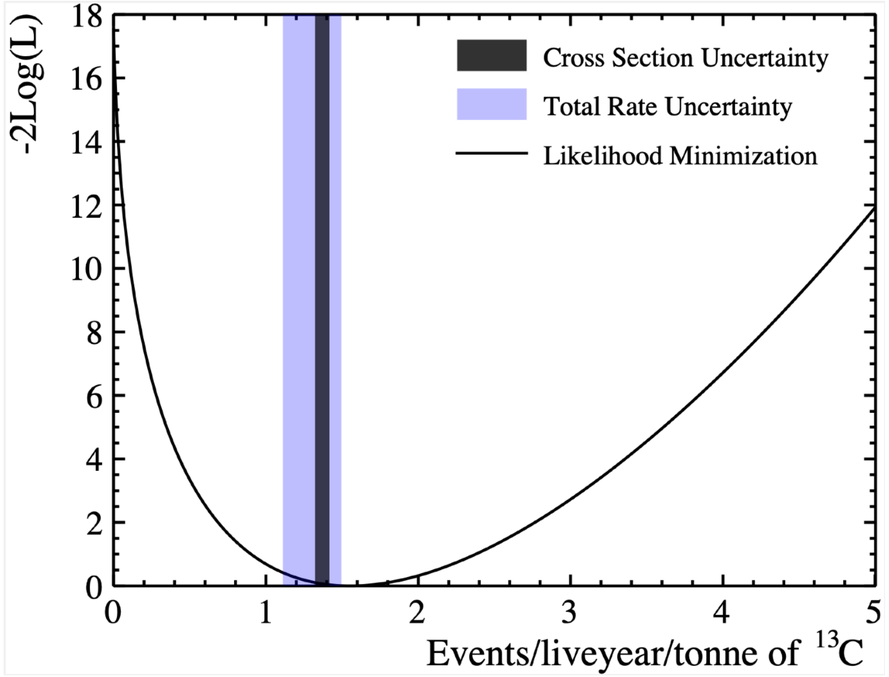

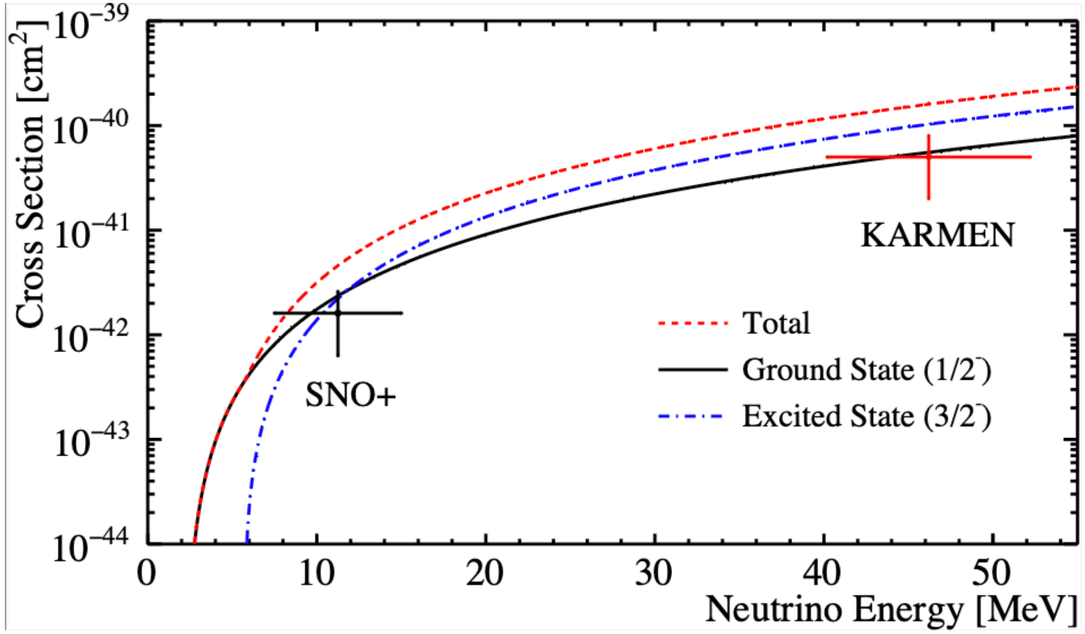

- First evidence of solar neutrino interactions on ^{13}C nucleus;
- 2nd real-time measurement of CC interactions from ^{8}B neutrinos;
- Lowest energy measurement of neutrino interactions on ^{13}C;
- First direct measurement of ground state cross section for $^{13}C + \nu_e \rightarrow ^{13}N + e^-$ in 5-15 MeV range:

$$(16.1^{+8.5}_{-6.7}(\text{stat.})^{+1.6}_{-2.7}(\text{syst.})) \times 10^{-43}\ \text{cm}^2$$

$$^{238}\mathrm{U} \rightarrow {}^{206}\mathrm{Pb} + 8\alpha + 8e^- + 6\bar{\nu}_e + 51.7\,\mathrm{MeV}$$

$$^{235}\mathrm{U} \rightarrow {}^{207}\mathrm{Pb} + 7\alpha + 4e^- + 4\bar{\nu}_e + 46.4\,\mathrm{MeV}$$

$$^{232}\mathrm{Th} \rightarrow {}^{208}\mathrm{Pb} + 6\alpha + 4e^- + 4\bar{\nu}_e + 42.7\,\mathrm{MeV}$$

$$^{40}\mathrm{K} \rightarrow {}^{40}\mathrm{Ca} + e^- + \bar{\nu}_e + 1.31\,\mathrm{MeV}\ (89.3\%)$$

$$^{40}\mathrm{K} + e^- \rightarrow {}^{40}\mathrm{Ar} + \nu_e + 1.505\,\mathrm{MeV}\ (10.7\%)$$

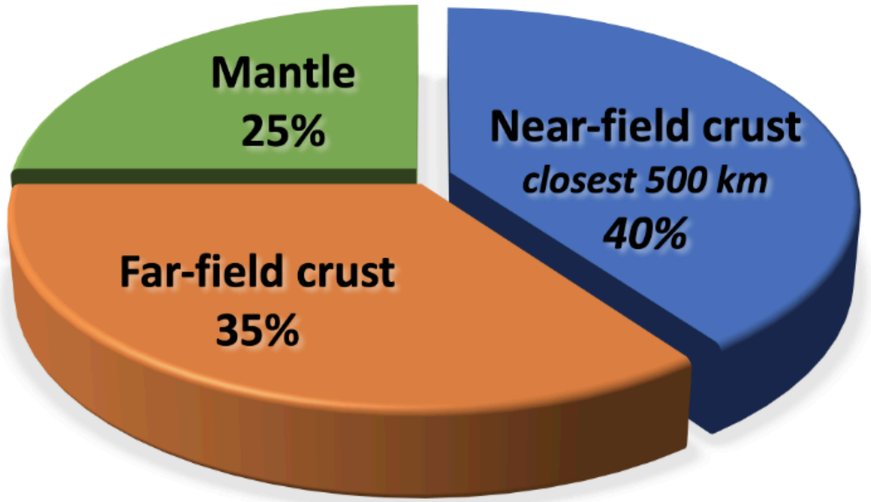

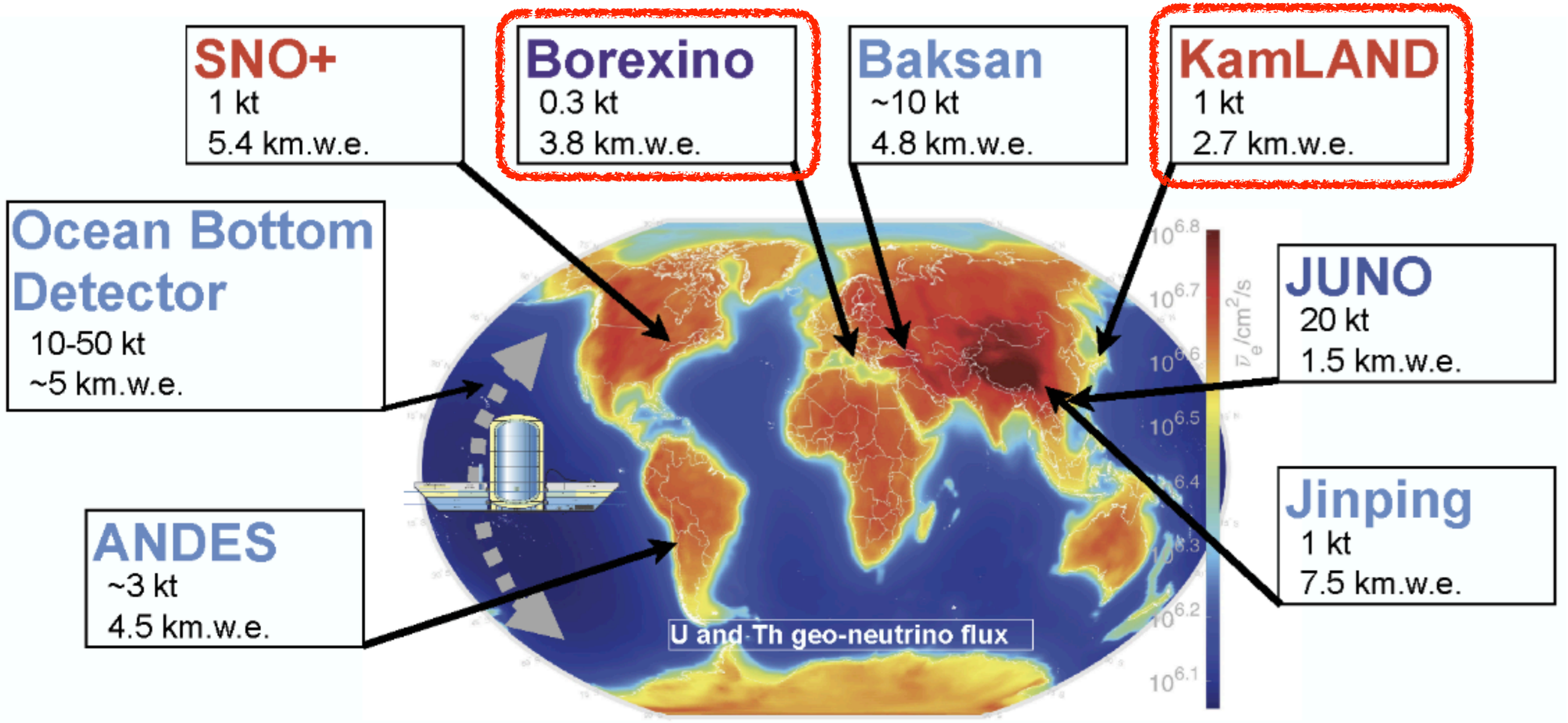

Neutrino Geoscience: Review, survey, future prospects
W. F. McDonough, H. Watanabe, arXiv:2209.13746 (2022)

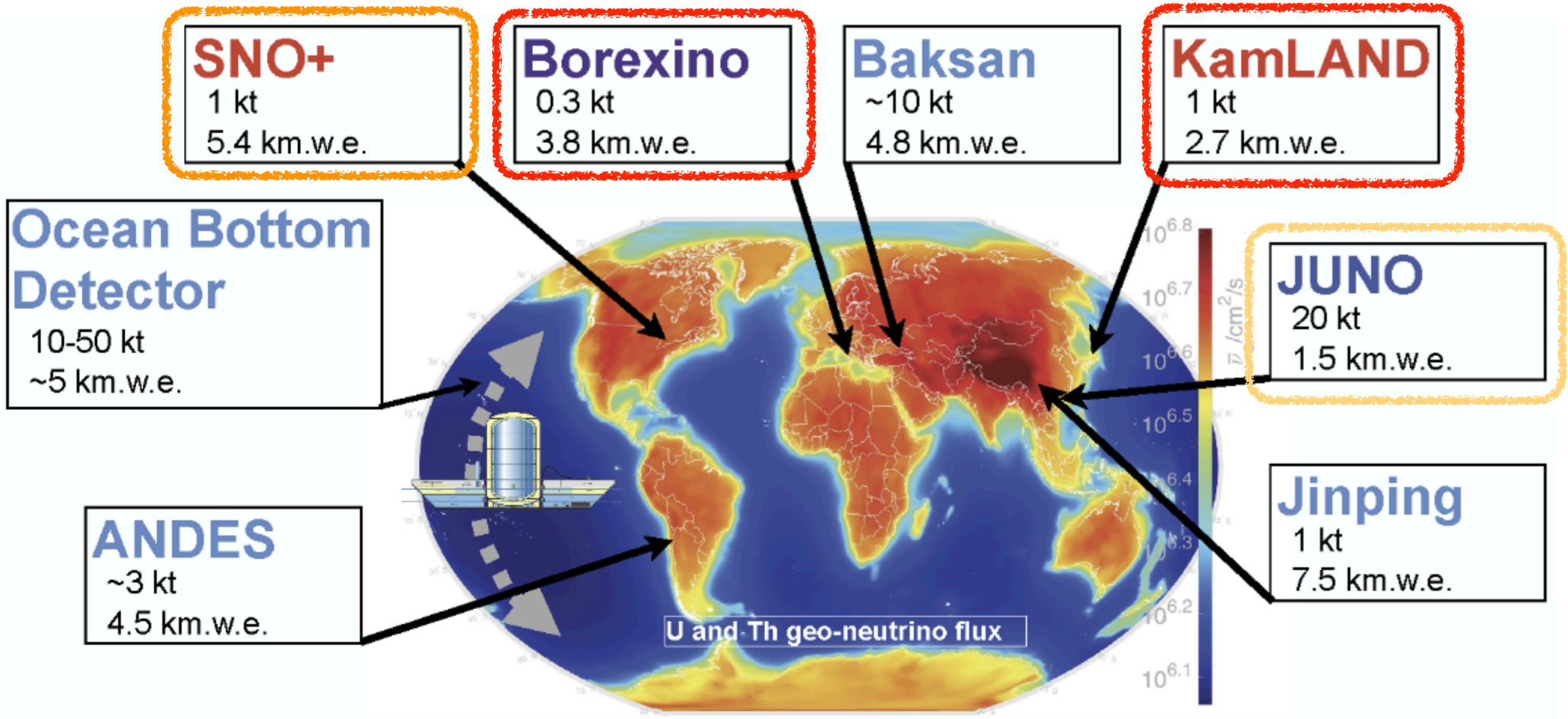

Neutrino Geoscience: Review, survey, future prospects
W. F. McDonough, H. Watanabe, arXiv:2209.13746 (2022)

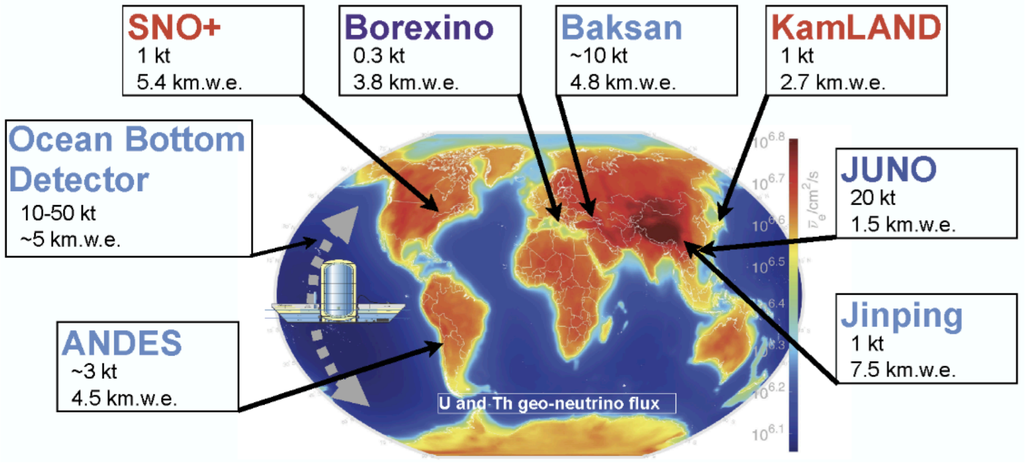

Table 4. Geological estimates of the signal contributions at various antineutrino detectors

Detector	reference	total signal	global crustal contribution	FFC	NFC	†mantle contribution
KamLAND	(Enomoto et al., 2007)	38.5	28.2	10.5	17.7	10.3
KamLAND	(Huang et al., 2013)	30.7	20.6	7.3	13.3	8.8
KamLAND	(Fiorentini et al., 2012)	–	26.5	8.8	17.7	–
KamLAND	(Wipperfurth et al., 2020)	37.9	27.0	8.8	18.2	9.4
Borexino	(Huang et al., 2013)	43.5	29.0	13.7	15.3	8.7
Borexino	(Coltorti et al., 2011)	43.5	26.2	16.0	10.2	9.9
Borexino	(Fiorentini et al., 2012)	–	25.3	15.7	9.7	–
Borexino	(Agostini et al., 2020)	47.0	25.5	16.3	9.2	20.6
Borexino	(Wipperfurth et al., 2020)	43.9	32.5	14.8	18.2	9.4
SNO+	(Huang et al., 2014)	40.0	30.7	15.1	15.6	7.0
SNO+	(Strati et al., 2017)	43.1	30.5	15.2	15.3	6.9
SNO+	(Wipperfurth et al., 2020)	46.8	34.3	14.7	19.6	9.1
JUNO	(Strati et al., 2015)	39.7	28.2	13.4	17.4	8.8
JUNO	(Gao et al., 2020)	49.1	38.3	9.8	28.5*	8.7
JUNO	(Wipperfurth et al., 2020)	40.5	29.8	12.7	17.1	9.5
Jinping	(Šrámek et al., 2016)	58.5	50.3	16.1	27.2	8.2
Jinping	(Wan et al., 2017)	59.4	49.0	–	–	10.4
Jinping	(Wipperfurth et al., 2020)	60.0	48.8	18.7	30.3	9.3
Hanohano	(Huang et al., 2013)	12.0	2.6	2.6	–	9.0

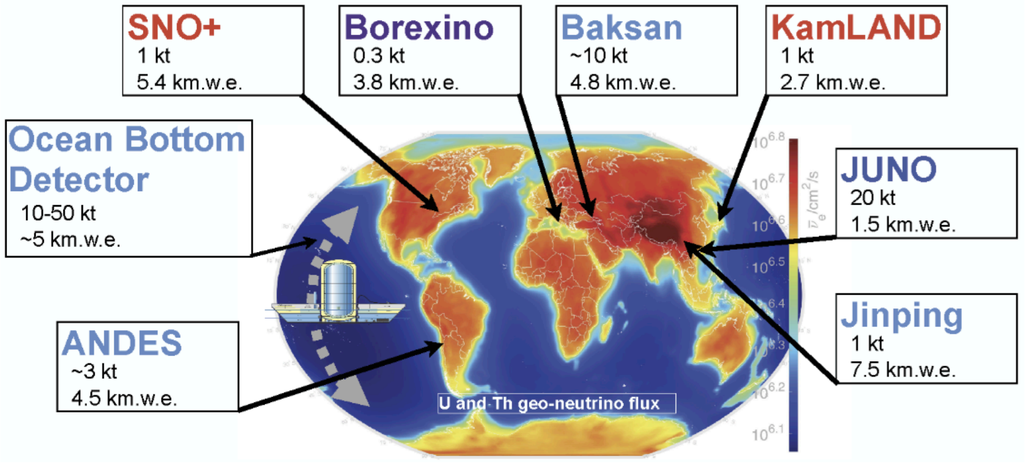

Table 4. Geological estimates of the signal contributions at various antineutrino detectors

Detector	reference	total signal	global crustal contribution	FFC	NFC	†mantle contribution
KamLAND	(Enomoto et al., 2007)	38.5	28.2	10.5	17.7	10.3
KamLAND	(Huang et al., 2013)	30.7	20.6	7.3	13.3	8.8
KamLAND	(Fiorentini et al., 2012)	–	26.5	8.8	17.7	–
KamLAND	(Wipperfurth et al., 2020)	37.9	27.0	8.8	18.2	9.4
Borexino	(Huang et al., 2013)	43.5	29.0	13.7	15.3	8.7
Borexino	(Coltorti et al., 2011)	43.5	26.2	16.0	10.2	9.9
Borexino	(Fiorentini et al., 2012)	–	25.3	15.7	9.7	–
Borexino	(Agostini et al., 2020)	47.0	25.5	16.3	9.2	20.6
Borexino	(Wipperfurth et al., 2020)	43.9	32.5	14.8	18.2	9.4
SNO+	(Huang et al., 2014)	40.0	30.7	15.1	15.6	7.0
SNO+	(Strati et al., 2017)	43.1	30.5	15.2	15.3	6.9
SNO+	(Wipperfurth et al., 2020)	46.8	34.3	14.7	19.6	9.1
JUNO	(Strati et al., 2015)	39.7	28.2	13.4	17.4	8.8
JUNO	(Gao et al., 2020)	49.1	38.3	9.8	28.5*	8.7
JUNO	(Wipperfurth et al., 2020)	40.5	29.8	12.7	17.1	9.5
Jinping	(Šrámek et al., 2016)	58.5	50.3	16.1	27.2	8.2
Jinping	(Wan et al., 2017)	59.4	49.0	–	–	10.4
Jinping	(Wipperfurth et al., 2020)	60.0	48.8	18.7	30.3	9.3
Hanohano	(Huang et al., 2013)	12.0	2.6	2.6	–	9.0

Comprehensive geoneutrino analysis with Borexino,

Agostini et al., Phys. Rev. D 101, 012009 (2020)

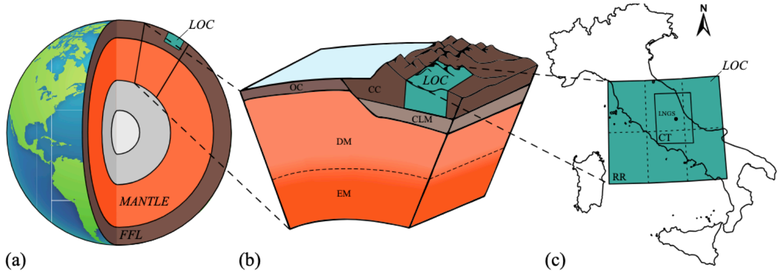

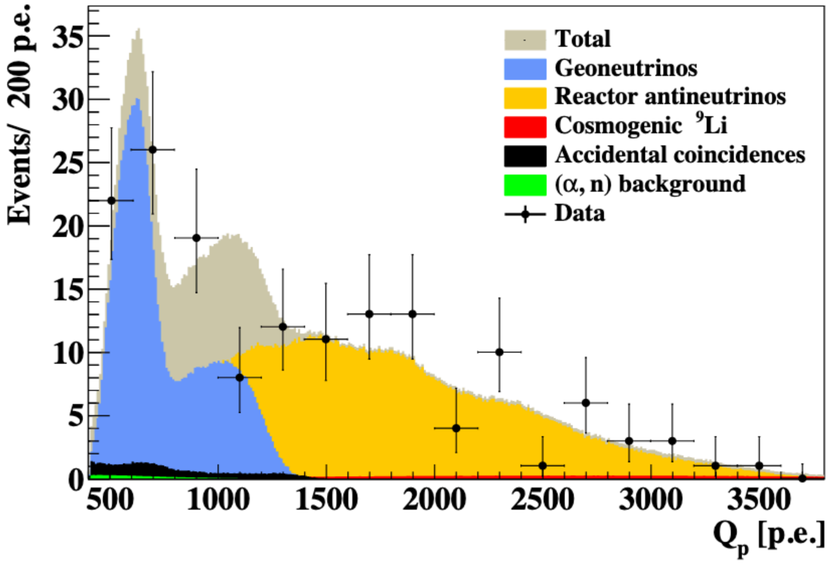

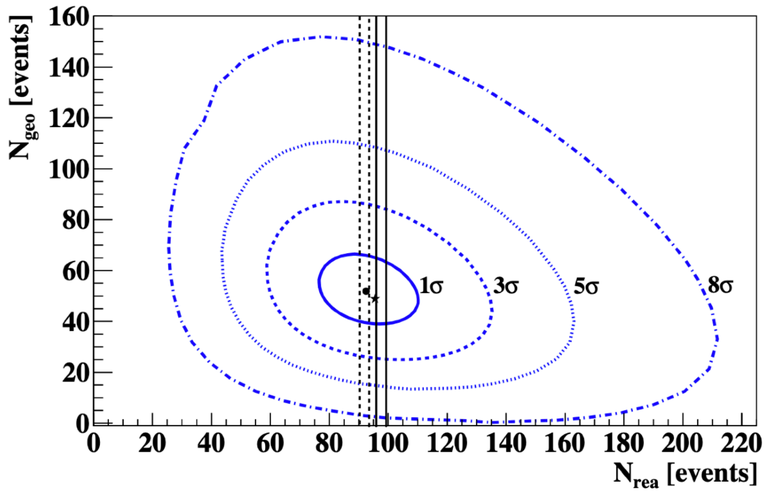

Comprehensive geoneutrino analysis with Borexino,

Agostini et al., Phys. Rev. D 101, 012009 (2020)

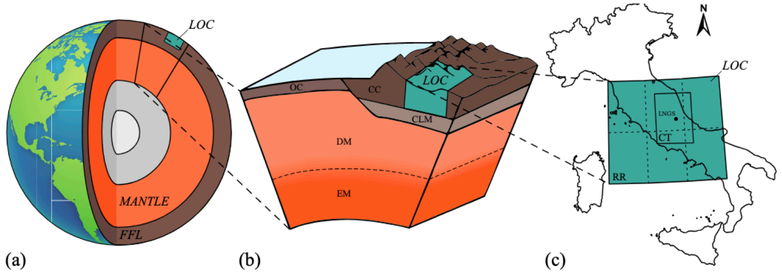

constrained from calculations of local contribution

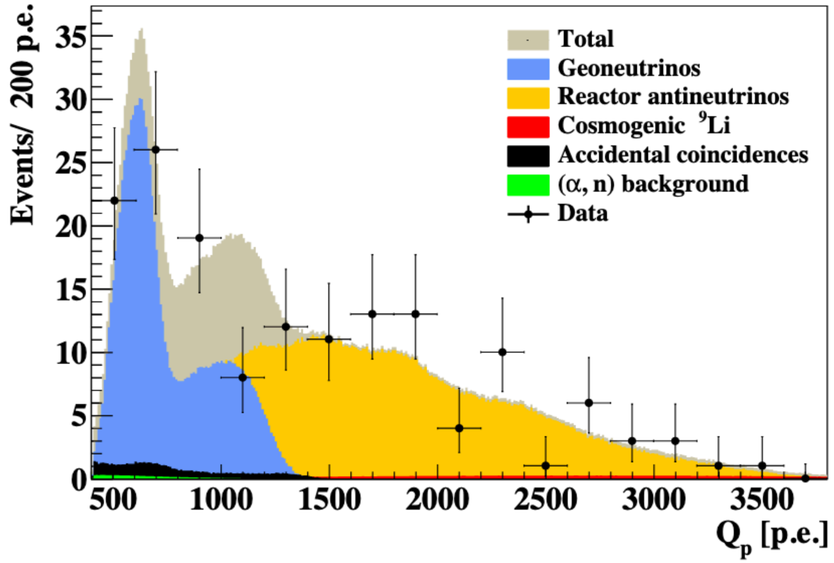

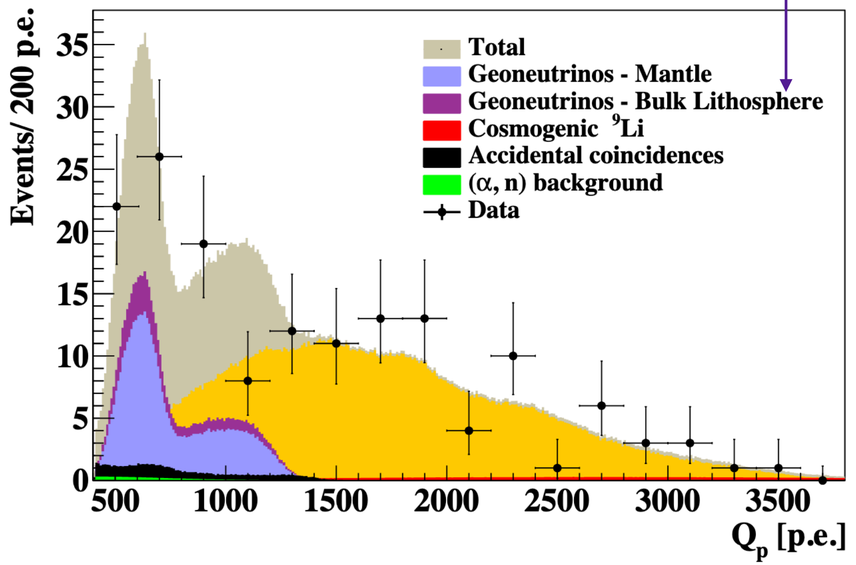

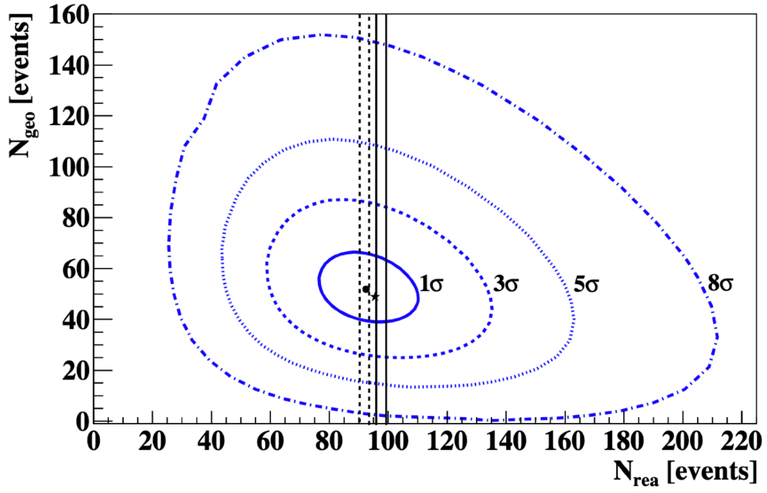

Comprehensive geoneutrino analysis with Borexino,

Agostini et al., Phys. Rev. D 101, 012009 (2020)

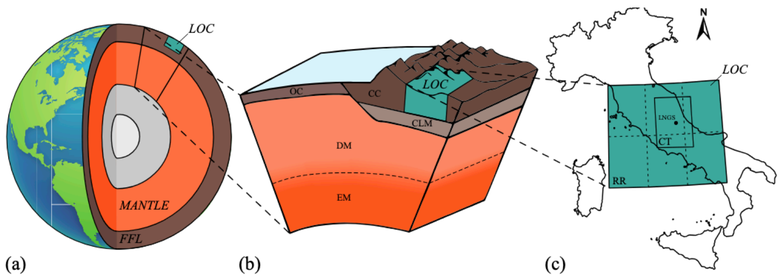

constrained from calculations of local contribution

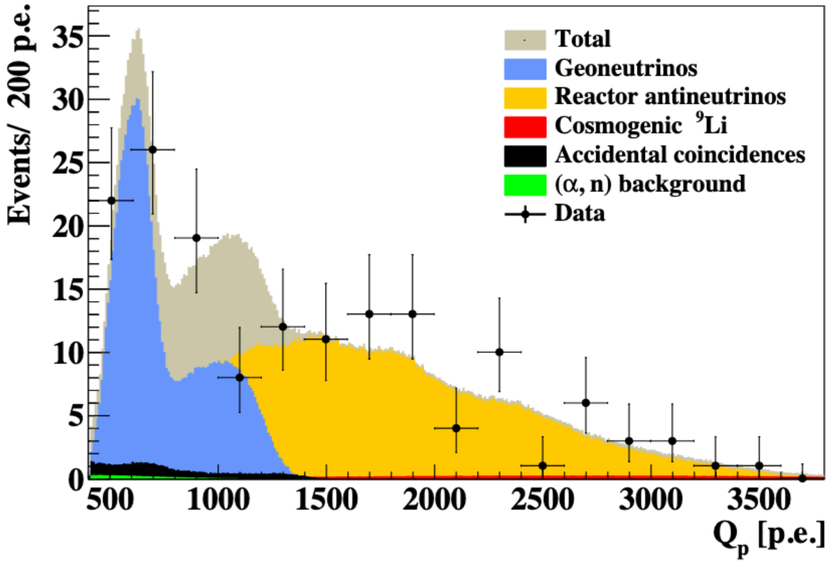

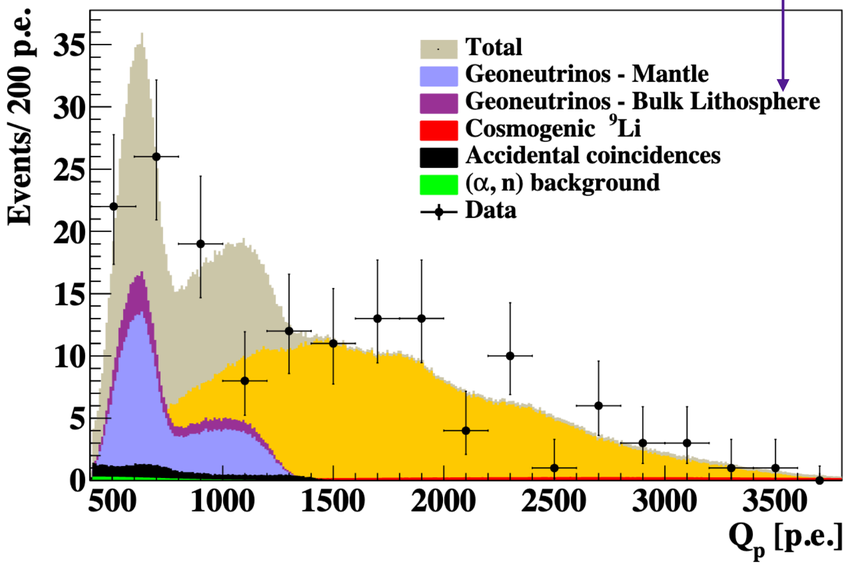

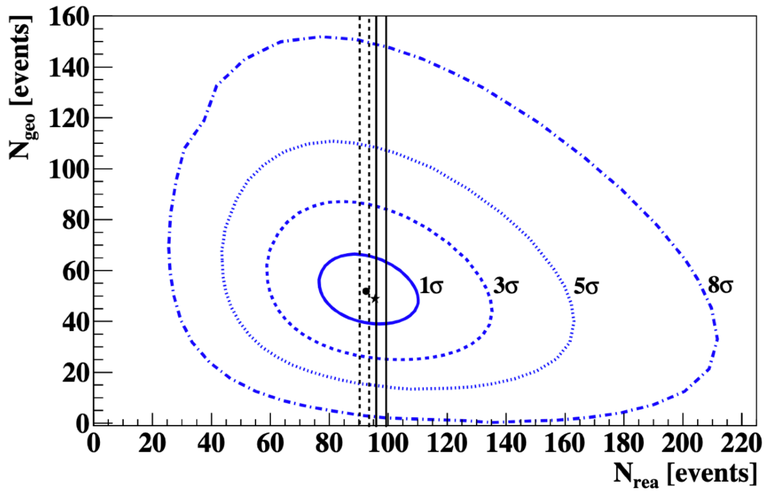

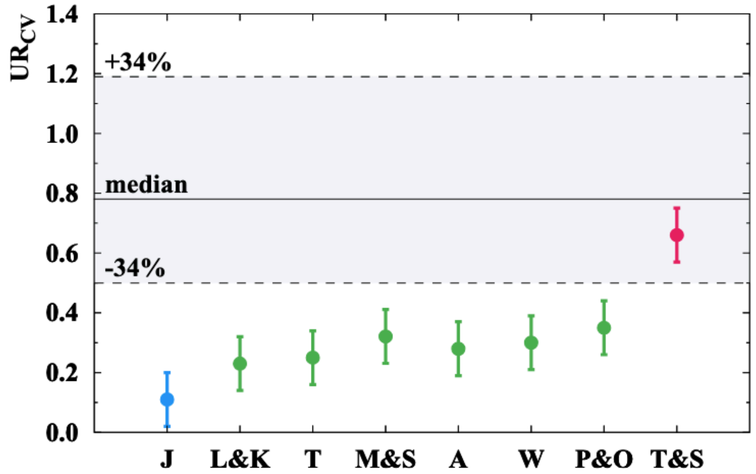

UR_{CV} = ratio of internal heat generation in the mantle over the mantle heat flux

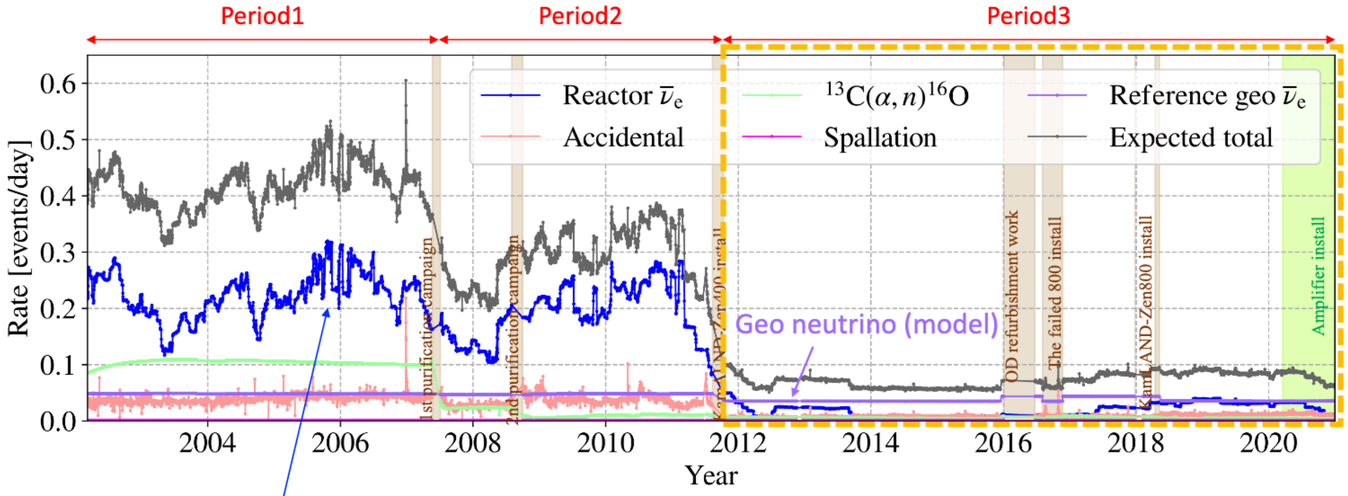

Reactor neutrino is the dominant background of geoneutrino signals.

Most of Japanese reactors have been shut down due to the 3.11 earthquake in 2011.

Nanami Kawada, TAUP 2023

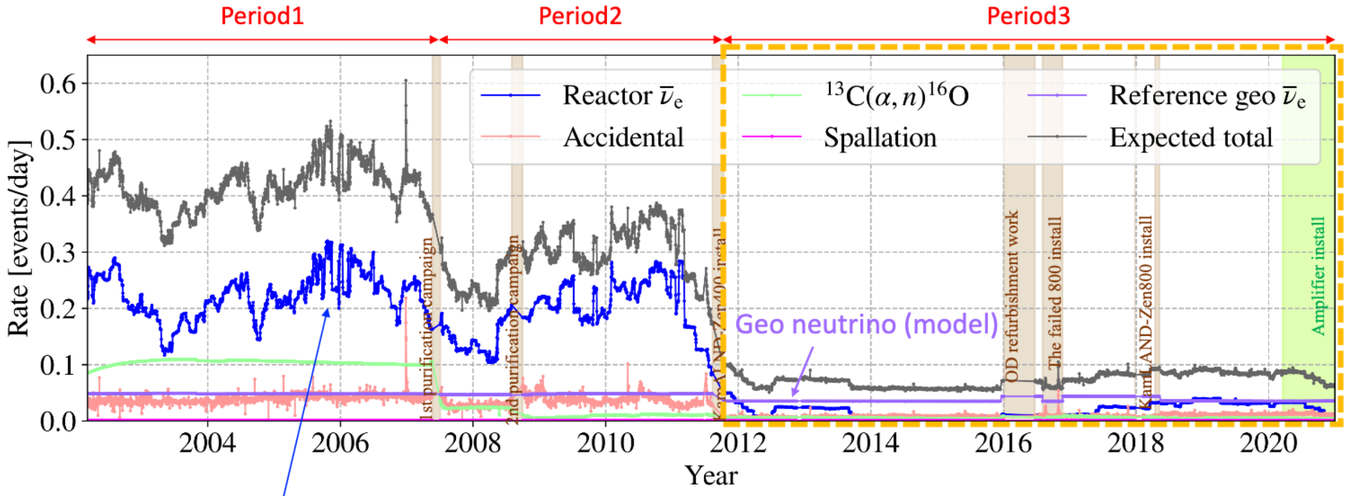

Reactor neutrino is the dominant background of geoneutrino signals.

Most of Japanese reactors have been shut down due to the 3.11 earthquake in 2011.

Nanami Kawada, TAUP 2023

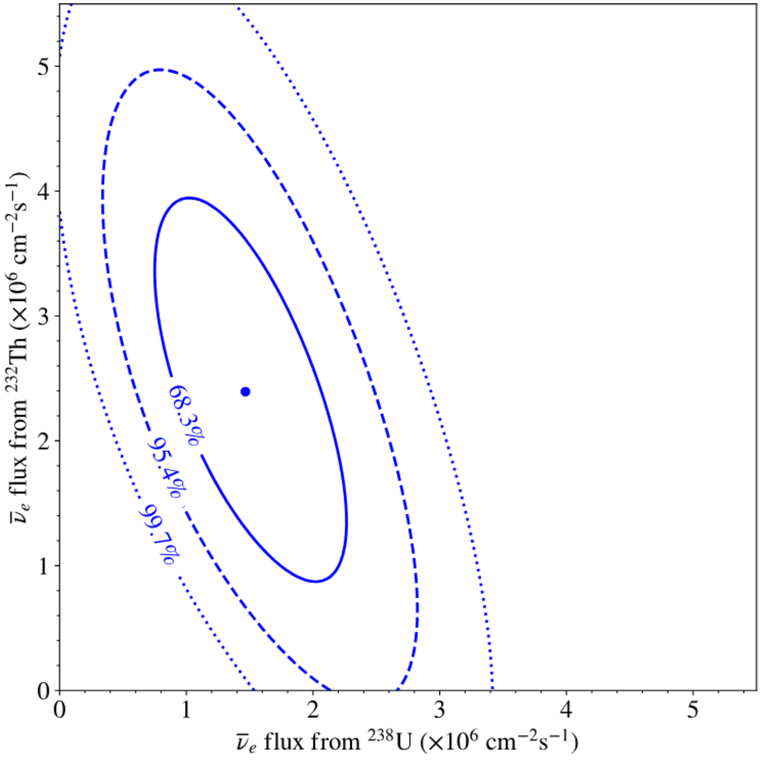

	$N_{\mathrm{U/Th}}$ [event]	flux [$\times 10^5$ cm^{-2}s^{-1}]	flux [TNU]	0-signal rejection
U	$116.6^{+41.0}_{-38.5}$	$14.7^{+5.2}_{-4.8}$	$19.1^{+6.7}_{-6.3}$	3.343σ
Th	$57.5^{+24.5}_{-24.1}$	$23.9^{+10.2}_{-10.0}$	$9.7^{+4.1}_{-4.1}$	2.386σ
U + Th	$173.7^{+29.2}_{-27.7}$	$32.1^{+5.8}_{-5.3}$	$28.6^{+5.1}_{-4.8}$	8.3σ

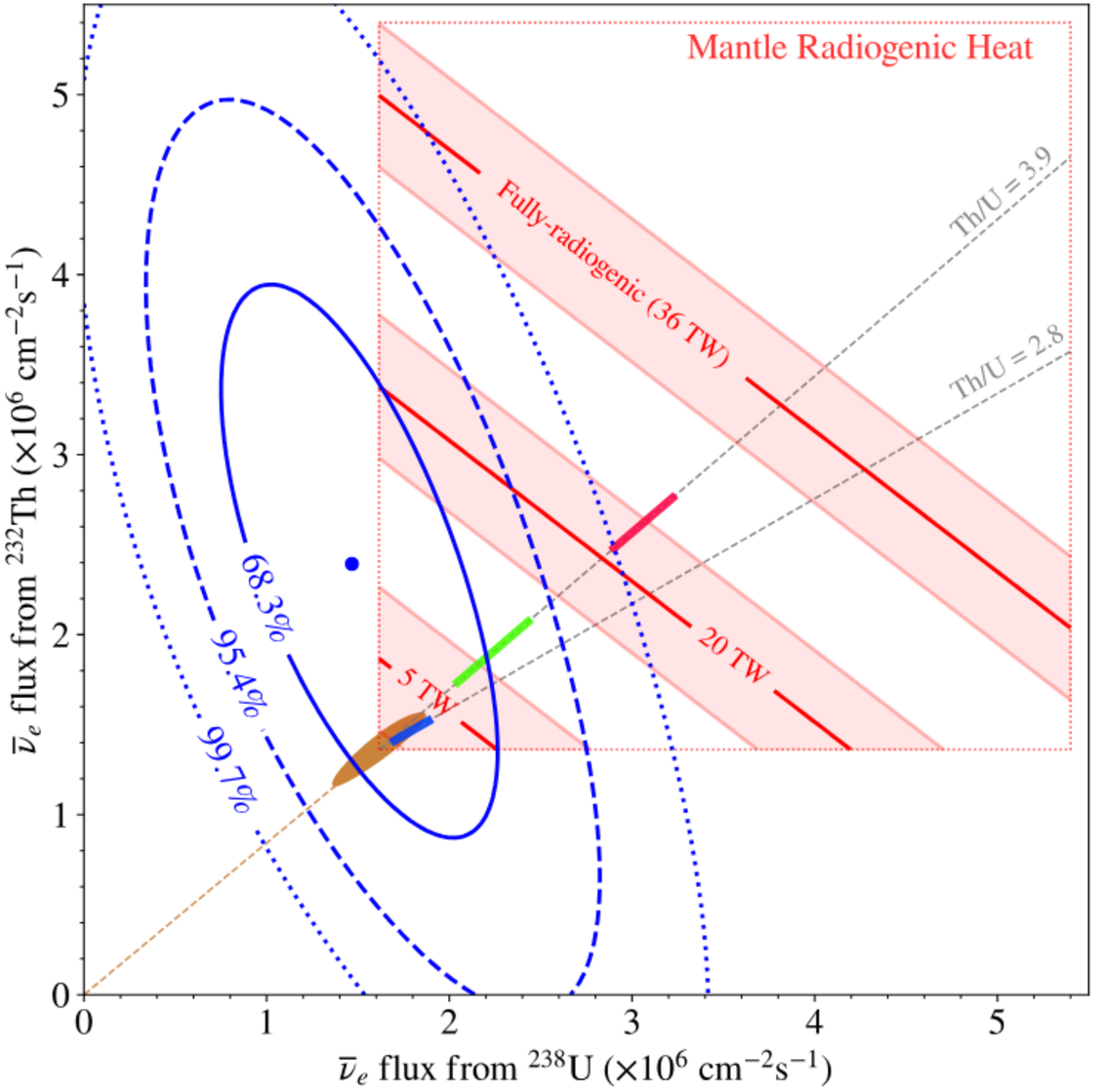

BSE models (Sramek et al 2013)

Low-Q (10-15 TW)
Based on compositional analysis of enstatite chondrites and isotopic constraints
(U : 12±2 ppb, Th : 43±4 ppb)

Middle-Q (17-22 TW)
Based on compositional analysis of CI carbonaceous chondrites and earth samples
(U : 20±4 ppb, Th : 80±13 ppb)

Consistent with the KamLAND data.

High-Q (>25 TW)
Based on balancing mantle viscosity and heat dissipation.
Predicting relatively large amount of radiogenic heat for mantle convection.
(U : 35±4 ppb, Th : 140±14 ppb)

Inconsistent with the KamLAND data

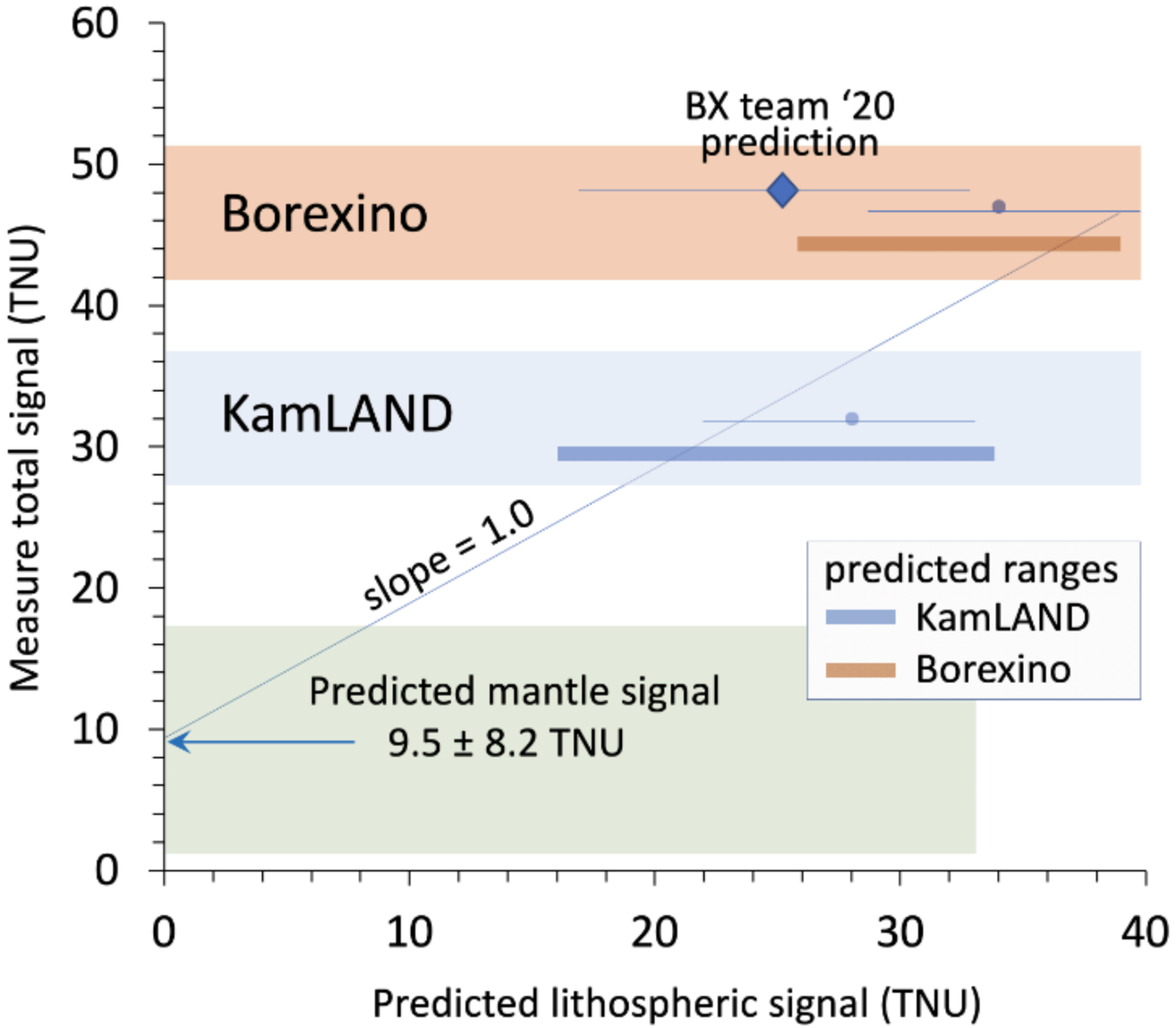

Neutrino Geoscience: Review, survey, future prospects
W. F. McDonough, H. Watanabe, arXiv:2209.13746 (2022)

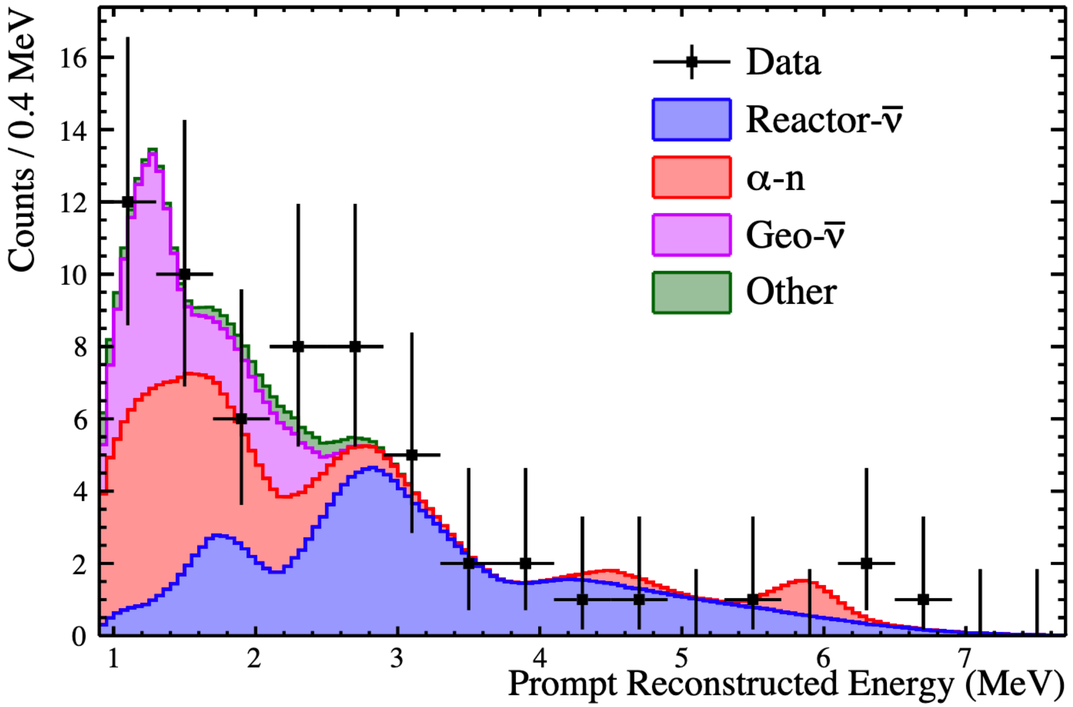

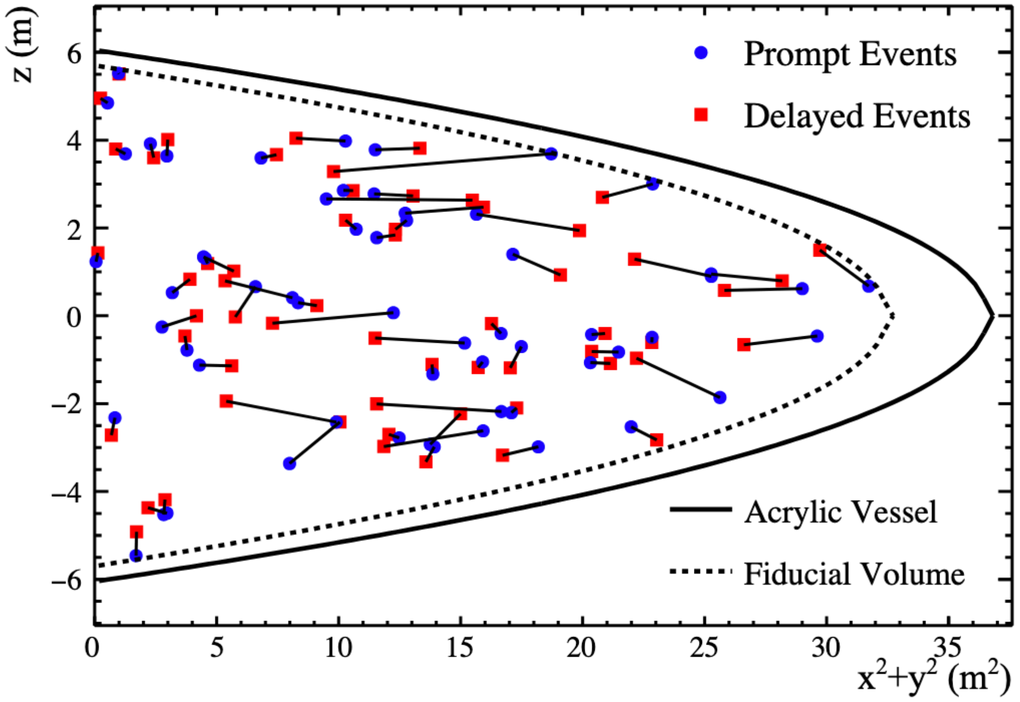

	Fit (Uncon.)	Fit (Con.)
Δm^2_{21} ($\times 10^{-5}$eV^2)	$7.96^{+0.48}_{-0.42}$	$7.58^{+0.18}_{-0.17}$
$\sin^2\theta_{12}$	$0.62^{+0.16}_{-0.40}$	0.308 ± 0.013
Geo-$\bar{\nu}$ IBD rate (TNU)	79^{+49}_{-44}	73^{+47}_{-43}

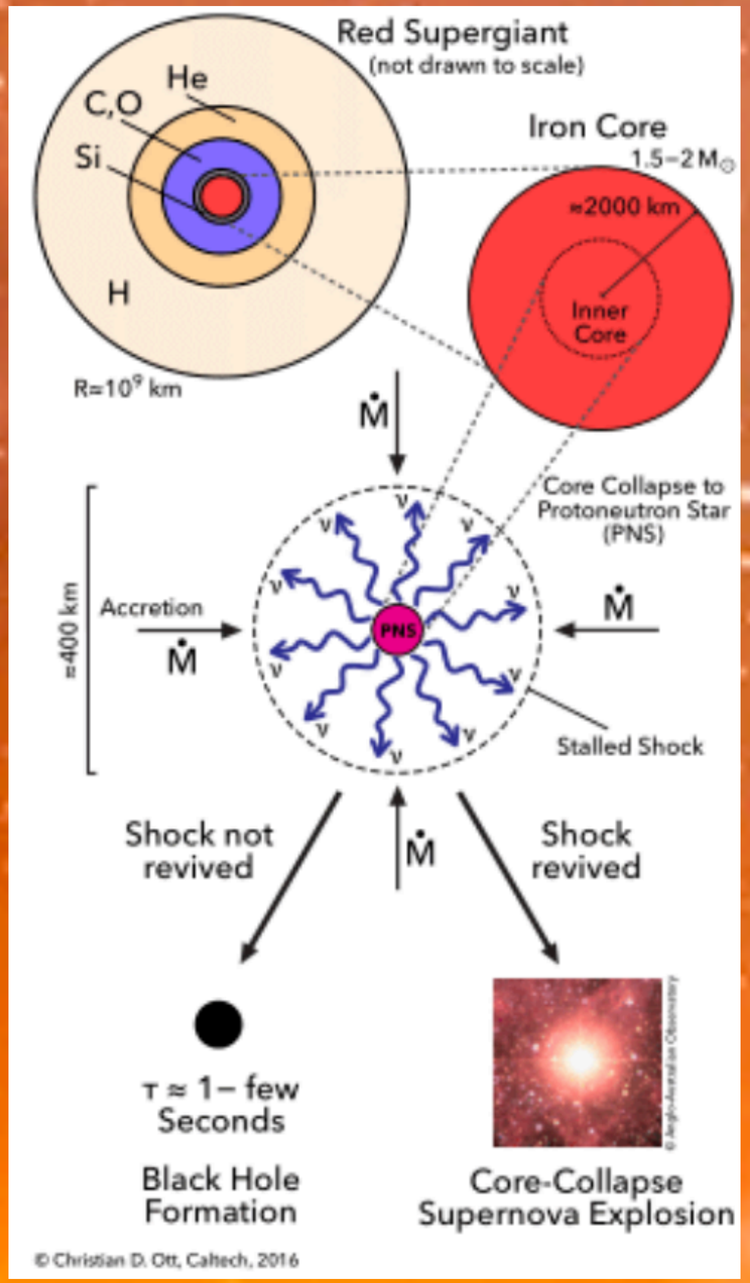

- Neutrino masses and mass ordering
- Dark matter
- Non-standard neutrino interactions
- Fast flavor conversions
- Hadron-quark phase transition
- Proton spin from strangeness
-
-
-

Recent Results from Supernova Neutrino Detection:

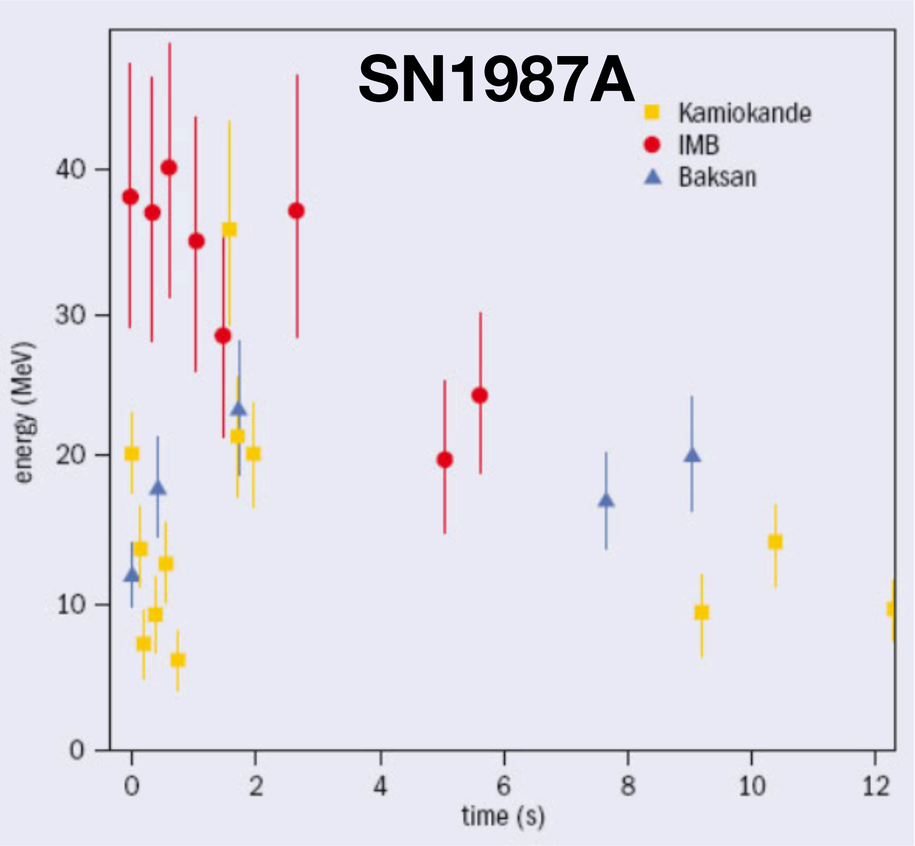

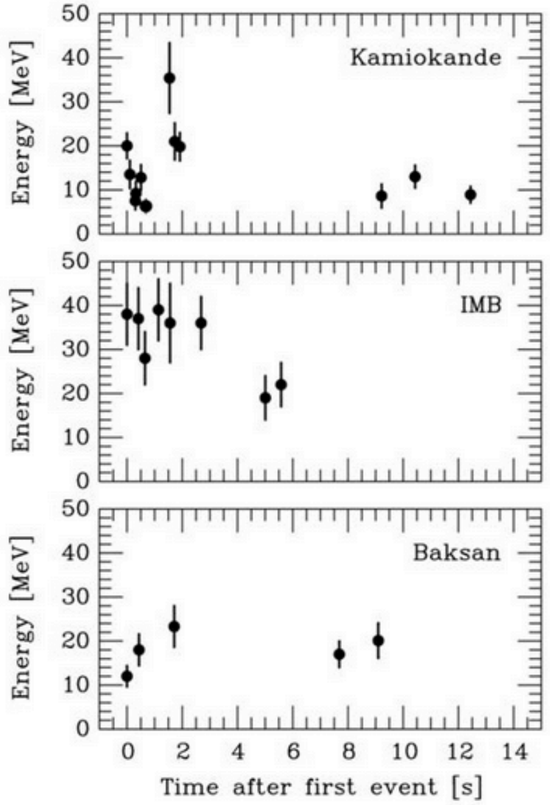

Kamiokande-II (Japan)
Water Cherenkov detector
2140 tons
Clock uncertainty ±1 min

Irvine-Michigan-Brookhaven (US)
Water Cherenkov detector
6800 tons
Clock uncertainty ±50 ms

Baksan Scintillator Telescope
(Soviet Union), 200 tons
Random event cluster ~ 0.7/day
Clock uncertainty +2/−54 s

Within clock uncertainties,
all signals are contemporaneous

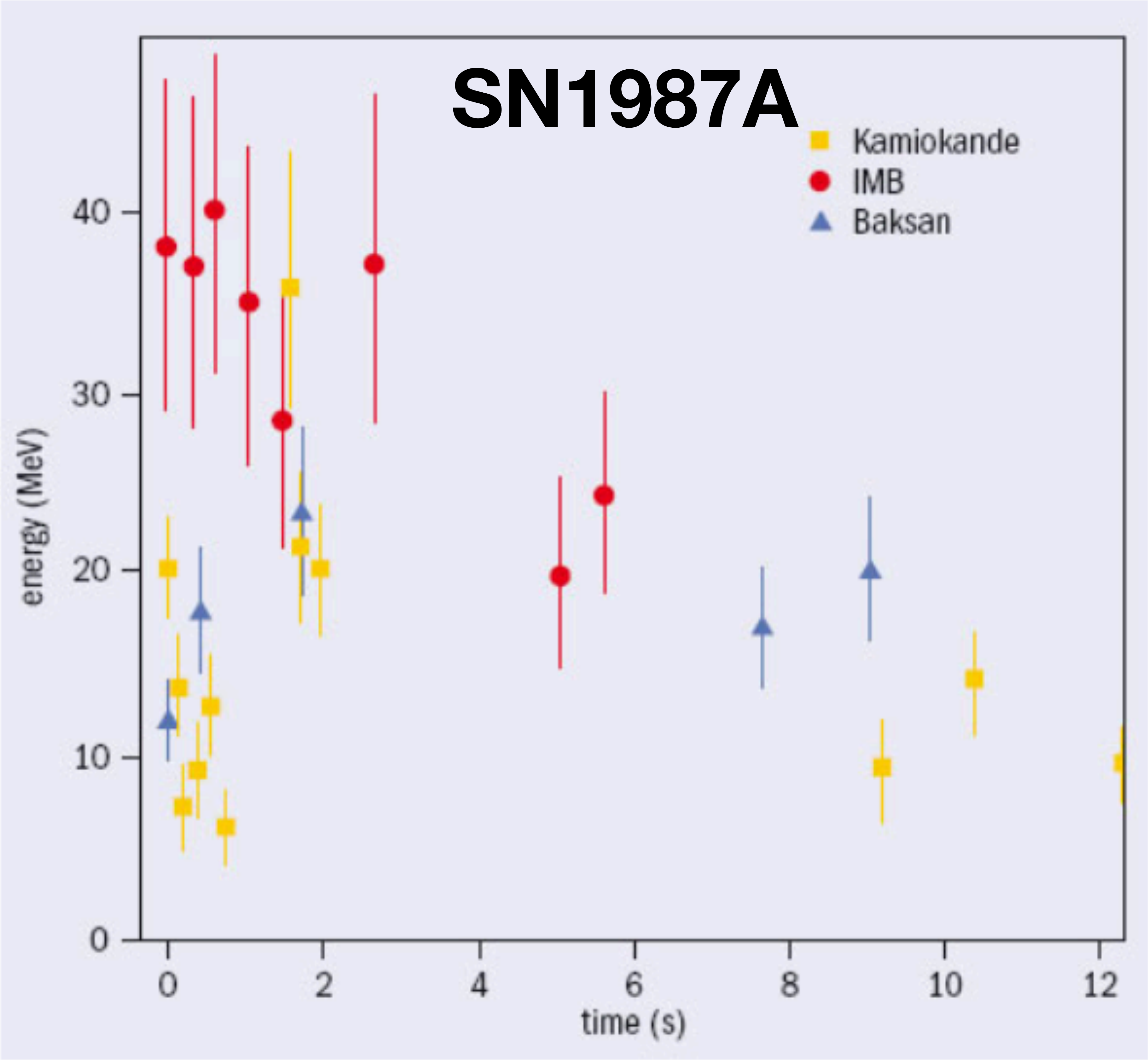

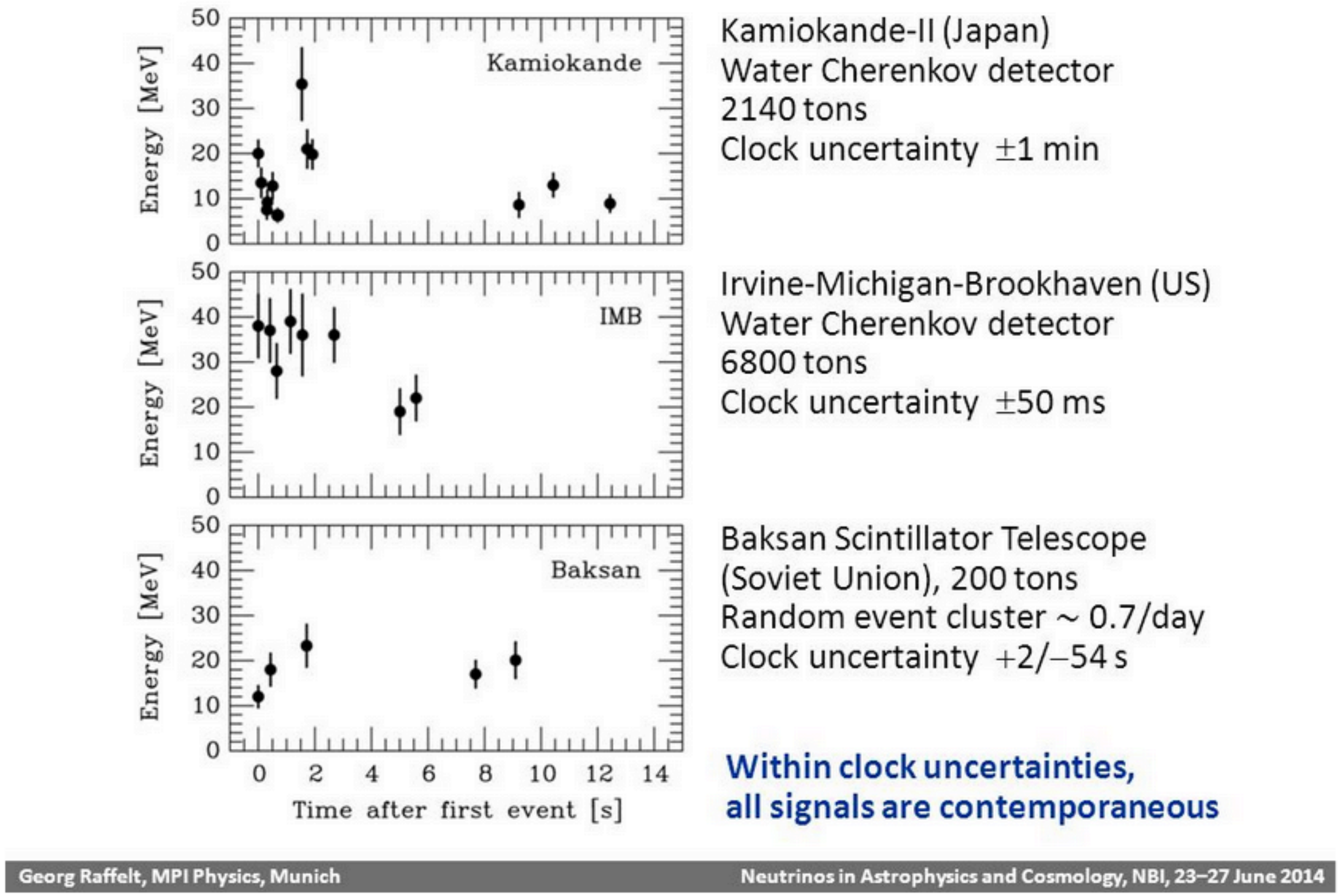

1. arXiv:2507.21845 [pdf, ps, other] hep-ph astro-ph.SR hep-ex nucl-ex nucl-th

Neutrino non-radiative decay in matter: constraints and prospects

Authors: Pilar Iváñez-Ballesteros, M. Cristina Volpe

Abstract: ...events from SN1987A. We then explore the prospects of neutrino-Majoron couplings from a future galactic core-collapse supernova, leaving either a neutron star or a black-hole. To this aim, we use information from detailed one-dimensional supernova simulations. We consider the supernova neutrino signal associated with inverse-beta decay in the upcoming JUNO… ▽ More

Submitted 29 July, 2025; originally announced July 2025.

Comments: 38 pages + 2 Appendices, 21 figures

2. arXiv:2506.20758 [pdf, ps, other] astro-ph.IM astro-ph.HE stat.AP stat.ML

Latent-space Field Tension for Astrophysical Component Detection An application to X-ray imaging

Authors: Matteo Guardiani, Vincent Eberle, Margret Westerkamp, Julian Rüstig, Philipp Frank, Torsten Enßlin

Abstract: ...the effectiveness of this method on synthetic multi-frequency imaging data and apply it to observational X-ray data from the eROSITA Early Data Release (EDR) of the SN1987A region in the Large Magellanic Cloud (LMC). Our results highlight the method's capability to reconstruct astrophysical components with high accuracy, achieving sub-pixel localization… ▽ More

Submitted 25 June, 2025; originally announced June 2025.

3. arXiv:2505.14332 hep-ph

Constraints on Neutrino Secret Interactions from Multi-messenger Neutrinos Scattering on CνB

Authors: Maria Petropavlova, Adam Smetana, Andreas Trautner

Abstract: ...SI) by studying high-energy neutrinos from well-known astrophysical sources, such as SN1987A, the blazars TXS $0506+056$ and PKS $0735+178$, the active galaxy NGC 1068, and KM3-230213A neutrino event. We extend existing limits by covering a previously unconstrained region of the mediator mass parameter space. Our analysis focuses on Dirac neutrinos interacti… ▽ More

Submitted 21 May, 2025; v1 submitted 20 May, 2025; originally announced May 2025.

Comments: Due to a lack of communication on my part, the manuscript was submitted without the full consent of all listed co-authors. I am therefore withdrawing it in order to resolve the authorship and submission issues appropriately

4. arXiv:2505.07479 [pdf, ps, other] astro-ph.HE

Thermal and Kinematic Properties of Ejecta in SN1987A revealed by XRISM

Authors: XRISM collaboration

Abstract: We present an analysis of high-resolution spectra from the shock-heated plasmas in SN~1987A, based on an observation using the Resolve instrument onboard the X-Ray Imaging and Spectroscopy Mission (XRISM).The 1.7--10 keV Resolve spectra are accurately represented by a single component, plane-parallel shock plasma model, with a temperature of $2.84^{+0.09}_{-0.08}$ keV and an ionization parameter o… ▽ More

Submitted 14 June, 2025; v1 submitted 12 May, 2025; originally announced May 2025.

Comments: 16 pages,11 figures, 4 tables, accept for publication in PASJ XRISM special issue. Corresponding authors are Yukikatsu Terada, Koji Mori, Tsukasa Matsushima, Satoru Katsuda, and Aya Bamba

5. arXiv:2505.03882 [pdf, other] hep-ph astro-ph.GA astro-ph.HE hep-th

The Dark Matter Diffused Supernova Neutrino Background

Authors: Garv Chauhan, R. Andrew Gustafson, Gonzalo Herrera, Taj Johnson, Ian Shoemaker

Abstract: ...GeV, which is the strongest bound to date on dark matter-neutrino scatterings at MeV energies, and stronger than bounds set from SN1987A neutrino attenuation by an order of magnitude. We end by discussing how the DMDSNB could be distinguished from the DSNB. ▽ More

Submitted 6 May, 2025; originally announced May 2025.

Comments: 10 pages, 7 figures

6. arXiv:2504.10928 [pdf, other] astro-ph.SR astro-ph.GA astro-ph.HE doi 10.1051/0004-6361/202555161

Radiative-transfer models for dusty Type II supernovae

Authors: Luc Dessart, D. John Hillier, Arkaprabha Sarangi

Abstract: ...favor of the H-rich material which generates the Halpha and FeII emission below 5500A. Our model with 5e-4Msun of dust below 2000km/s matches closely the optical spectrum of SN1987A at 714d. Modeling historical SNe requires treating both the ejecta material and the dust, as well as multiple power sources, although interaction power will generally dominate. ▽ More

Submitted 27 May, 2025; v1 submitted 15 April, 2025; originally announced April 2025.

Comments: accepted to A&A

Journal ref: A&A 698, A293 (2025)

7. arXiv:2503.13607 [pdf, other] hep-ph astro-ph.HE

Supernova Gamma-Ray Constraints from Heavy Sterile Neutrino Decays

Authors: Garv Chauhan, R. Andrew Gustafson, Ian M. Shoemaker

Abstract: ...-rays from SN1987A by the Solar Maximum Mission (SMM) and constraints from the diffuse γ-ray background arising from sterile neutrino decays. We find that the constraints arising from both the SMM data and the diffuse γ-ray background are weaker than those that have previously appeared in the literature. Finally, we study the sensitivity of several prese… ▽ More

Submitted 17 March, 2025; originally announced March 2025.

Comments: 10 pages + 6 page appendix

8. arXiv:2503.09691 [pdf, other] hep-ph astro-ph.HE

New Supernova Constraints on Neutrinophilic Dark Sector

Authors: Christopher V. Cappiello, P. S. Bhupal Dev, Amol V. Patwardhan

Abstract: ...a supernova could copiously produce such neutrinophilic DM at a large enough rate to cause noticeable anomalous cooling. From the non-observation of such anomalous cooling in SN1987A, we thus set new constraints on neutrino-DM interactions, which provide up to four orders of magnitude improvement over the existing constraints for DM masses below $\mathcal{O}$(1… ▽ More

Submitted 12 March, 2025; originally announced March 2025.

Comments: 5 pages, 3 figures; 4 additional figures in Appendix

9. arXiv:2503.04573 [pdf, other] hep-ph astro-ph.SR hep-ex

SN1987A bounds on neutrino quantum decoherence

Authors: Christoph A. Ternes, Giulia Pagliaroli, Francesco L. Villante

Abstract: We obtain stringent bounds on neutrino quantum decoherence from the analysis of SN1987A data. We show that for the decoherence model considered here, which allows for neutrino-loss along the trajectory, the bounds are many orders of magnitude stronger than the ones that can be obtained from the analysis of data from reactor neutrino oscillation experiments o… ▽ More

Submitted 6 March, 2025; originally announced March 2025.

Comments: v1: 10 pages, 1 figure, 2 tables

10. arXiv:2502.13926 [pdf, ps, other] astro-ph.IM

A crude but efficient pipeline for JWST MIRI imager : the case of sn1987A

Authors: R. Gastaud, A. Coulais

Abstract: Most of the space projects or large observatories do have official tools like simulators, end-to-end pipelines developed during years by a large team of contributors. They are like {\em cathedrals}. In this paper, we show that very simplistic code using basic operators provided by high level language like GDL allows to write quickly high quality code to process raw data into scientifically validat… ▽ More

Submitted 19 February, 2025; originally announced February 2025.

Comments: 4 pages, 2 figures, ADASS conference 2024

11. arXiv:2502.01731 [pdf, other] hep-ph astro-ph.HE doi 10.1103/PhysRevLett.134.151002

Cooling the Shock: New Supernova Constraints on Dark Photons

Authors: Andrea Caputo, Hans-Thomas Janka, Georg Raffelt, Seokhoon Yun

Abstract: ...neutrino-driven explosions are expected to survive, the DP cooling of the core is too small to modify the neutrino signal, i.e., our new argument supersedes the traditional SN1987A cooling bound. ▽ More

Submitted 17 April, 2025; v1 submitted 3 February, 2025; originally announced February 2025.

Comments: Version published in PRL

Journal ref: Phys. Rev. Lett. 134, 151002, 16 April 2025

12. arXiv:2501.18689 [pdf, other] astro-ph.HE astro-ph.SR doi 10.1051/0004-6361/202451483

The initial mass-remnant mass relation for core collapse supernovae

Authors: C. Ugolini, M. Limongi, R. Schneider, A. Chieffi, U. N. Di Carlo, M. Spera

Abstract: ...the HYdrodynamic Ppm Explosion with Radiation diffusION (HYPERION) code (Limongi and Chieffi 2020), assuming a thermal bomb model calibrated to match the main properties of SN1987A. We find that the heaviest black hole that can form depends on the initial stellar rotation, metallicity, and the assumed criterion for the onset of pulsational pair-instability s… ▽ More

Submitted 30 January, 2025; originally announced January 2025.

Comments: Accepted for publication on A&A. 25 pages, 24 figures, 6 tables

Journal ref: A&A 695, A122 (2025)

13. arXiv:2501.09445 [pdf, other] hep-ph astro-ph.HE hep-ex

The flux of electron antineutrinos from supernova SN1987A data

Authors: Riccardo Maria Bozza, Vigilante di Risi, Giuseppe Matteucci, Veronica Oliviero, Giulia Ricciardi, Francesco Vissani

Abstract: ...antineutrino emission, we have made some steps forward in the analysis of the thermodynamical properties and temporal structure of neutrino emission from core collapse SN1987A. Our analysis, unlike similar previous ones, takes into account the times, energies and angles of arrival of the detected events in a reliable framework which includes a finite ramp in… ▽ More

Submitted 16 January, 2025; originally announced January 2025.

Comments: 26 pages, 13 images, 5 tables

14. arXiv:2501.08741 [pdf, other] hep-ph

Are there critical aspects in the time, energy and angular distributions of SN1987A?

Authors: Veronica Oliviero, Riccardo Maria Bozza, Vigilante di Risi, Giuseppe Matteucci, Giulia Ricciardi, Francesco Vissani

Abstract: ...this complex event are increasingly sophisticated, but the accuracy with which they describe the emission is unknown. The only event observed so far with neutrino telescopes, SN1987A, still plays a crucial role and deserves to be studied meticulously. With this in mind, we have undertaken a refined analysis of the observations, taking into account the knowle… ▽ More

Submitted 15 January, 2025; originally announced January 2025.

Comments: Proceeding for 13th Cosmic-Ray International Studies and Multi-Messenger Astroparticle Conference, (Trapani, Italy), June, 2024

15. arXiv:2501.08117 [pdf, ps, other] hep-ph astro-ph.HE

New Limits on Ultralight Axionlike Dark Matter from Reanalyzed Data

Authors: K. Y. Zhang, L. Y. Wu, H. Yan

Abstract: ...eV, the results improve upon previous laboratory limits by more than 3 orders of magnitude, exceeding for the first time the astrophysical limits from supernova SN1987A cooling. For the axion mass range of interest corresponding to ultralow frequencies, the crucial local phase of the axion field is considered. Furthermore, the obtained limits are nearly equ… ▽ More

Submitted 29 July, 2025; v1 submitted 14 January, 2025; originally announced January 2025.

Comments: Revised according to suggestions from referees; 6 pages, 5 figures

Event yields

Primary channels, SN at 10kpc

SNEWS2, New J Phys 23 (2021) 3, 031201

Experiment	Type	Mass [kt]	Location	11.2 $M_\odot$	27.0 $M_\odot$	40.0 $M_\odot$
Super-K	$H_2O/\bar{\nu}_e$	32	Japan	4000/4100	7800/7600	7600/4900
Hyper-K	$H_2O/\bar{\nu}_e$	220	Japan	28K/28K	53K/52K	52K/34K
IceCube	String/$\bar{\nu}_e$	2500*	South Pole	320K/330K	660K/660K	820K/630K
KM3NeT	String/$\bar{\nu}_e$	150*	Italy/France	17K/18K	37K/38K	47K/38K
LVD	$C_nH_{2n}/\bar{\nu}_e$	1	Italy	190/190	360/350	340/240
KamLAND	$C_nH_{2n}/\bar{\nu}_e$	1	Japan	190/190	360/350	340/240
Borexino	$C_nH_{2n}/\bar{\nu}_e$	0.278	Italy	52/52	100/97	96/65
JUNO	$C_nH_{2n}/\bar{\nu}_e$	20	China	3800/3800	7200/7000	6900/4700
SNO+	$C_nH_{2n}/\bar{\nu}_e$	0.78	Canada	150/150	280/270	270/180
NOνA	$C_nH_{2n}/\bar{\nu}_e$	14	USA	1900/2000	3700/3600	3600/2500
Baksan	$C_nH_{2n}/\bar{\nu}_e$	0.24	Russia	45/45	86/84	82/56
HALO	Lead/ν_e	0.079	Canada	4/3	9/8	9/9
HALO-1kT	Lead/ν_e	1	Italy	53/47	120/100	120/120
DUNE	Ar/ν_e	40	USA	2700/2500	5500/5200	5800/6000
MicroBooNe	Ar/ν_e	0.09	USA	6/5	12/11	13/13
SBND	Ar/ν_e	0.12	USA	8/7	16/15	17/18
DarkSide-20k	Ar/any ν	0.0386	Italy	-	250	-
XENONnT	Xe/any ν	0.006	Italy	56	106	-
LZ	Xe/any ν	0.007	USA	65	123	-
PandaX-4T	Xe/any ν	0.004	China	37	70	-

Interaction channels

SNO+: 780t organic liquid scintillator

Reaction	Yield
NC: $\nu p \to \nu p$	429.1 ± 12.0
CC: $\overline{\nu}_e p \to e^+ n$	194.7 ± 1.0
CC: $\overline{\nu}_e\ ^{12}C \to e^+\ ^{12}B_{gs}$	7.0 ± 0.7
CC: $\nu_e\ ^{12}C \to e^-\ ^{12}N_{gs}$	2.7 ± 0.3
NC: $\nu\ ^{12}C \to \nu'\ ^{12}C^*(15.1\ \text{MeV})$	43.8 ± 8.7
CC/NC: $\nu\ ^{12}C \to\ ^{11}C$ or $^{11}B+X$	2.4 ± 0.5
νe elastic scattering	13.1

SNO+, Adv HEP 2016 (2016) 6194250

Super-Kamiokande: 32kt water Cherenkov + Gd

Reconstructed	Hüdepohl			Fischer			Tamborra		
	No Osc.	NMO	IMO	No Osc.	NMO	IMO	No Osc.	NMO	IMO
IBD ($\bar{\nu}_e$)	1936	1939	1935	1186	1260	1437	2505	2283	1786
ES (ν_e)	38	39	39	22	29	26	46	33	37
ES ($\bar{\nu}_e$)	9	8	8	5	6	6	12	10	8
ES (ν_x)	12	12	12	9	8	8	10	12	12
ES ($\bar{\nu}_x$)	10	10	10	7	7	7	8	9	10
^{16}O CC (ν_e)	7	19	16	3	17	13	35	58	51
^{16}O CC ($\bar{\nu}_e$)	19	20	21	9	11	17	62	58	49
^{16}O NC (ν_e,^{15}N)	0	0	0	0	0	0	0	0	0
^{16}O NC ($\bar{\nu}_e$,^{15}N)	0	0	0	0	0	0	0	0	0
^{16}O NC (ν_x,^{15}N)	0	0	0	0	0	0	0	0	0
^{16}O NC ($\bar{\nu}_x$,^{15}N)	0	0	0	0	0	0	0	0	0
^{16}O NC (ν_e,^{15}O)	0	0	0	0	0	0	0	0	0
^{16}O NC ($\bar{\nu}_e$,^{15}O)	0	0	0	0	0	0	0	0	0
^{16}O NC (ν_x,^{15}O)	0	0	0	0	0	0	0	0	0
^{16}O NC ($\bar{\nu}_x$,^{15}O)	0	0	0	0	0	0	0	0	0
total	2031	2037	2041	1241	1338	1514	2678	2463	1953

Super-K, arxiv:2403.06760

SNEWS
SUPERNOVA EARLY WARNING SYSTEM

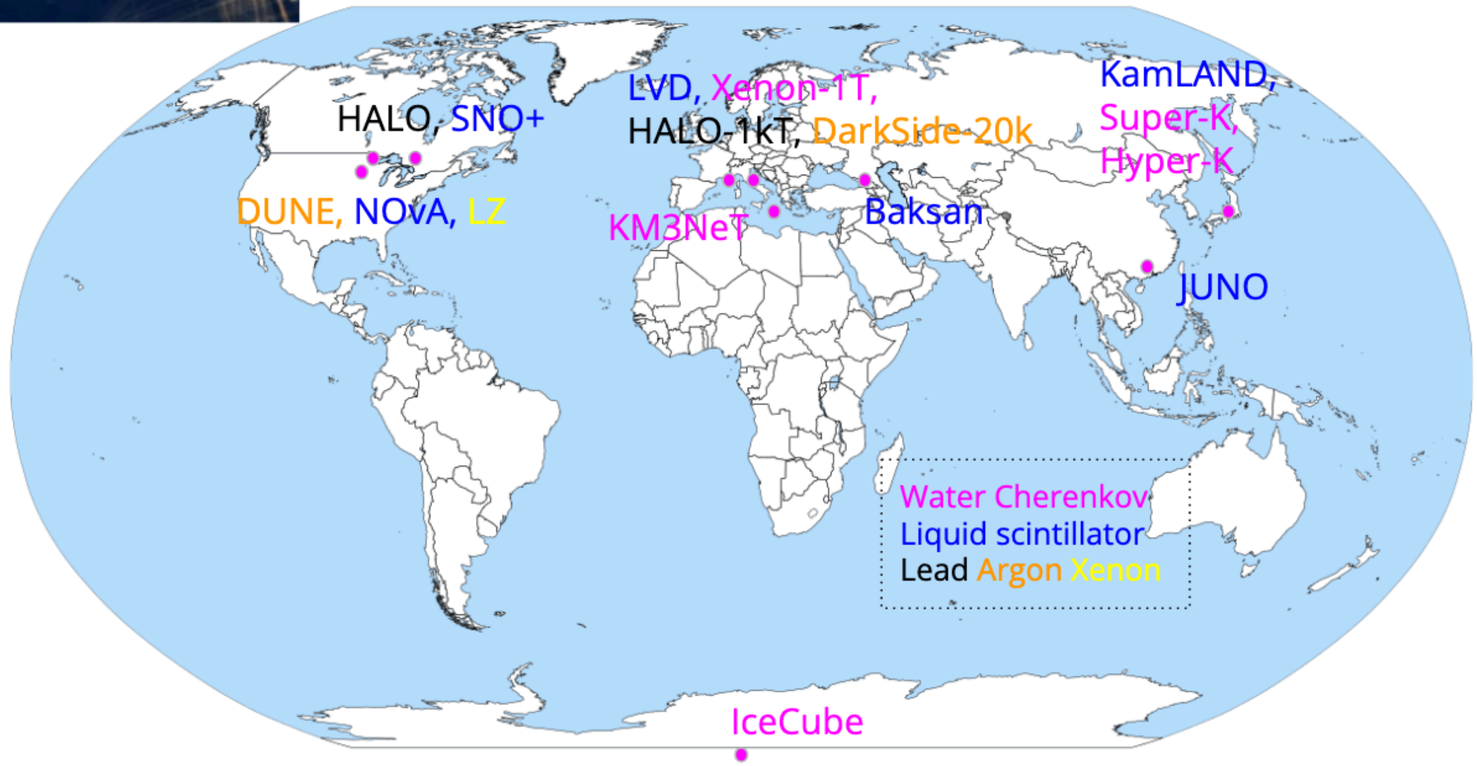

- Provide rapid calculation of observationally relevant quantities
- Direction
- Distance
- Features

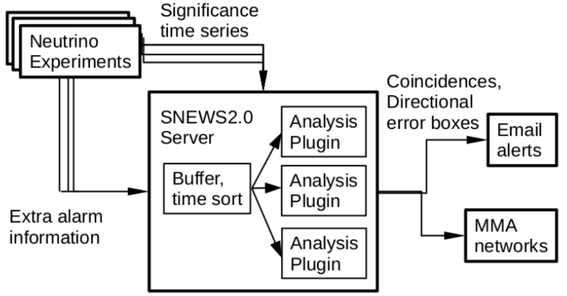

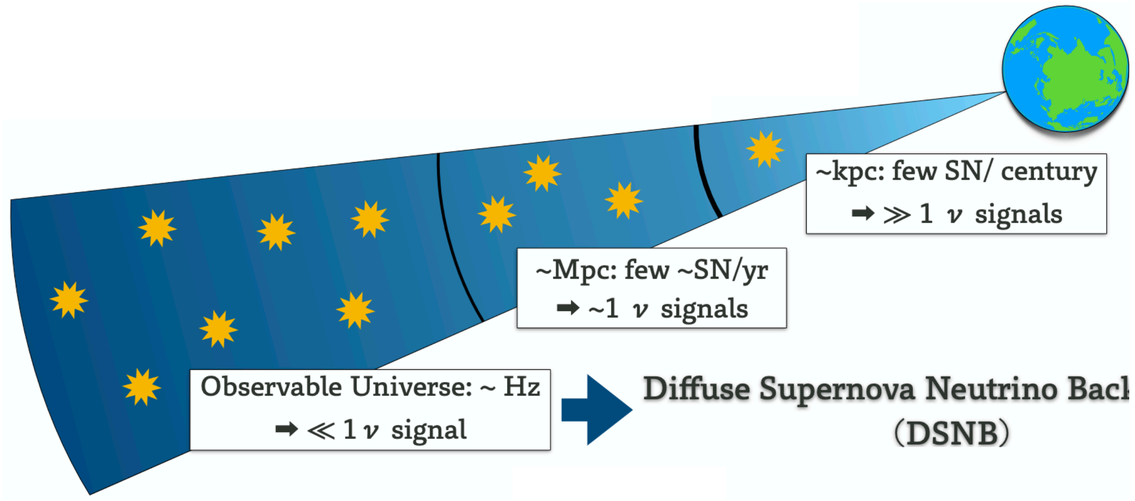
~kpc: few SN/ century
➡ ≫ 1 ν signals
~Mpc: few ~SN/yr
➡ ~1 ν signals
Observable Universe: ~ Hz
➡ ≪ 1 ν signal
Diffuse Supernova Neutrino Bacl
(DSNB)

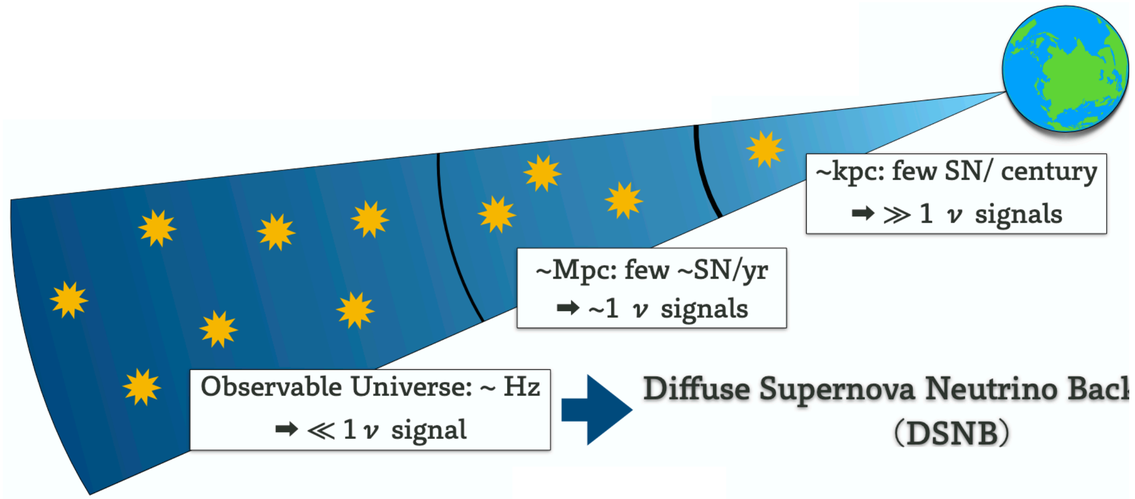

Look for high energy anti-nu signal
(coincidence detection reduces background to the very small signal)

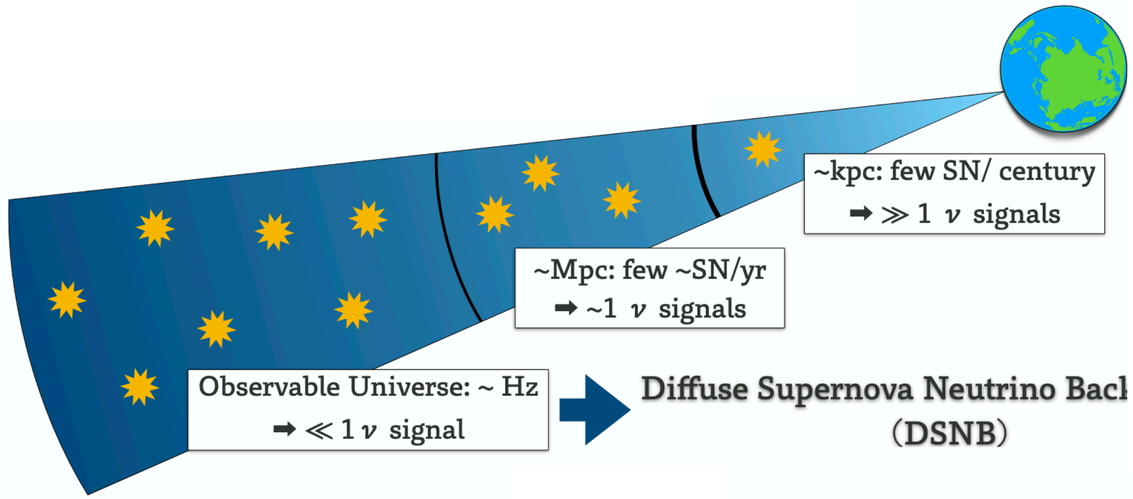

Look for high energy anti-nu signal
(coincidence detection reduces background to the very small signal)

Super-Kamiokande

The world largest underground water Cherenkov detector

- Super-Kamiokande (SK): WC detector
  - Location: 1000 m underground@Kamioka mine, Japan
- Phase: exposure with 22.5 kton times…
  - No neutron tagging (1996 - 2008): 3033 d (SK-I — III)
  - pure-water with neutron tagging (2008 - 2018): 2970 d (SK-IV)
  - **Gd-loaded water with neutron tagging (2020-present): >956 d (SK-VI, VII)**

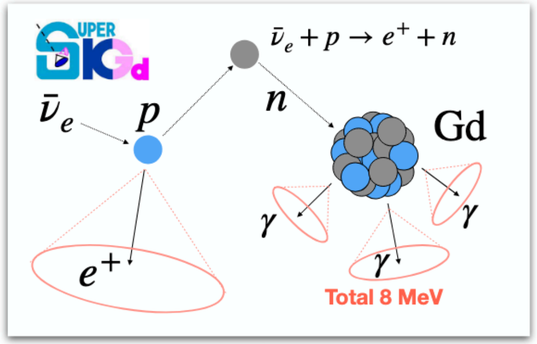

Beacom and Vagins (2004)

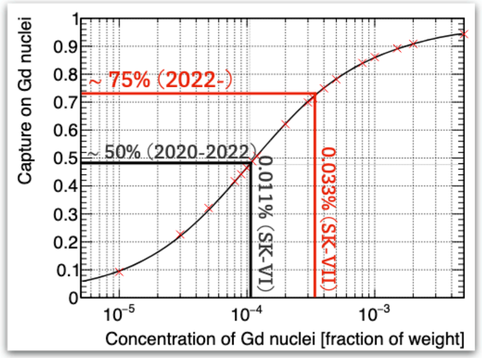

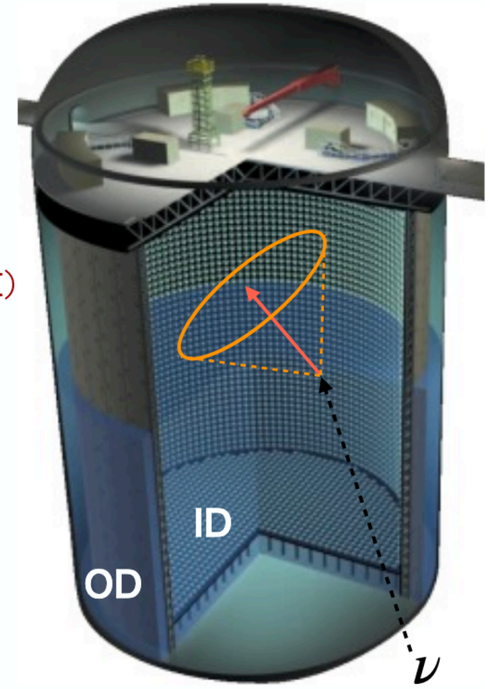

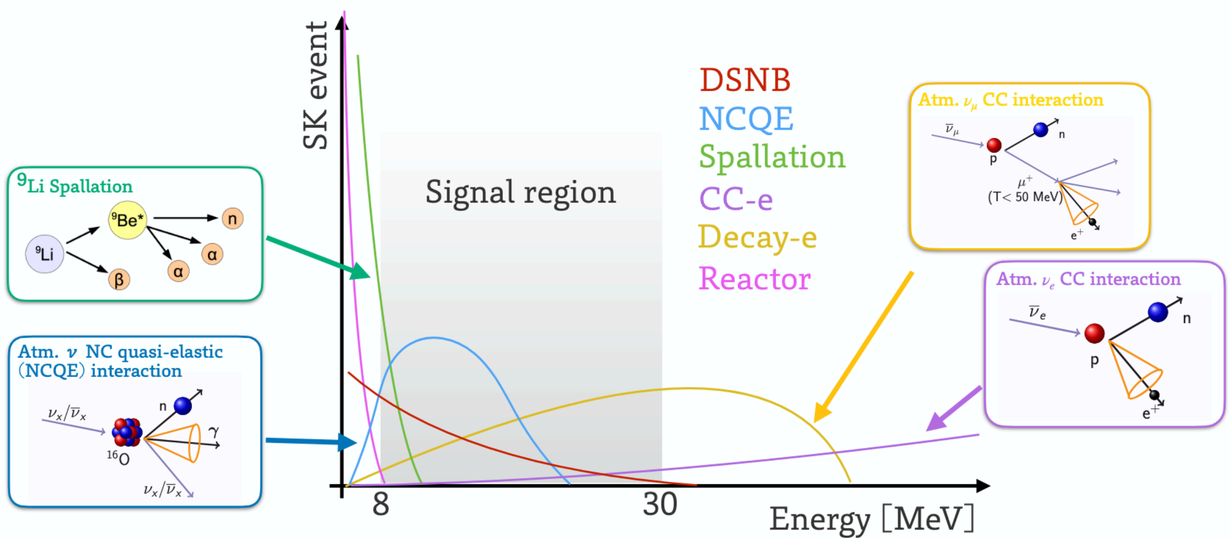
SK event
Signal region
DSNB
NCQE
Spallation
CC-e
Decay-e
Reactor
^{9}Li Spallation
^{9}Li
^{9}Be*
n
α
α
β
Atm. ν NC quasi-elastic (NCQE) interaction
$\nu_x/\bar{\nu}_x$
n
γ
^{16}O
$\nu_x/\bar{\nu}_x$
Atm. ν_μ CC interaction
$\bar{\nu}_\mu$
p
n
μ^+
(T< 50 MeV)
e^+
Atm. ν_e CC interaction
$\bar{\nu}_e$
p
n
e^+
8
30
Energy [MeV]

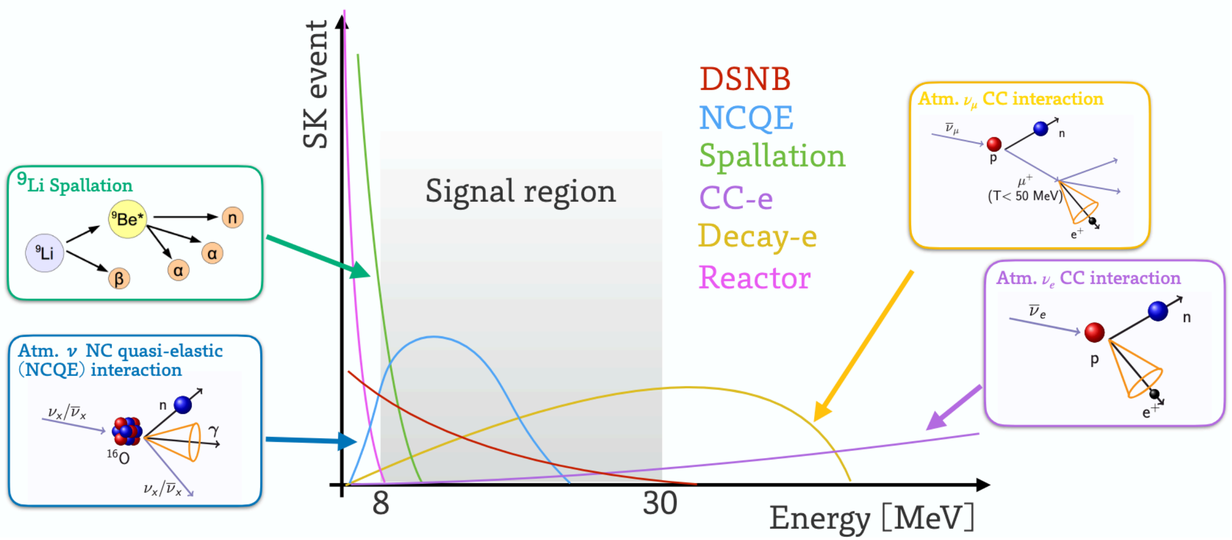

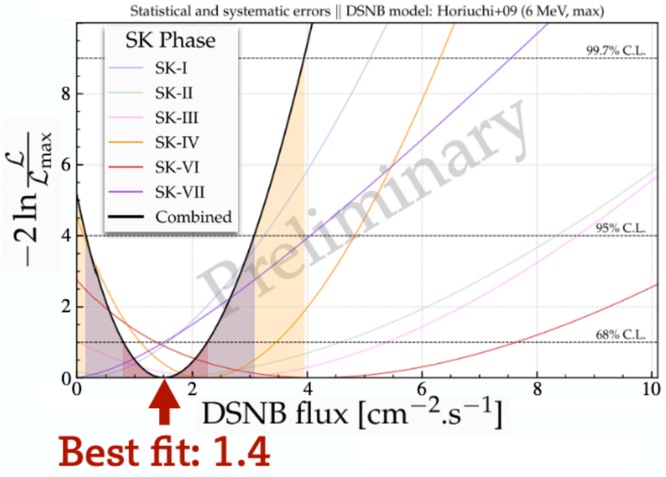

Best fit: 1.4

Highlight:

- 956 days of SK-Gd with Gd 0.01%(552 d)+0.03%(404 d)
  Spectrum independent analysis
  - Only use $N_n = 1$ events
  - Differential upper limit for $9.3 < E_\nu < 31.3$ MeV
- **Update the world stringent sensitivity for almost all bins**

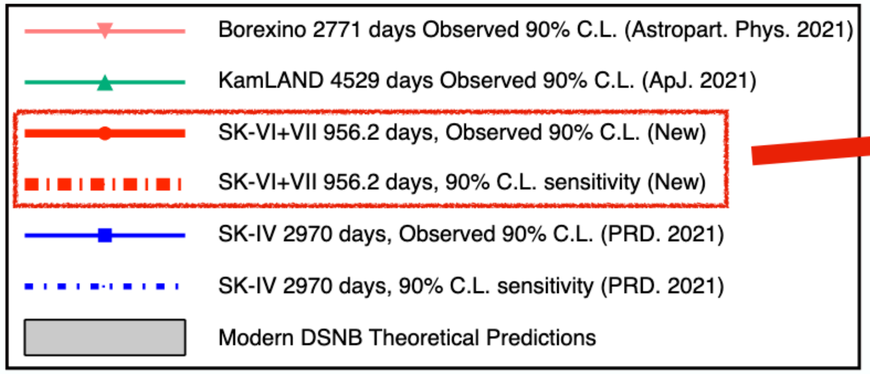

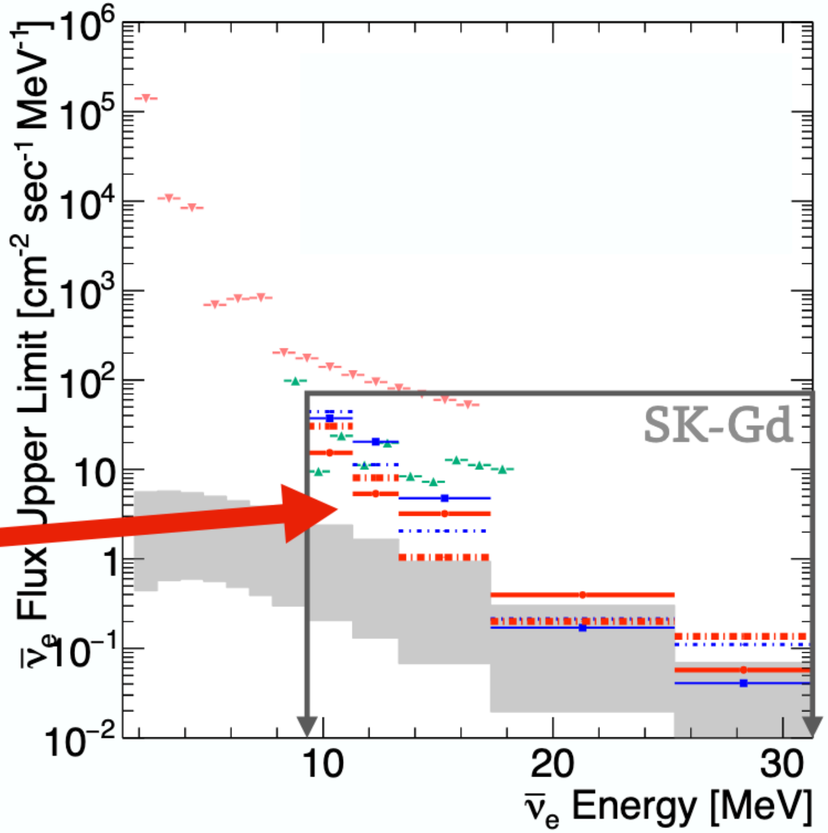

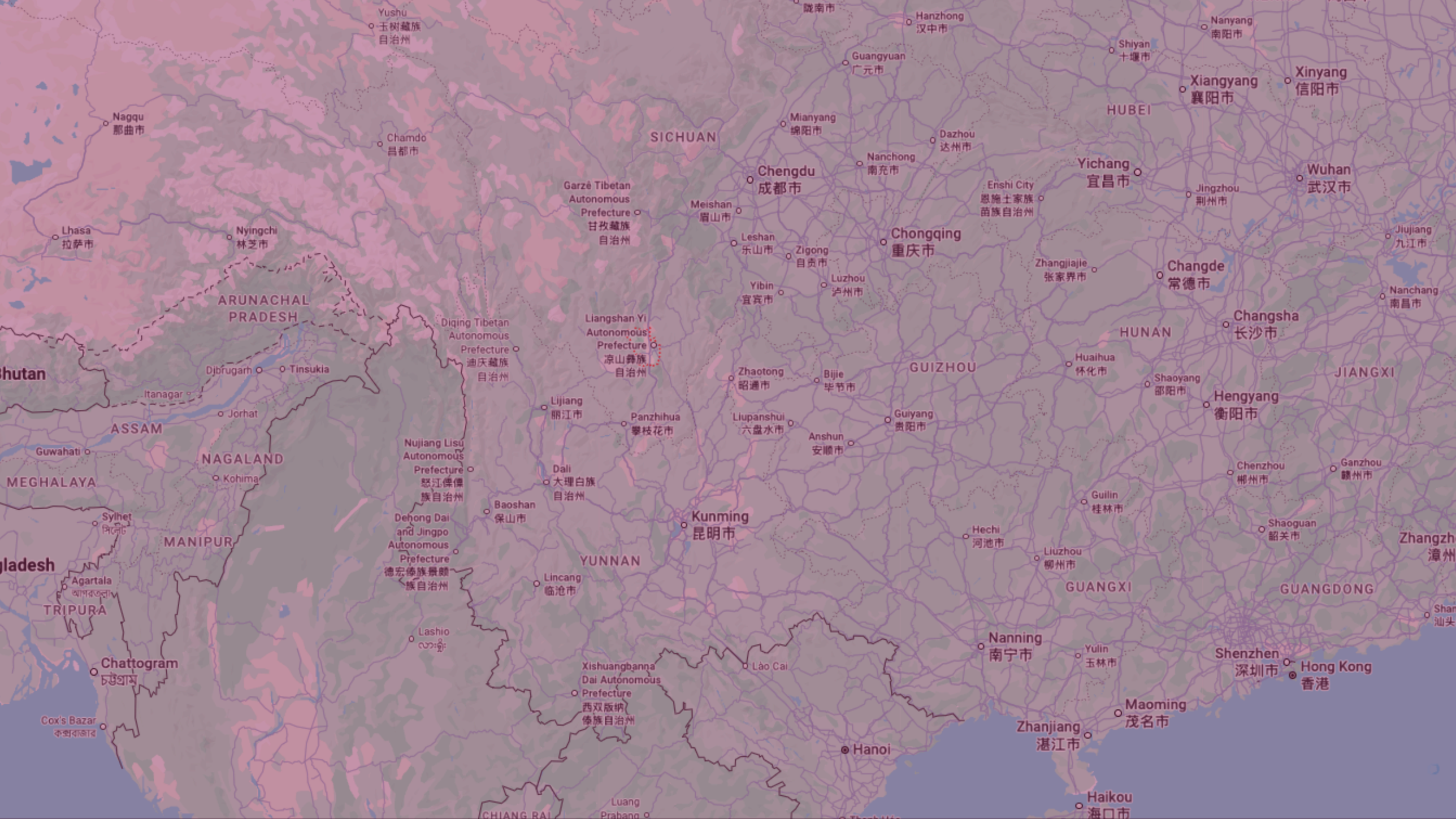
Yushu
玉树藏族
自治州
Hanzhong
汉中市
Nanyang
南阳市
Shiyan
十堰市
Guangyuan
广元市
Xiangyang
襄阳市
Xinyang
信阳市
HUBEI
Nagqu
那曲市
Chamdo
昌都市
SICHUAN
Mianyang
绵阳市
Dazhou
达州市
Nanchong
南充市
Chengdu
成都市
Yichang
宜昌市
Wuhan
武汉市
Enshi City
恩施土家族
苗族自治州
Jingzhou
荆州市
Garzê Tibetan
Autonomous
Prefecture
甘孜藏族
自治州
Meishan
眉山市
Lhasa
拉萨市
Nyingchi
林芝市
Leshan
乐山市
Zigong
自贡市
Chongqing
重庆市
Jiujiang
九江市
Zhangjiajie
张家界市
Changde
常德市
Yibin
宜宾市
Luzhou
泸州市
Nanchang
南昌市
ARUNACHAL
PRADESH
Liangshan Yi
Autonomous
Prefecture
凉山彝族
自治州
Diqing Tibetan
Autonomous
Prefecture
迪庆藏族
自治州
Changsha
长沙市
HUNAN
Huaihua
怀化市
Djibugarh
Tinsukia
Itanagar
Zhaotong
昭通市
Bijie
毕节市
GUIZHOU
Shaoyang
邵阳市
JIANGXI
Hengyang
衡阳市
Lijiang
丽江市
Jorhat
Panzhihua
攀枝花市
Liupanshui
六盘水市
Guiyang
贵阳市
ASSAM
Anshun
安顺市
Nujiang Lisu
Autonomous
Prefecture
怒江傈僳
族自治州
Guwahati
NAGALAND
Kohima
Dali
大理白族
自治州
Chenzhou
郴州市
Ganzhou
赣州市
MEGHALAYA
Baoshan
保山市
Guilin
桂林市
Sylhet
সিলেট
Dehong Dai
and Jingpo
Autonomous
Prefecture
德宏傣族景颇
族自治州
Kunming
昆明市
Shaoguan
韶关市
MANIPUR
Hechi
河池市
Liuzhou
柳州市
YUNNAN
Agartala
আগরতলা
Lincang
临沧市
GUANGXI
GUANGDONG
TRIPURA
Lashio
Nanning
南宁市
Yulin
玉林市
Shenzhen
深圳市
Hong Kong
香港
Chattogram
চট্টগ্রাম
Xishuangbanna
Dai Autonomous
Prefecture
西双版纳
傣族自治州
Lào Cai
Maoming
茂名市
Cox's Bazar
কক্সবাজার
Zhanjiang
湛江市
Hanoi
Haikou
海口市
Luang
Prabang
CHIANG RAI


谢谢
步行栈道及沿岸水域禁
游泳、戏水、捕捞